
Theses and Dissertations

Fall 2011

Biomechanical effects of multi-level laminoplasty and laminectomy: an experimental and finite element investigation

Swathi Kode
University of Iowa

Copyright 2011 Swathi Kode

This dissertation is available at Iowa Research Online: <http://ir.uiowa.edu/etd/2730>

Recommended Citation

Kode, Swathi. "Biomechanical effects of multi-level laminoplasty and laminectomy: an experimental and finite element investigation." PhD (Doctor of Philosophy) thesis, University of Iowa, 2011.
<http://ir.uiowa.edu/etd/2730>.

Follow this and additional works at: <http://ir.uiowa.edu/etd>

 Part of the [Biomedical Engineering and Bioengineering Commons](#)

BIOMECHANICAL EFFECTS OF MULTI-LEVEL LAMINOPLASTY AND
LAMINECTOMY: AN EXPERIMENTAL AND FINITE ELEMENT
INVESTIGATION

by
Swathi Kode

An Abstract

Of a thesis submitted in partial fulfillment
of the requirements for the Doctor of
Philosophy degree in Biomedical Engineering
in the Graduate College of
The University of Iowa

December 2011

Thesis Supervisor: Associate Professor Nicole M. Grosland

ABSTRACT

Cervical spondylotic myelopathy is the most common spinal cord disorder in persons over 55 years of age in North America and perhaps in the world. Surgical options are broadly classified into two categories namely, anterior and posterior approaches. This study focuses on the posterior based approach (i.e. laminectomy or laminoplasty) which is considered when multiple levels of the spine have to be decompressed or when most of the cord compression results from posterior pathological conditions. The external and internal behavior of the spine after laminoplasty and laminectomy has been evaluated using both experimental and computational methods.

Computationally, a validated intact 3D finite element model of the cervical spine (C2-T1) was modified to simulate laminectomy and laminoplasty (open door (ODL) and double door (DDL)) at levels C3-C6. During flexion, after ODL the adjacent levels C2-C3 and C6-C7 showed a 39% and 20% increase in the motion respectively; while no substantial changes were observed at the surgically altered levels. The percent increase in motion after DDL varied from 4.3% to 34.6%. The inclination towards increased motion during flexion after double door laminoplasty explains the role of the lamina-ligamentum flavum complex in the stability of spine. Compared to the intact model, laminectomy at C3-C6 led to a profound increase (37.5% to 79.6%) in motion across the levels C2-C3 to C6-C7. Furthermore, the changes in the von Mises stresses of the intervertebral disc observed after laminoplasty and laminectomy during flexion can be correlated to the changes in the intersegmental motions.

An in-vitro biomechanical study was conducted to address the effects of laminoplasty (two-level and four-level) and four-level laminectomy on the flexibility of the cervical spine. Both two-level and four-level laminoplasty resulted in minimal changes in C2-T1 range of motion. For flexion/extension, two-level and multi-level laminoplasty showed an approximate 20% decrease ($p>0.05$) in the range of motion at

C4-C5 and C2-C3 respectively due to the encroachment of the spinous process into the opened lamina. The decrease was mostly observed in older specimens and specimens with adjacent laminae close to each other; thus leading to the encroachment of the spinous process into the opened lamina. Laminectomy resulted in a statistically significant ($p < 0.05$) increase in the range of motion compared to the intact condition during the three loading modes. These results correspond well with the finite element predictions, where a four-level ODL and laminectomy resulted in a minimal 5.4% and a substantial 57.5% increase in C2-T1 motion respectively during flexion.

Adaptive bone remodeling theory was applied to the open door laminoplasty model to understand the effect of the surgical procedure on the internal architecture of bone. Bone remodeling was implemented at the C5 vertebra by quantifying the changes in apparent bone density in terms of the mechanical stimulus (i.e. SED/density). After laminoplasty, the increased load distribution through the bony hinge region led to the increased bone density during extension. This increased bone density could eventually lead to bone formation in those regions through external remodeling.

The current study proved laminoplasty to be a motion preservation technique wherein the plates and spacer provided additional stability via reconstruction of the laminar arch while laminectomy can cause instability of spine especially during flexion. In the future, patient-specific finite element models that incorporate geometry-related differences could be developed to optimize the number of operated levels and to further explain the effect of surgical procedure on the unaltered levels.

Abstract Approved: _____
 Thesis Supervisor

 Title and Department

 Date

BIOMECHANICAL EFFECTS OF MULTI-LEVEL LAMINOPLASTY AND
LAMINECTOMY: AN EXPERIMENTAL AND FINITE ELEMENT
INVESTIGATION

by
Swathi Kode

A thesis submitted in partial fulfillment
of the requirements for the Doctor of
Philosophy degree in Biomedical Engineering
in the Graduate College of
The University of Iowa

December 2011

Thesis Supervisor: Associate Professor Nicole M. Grosland

Copyright by
SWATHI KODE
2011
All Rights Reserved

Graduate College
The University of Iowa
Iowa City, Iowa

CERTIFICATE OF APPROVAL

PH.D. THESIS

This is to certify that the Ph.D. thesis of

Swathi Kode

has been approved by the Examining Committee
for the thesis requirement for the Doctor of Philosophy
degree in Biomedical Engineering at the December 2011 graduation.

Thesis Committee: _____
Nicole M. Grosland, Thesis Supervisor

Joseph D. Smucker

Tae-Hong Lim

David G. Wilder

M. Asghar Bhatti

To all those people who are suffering from spinal problems

Learn from yesterday, live for today, hope for tomorrow

Albert Einstein

ACKNOWLEDGMENTS

I have been grateful to receive the support of many people through the completion of my doctoral work. Thank you to each and everyone. The whole process taught me many valuable lessons and helped me grow both professionally as well as personally.

I would like to first thank my advisor Dr. Nicole Grosland who has been a great support and mentor during the course of my study. Her guidance, understanding and suggestions during the development of my thesis have been invaluable.

I would like to extend my special thanks to Dr. Joseph Smucker for providing valuable inputs and guidance while simulating the surgical techniques. I am also grateful to Professors David Wilder, Tae-Hong Lim and Asghar Bhatti for serving on the committee. Their valuable advice and suggestions helped me shape the thesis better. Many thanks to Douglas Fredericks for taking time out of his busy schedule to perform the surgical procedures.

My special thanks to Anup Gandhi who showed great interest and support during the experimental testing of the specimens. I would also like to thank Nicole Kallemeyn, Srinivas Tadepalli and Kiran Shivanna for their valuable assistance in finite element modeling and programming. I am grateful to the Bone Healing Research Lab for their financial support thus helping me finish my work with no hurdles. I would also like to acknowledge Dr. Yubo Gao for assistance with statistical analysis and Amy Criswell for help during biomechanical testing.

It was also a great pleasure to share my doctoral life with people like Nicole DeVries, Amla Natarajan and Austin Ramme, making my experience at Iowa a memorable one. I have been fortunate to have the support of many good friends who have made my life outside the lab a fun-filled one. Pallavi, you were tolerant enough to live with me for three years; Sharada, Hema, and Jyothsna, I will always cherish those long

Friday nights and lengthy chats; and Divya, I couldn't ask you more, you stayed with me through thick and thin.

Finally, I am indebted to my wonderful parents and family who have been instrumental in defining me. Thanks to my mom for always being there for me and to my dad for being a constant source of inspiration and encouragement. Their unconditional love and support helped me reach my goals.

TABLE OF CONTENTS

LIST OF TABLES	viii
LIST OF FIGURES	ix
LIST OF ABBREVIATIONS.....	xiii
CHAPTER 1: SIGNIFICANCE AND SPECIFIC AIMS.....	1
1.1 Significance of the Current Study.....	2
1.2 Specific Aims.....	4
CHAPTER 2: INTRODUCTION.....	5
2.1 Relevant Anatomy of Cervical Spine	6
2.1.1 Cervical Vertebrae.....	7
2.1.2 Intervertebral Disc and Facet Joints	8
2.1.3 Ligaments	9
2.1.4 Spinal Cord.....	9
2.2 Cervical Spondylotic Myelopathy	9
2.2.1 Operative Management	12
2.2.1.1 Anterior Approach.....	13
2.2.1.2 Posterior Approach.....	14
2.2.1.2.1 Laminectomy	15
2.2.1.2.2 Laminoplasty.....	15
CHAPTER 3: FINITE ELEMENT MODELS OF INTACT AND SURGICALLY SIMULATED CERVICAL SPINE	19
3.1 Modification of the Existing Intact C2-C7 Finite Element Model	20
3.1.1 Addition of T1 to C2-C7 model	20
3.1.2 Updating the Model to 2Nm.....	22
3.1.2.1 Boundary and Loading Conditions	25
3.1.2.2 Flexibility Testing	25
3.1.2.3 Validation of the Intact Finite Element Model.....	25
3.1.2.4 Results	29
3.2 Laminectomy in the Cervical Spine	32
3.2.1 Background and Literature Review.....	33
3.2.2 Simulation of Laminectomy in a Finite Element Model.....	34
3.3 Open Door Laminoplasty in the Cervical Spine.....	36
3.3.1 Background and Literature Review.....	36
3.3.2 Simulation of ODL at Levels C3-C6.....	40
3.4 Double Door Laminoplasty in the Cervical Spine.....	46
3.4.1 Background and Literature Review.....	46
3.4.2 Simulation of DDL at Levels C3-C6.....	50
3.5 Results.....	54
3.5.1 Comparison of Spinal Canal Area.....	54
3.5.2 Stress Distribution in the Cortical Bone.....	56
3.5.3 Stress Distribution in Laminoplasty Constructs	56
3.5.4 Flexibility Test.....	60
3.6 Discussion.....	63

CHAPTER 4. EXPERIMENTAL TESTING OF CADAVERIC CERVICAL SPINE SPECIMENS AFTER LAMINOPLASTY AND LAMINECTOMY	68
4.1 Introduction.....	68
4.2 Materials and Methods	69
4.2.1 Specimen Preparation	69
4.2.2 Biomechanical Testing	69
4.2.2.1 Test Setup	70
4.2.2.2 Test Protocol	71
4.2.3 Surgical Techniques	73
4.2.3.1 Laminoplasty (C5-C6).....	73
4.2.3.2 Laminoplasty (C3-C6).....	74
4.2.3.3 Laminectomy (C3-C6)	74
4.2.4 Data Analysis.....	75
4.3 Results.....	76
4.4 Discussion.....	80
4.5 Conclusion.....	83
 CHAPTER 5: APPLICATION OF ADAPTIVE BONE REMODELING THEORY TO CERVICAL LAMINOPLASTY	 84
5.1 Introduction.....	84
5.1.1 Bone Remodeling Theories	85
5.2 Methods	89
5.2.1 Finite Element Model	89
5.2.1.1 Loading and Boundary Conditions	89
5.2.2 Bone Remodeling Algorithm	89
5.2.3 Analysis	92
5.3 Results.....	93
5.4 Discussion.....	96
 CHAPTER 6: CONCLUSION	 99
6.1 Future Work.....	101
 REFERENCES	 103

LIST OF TABLES

Table 1. Young's Modulus of Annulus fibrosus for different levels.....	23
--	----

LIST OF FIGURES

Figure 1. Spinal Column (Left) Lateral view; (Right) Posterior view.....	5
Figure 2. Anatomy of cervical spine highlighting the various bony elements. Atlas and axis differ from the subaxial spine	6
Figure 3. Anatomy of a typical cervical vertebra (C3-C6).....	7
Figure 4. Intervertebral disc with clearly defined annulus fibrosus and nucleus pulposus.....	8
Figure 5. Static mechanical factors in cervical spondylotic myelopathy (Herniated Disc, Bone Spurs and Thickened Ligamentum Flavum)	11
Figure 6. Dynamic mechanical factors in cervical Spondylotic Myelopathy. (Left) During flexion, lengthened spinal cord hits the anterior osteophytes; (Right) During extension, buckled ligamentum flavum decreases the available spinal canal area.....	12
Figure 7. Anterior Cervical Decompression and Fusion; anterior plating for stabilization	14
Figure 8. Cervical Laminectomy of C4, C5 and C6 levels. It shows the removal of lamina and spinous process	16
Figure 9. Types of Laminoplasty: (A) Creation of open and hinge side with the use of a high speed burr for open door laminoplasty (B) Creation of bilateral hinges for double door laminoplasty with the use of a high speed burr. Spinous process are split in the midline (C) Open door laminoplasty: Lamina stabilized with plates and screw after open door laminoplasty (D) Double door laminoplasty: Spinous process are spread in the midline and held open with either sutures or spacers.....	17
Figure 10. Intervertebral Disc showing the annulus and nucleus. Annulus was further divided into anterior, lateral and posterior regions	21
Figure 11. C2-T1 Intact finite element model of cervical spine.....	24
Figure 12. C2-C7 Model Validation in Flexion/Extension. Experimental data is represented red in color and blue triangular dots denote the finite element predictions	27
Figure 13. C2-C7 Model Validation in Right/Left Lateral Bending. Experimental data is represented red in color and blue triangular dots denote the finite element predictions	28
Figure 14. C2-C7 Model Validation in Left/Right Axial Rotation. Experimental data is represented red in color and blue triangular dots denote the finite element predictions	29

Figure 15. C7-T1 Range of motion obtained from (A) Finite element model (B) Experimental study in flexion/extension	30
Figure 16. C2-T1 Range of motion obtained from (A) Finite element model (B) Experimental study in flexion/extension	31
Figure 17. Cervical decompressive laminectomy	32
Figure 18. Laminectomy of C5 vertebra.....	34
Figure 19. C2-T1 model with laminectomy at C3-C6	35
Figure 20. Open door Laminoplasty stabilized by (A) Anchor system (B) Spacer	37
Figure 21. Axial CT image of plate in situ	39
Figure 22. Superior view of a vertebra showing the hinge and cut end of the lamina	41
Figure 23. Superior view of C5 vertebrae showing laminar opening.....	42
Figure 24. C5 vertebra showing holes in lateral mass and lamina.....	42
Figure 25. ProE Model of the laminoplasty plate and screw	43
Figure 26. Finite element mesh of the plate and screw.....	44
Figure 27. von Mises stress (MPa) distribution in C5 vertebra stabilized with plate and screws.....	45
Figure 28. C2-T1 finite element model with open door laminoplasty performed at levels C3-C6. (Left) Full model; (Right) Local zoom	46
Figure 29. Hydroxyapatite Spacer	48
Figure 30. DDL with HA spacer stabilized with (A) sutures and (B) screws	49
Figure 31. Superior view of a vertebra following laminar opening for DDL ; highlighting the bilateral hinges and Laminar Opening Space (LOS) of 10 mm	51
Figure 32. Trapezoid shaped spacer. (Left) Solid model; (Right) Finite element mesh	52
Figure 33. C6 Vertebra stabilized with spacer.....	53
Figure 34. C2-T1 finite element model with double door laminoplasty performed at levels C3-C6. (Left) Full model; (Right) Local zoom.	54
Figure 35. Comparison of spinal canal area of the three models (intact, open door and double door) with the literature data	55
Figure 36. Posterior view of the von Mises stress distributon in the vertebral bodies (C3-C6) after open and double door laminoplasty	57

Figure 37. Maximum von Mises stress in the (Top) anterior and (Bottom) posterior regions of the vertebral bodies after the laminar opening for open and double door laminoplasty.....	58
Figure 38. von Mises Stress (MPa) distribution in the laminoplasty plate.....	59
Figure 39: von Mises Stress (MPa) distribution in the spacer.....	59
Figure 40. Percent changes in C2-T1 range of motion after ODL, DDL and laminectomy.....	61
Figure 41. Percent change in intersegmental motion after the three surgical techniques for the six loading modes.....	62
Figure 42. Percent change in stresses in the annular regions of the intervertebral discs after the three surgical techniques during the six loading modes.....	63
Figure 43. Experimental data (A) C2-T1 motion after Open Door Laminoplasty and Laminectomy (B) Intersegmental motions after Double Door Laminoplasty.....	66
Figure 44. Photograph of a specimen mounted for testing on servo hydraulic materials testing machine (858Bionix II, MTS Corporation, Eden Prairie, MN). XZ table was placed below the bottom gimbal to offset any shear forces by translating in the required direction. Rigid body markers (IREDS) were attached to the vertebral bodies of spine.....	72
Figure 45. Flowchart showing the sequential order of biomechanical testing.	73
Figure 46. Photograph showing a 10mm open door laminoplasty plate and screw. The left end of the plate sits on the lateral mass while the U-shaped slot holds the lamina via screws.	74
Figure 47. Photograph depicting the procedures of (A) Open door laminoplasty performed on the left side at C3-C6; the laminae were held open with plates and screws and (B) Laminectomy with the complete resection of lamina and associated ligaments at C3-C6 levels.....	75
Figure 48. Sample Moment-Rotation curve from the three-dimensional flexibility test. Graph shows the segmental rotations plotted against moment for an intact specimen during flexion/extension.....	76
Figure 49. Moment-Rotation curves of the intact, two-level laminoplasty (LP_C56), multi-level laminoplasty (LP_C3456), multi-level laminectomy (LT_C3456) from the three dimensional flexibility test (flexion/extension).....	77
Figure 50. Percent change in C2-T1 range of motion during the three loading modes, FE (Flexion/Extension), LB (Lateral Bending) and AR (Axial Rotation). Laminoplasty (LP_C56 and LP_C3456) resulted in minimal changes while laminectomy reported significant increase in the motion compared to the intact state.....	78

Figure 51. Mean intervertebral rotations (\pm standard deviation) for each level (C2-C3 to C7-T1) during (A) Flexion + Extension; (B) Right + Left lateral bending; (C) Right + Left axial rotation.	79
Figure 52. Basic Multicellular Unit	86
Figure 53. Biological control mechanism of adaptive bone remodeling	87
Figure 54. Adaptive bone remodeling algorithm.....	90
Figure 55. Graphical representation of the rate of change of bone density with the remodeling signal (strain energy density).....	91
Figure 56. Flowchart showing the application of site-specific bone remodeling algorithm to cervical laminoplasty.....	93
Figure 57. Density distribution in an intact C5 vertebrae (A) CT based material properties (B) Optimized material properties (Superior View) (C) Optimized material properties (Sagittal View).....	95
Figure 58. Density distribution in a C5 vertebra after open door laminoplasty (A) site-specific material properties from the optimized intact model (B) Optimized material properties after convergence.	96

LIST OF ABBREVIATIONS

CSM	Cervical spondylotic myelopathy (CSM)
ACDF	Anterior cervical decompression and fusion ()
ODL	Open Door Laminoplasty
DDL	Double Door Laminoplasty
3D	Three Dimensional
ALL	Anterior Longitudinal Ligament
PLL	Posterior Longitudinal Ligament
CL	Capsular Ligament
LF	Ligamentum Flavum
IS	Interspinous Ligament
OPLL	Ossification of the Posterior Longitudinal Ligament
CT	Computed Tomography
MR	Magnetic Resonance
LOS	Laminar Opening Space
CAD	Computer-Aided Design
HA	Hydroxyapatite
JOA	Japanese Orthopaedic Association
FDL	French door laminoplasty
MTS	Materials Testing Machine
IRED	Infrared Light Emitting Diodes
SED	Strain Energy Density
HU	Hounsfield Units

CHAPTER 1: SIGNIFICANCE AND SPECIFIC AIMS

The spine is a long, slender, flexible column with a large range of mobility. The three main functions of the spine are: 1) to protect the spinal cord, nerve roots and several other internal organs 2) to provide structural support and balance to maintain an upright posture, and 3) to provide flexibility. Typically, the spine is divided into four main regions: cervical, thoracic, lumbar and sacral. Each region has specific characteristics and functions.

Cervical spondylotic myelopathy (CSM) is caused by degenerative disorders of spine. This spectrum includes neck-pain syndromes, radiculopathy and myelopathy. Proper imaging of the cervical spine is essential in the diagnosis, evaluation and preoperative planning for patients with cervical spondylotic myelopathy. It is generally accepted that an absolute anterior-posterior diameter of the spinal canal measuring less than 10mm presents a greater risk for the development of cervical spondylotic myelopathy [61].

Operative management is generally indicated for patients with progressive neurological deterioration. Anterior and posterior approaches are effective in decompressing the spinal cord. The pros and cons of each approach based on the patient's pathological conditions should be considered. Anterior cervical decompression and fusion (ACDF) and laminectomy are the traditional techniques widely used to decompress the spinal cord. However ACDF has been associated with several complications over the years such as graft failure, adjacent segment degeneration, and decrease in the rate of fusion with the increase in the number of levels [2-4]. Following laminectomy, several clinical studies reported loss of cervical curvature and development of clinical instability due to the loss of posterior structures [5, 6].

Cervical laminoplasty is a posterior based surgical approach intended to relieve pressure on the spinal cord while maintaining the stabilizing effects of the posterior

elements of the vertebrae. It may be an excellent option to allow the spinal cord to heal, and reverse the symptoms. Since its inception, several modifications have been made to the basic theme of this procedure. Currently, surgical procedure of laminoplasty can be broadly divided into open door type and double door type. Open door laminoplasty (ODL) was originally developed by Hirabayashi [7,8] as a primary treatment for ossification of posterior longitudinal ligament. Once the lamina is opened and the spinal cord is decompressed, preventing restenosis is a primary concern. Hirabayashi used sutures to hold the lamina open. Although simple, it resulted in several cases of recurrent stenosis as the lamina closed into its preoperative position. Subsequently, various authors have described numerous techniques which include the use of titanium miniplates, spacers or blocks to stabilize the posterior elements in the open position [9,10]. Our earlier studies on single-level open door laminoplasty have shown increased sagittal diameter and spinal canal area using this technique [11]. The *in vitro* and computational studies done on a single C5 vertebrae provided the information on the loads taken by posterior bone before the failure of the laminoplasty construct [12]. The current study uses titanium plates and screws to hold the lamina in the open position for ODL and hydroxyapatite spacers (HA) for double door laminoplasty (DDL).

Various authors compared multi-level laminectomy to laminoplasty via experimental studies to show the instability of spine after laminectomy [9,10,13,14]. However, most of the studies have been performed under lower moments and did not report the intersegmental motions after the surgical procedures.

The current study was designed to look at the internal and external responses of the spine to laminectomy and the two types of laminoplasty procedures.

1.1 Significance of the Current Study

In 2008 the U.S. laminoplasty market was valued at \$65.3 million, representing an increase of 9.5% over 2007. The market is predicted to continue growing over the

forecast period (2005-2015). Future growth will be driven by the advantages laminoplasty offers over its alternatives, most notably, that laminoplasty maintains spinal alignment and very often aids in preserving motion in the cervical region [15]. These numbers serve as another motivating factor to examine closely the biomechanical impact of the surgical procedure.

Although, *in vitro* and *in vivo* experiments give valuable data, little information can be obtained about the internal responses. Hence, a commonly employed technique to study the spinal biomechanics is through the construction of mathematical models and their solution using numerical methods (e.g. finite element method). Finite element methods have been demonstrated to be very useful in quantifying variables not directly measurable in experimental studies like local stresses, as they help in determining the effect a particular parameter on the resulting complex structures. The current study emphasizes simulating multi-level laminoplasty and laminectomy in a finite element model. Earlier studies that compared the two laminoplasty techniques have been mostly clinical in nature and hence have only looked at the differences pertaining to spinal canal area and range of motion. This is the first study looking at the differences in terms of flexibility and stress distribution in the implants, vertebral bodies and intervertebral discs. It is well known that the main aim of laminoplasty is to create a stable laminar arch to preserve the laminar opening. As hinge failure is a commonly encountered problem during laminoplasty, it is necessary to understand the process of bone remodeling post laminoplasty. The study aims at implementing a computer simulation method to predict changes in bone density distribution in accordance with Wolff's Law. Most of the previous *in vitro* studies were conducted on C2-C7 spines under a moment of $\leq 1.5\text{Nm}$ using different experimental setups. In order to have a direct and robust comparison with our finite element studies, an experimental study was undertaken to study the multidirectional flexibility after multi-level laminoplasty and laminectomy under similar loading and boundary conditions.

1.2 Specific Aims

The thesis is divided into six chapters. The second chapter of the thesis introduces cervical spinal anatomy, and discusses the operative management of the cervical spondylotic myelopathy. Thereafter, each specific aim is addressed separately in greater detail discussing the background, methodology, and the results. The last chapter of the thesis summarizes the findings of the current study and concludes with the ideas for related future research.

The specific aims of the current study can be summarized as follows:

- To extend the previously developed intact C2-C7 finite element model to include T1, thereby a detailed specimen-specific, validated three-dimensional (3D) finite element model of the cervical spine (C2-T1) was used. For better kinematic predictions following the surgical simulations, the model was also updated to 2Nm.
- To simulate two different laminoplasty procedures namely open-door, double-door laminoplasty and laminectomy at C3-C6 levels of a C2-T1 finite element model.
- To experimentally test cadaveric cervical spine specimens after laminoplasty (2-level, 4-level) and laminectomy.
- To predict the changes in the bone density by applying an adaptive bone remodeling theory to the open door laminoplasty model.

CHAPTER 2: INTRODUCTION

The spine is a complex structure with hard and soft tissue constituents. It is tied together by ligaments and is actuated by muscles. The spine is divided into cervical, thoracic, lumbar and sacral regions as shown in Figure 1. Each region of the spine has a natural curve. The cervical and lumbar sections are lordotic; while the thoracic and sacral sections are kyphotic in nature. These curves help to distribute mechanical stress as the body moves. The entire spinal column provides structural support for the trunk of the body and protects the spinal cord.

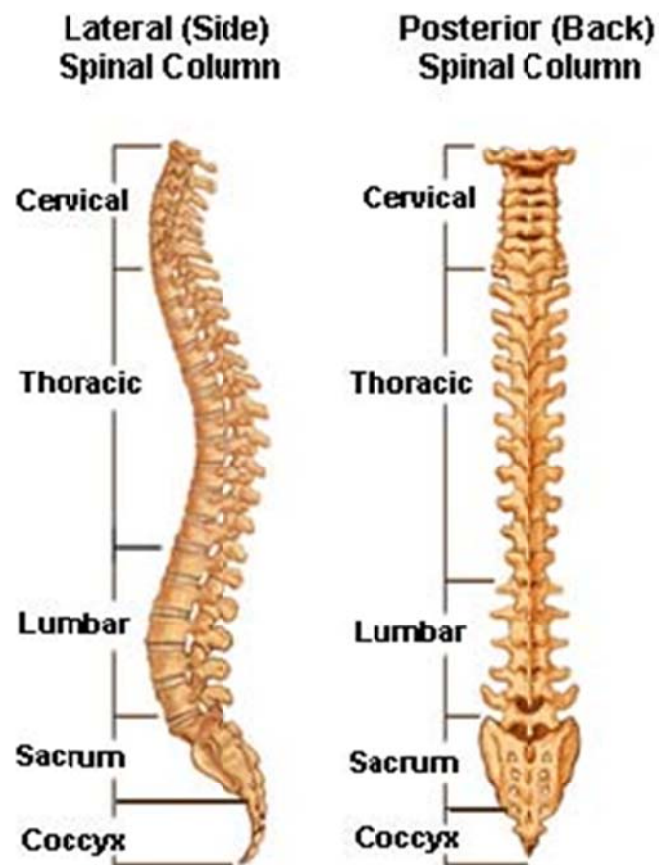


Figure 1. Spinal Column (Left) Lateral view; (Right) Posterior view [16].

2.1 Relevant Anatomy of Cervical Spine

The cervical spine is made up of the first seven vertebrae in the spine (Figure 2). It has a lordotic curvature and is much more mobile than the thoracic and lumbar regions of the spine. The purpose of the cervical spine is to contain and protect the spinal cord, support the skull, and enable diverse head movement (e.g., rotate side to side, flexion and extension).

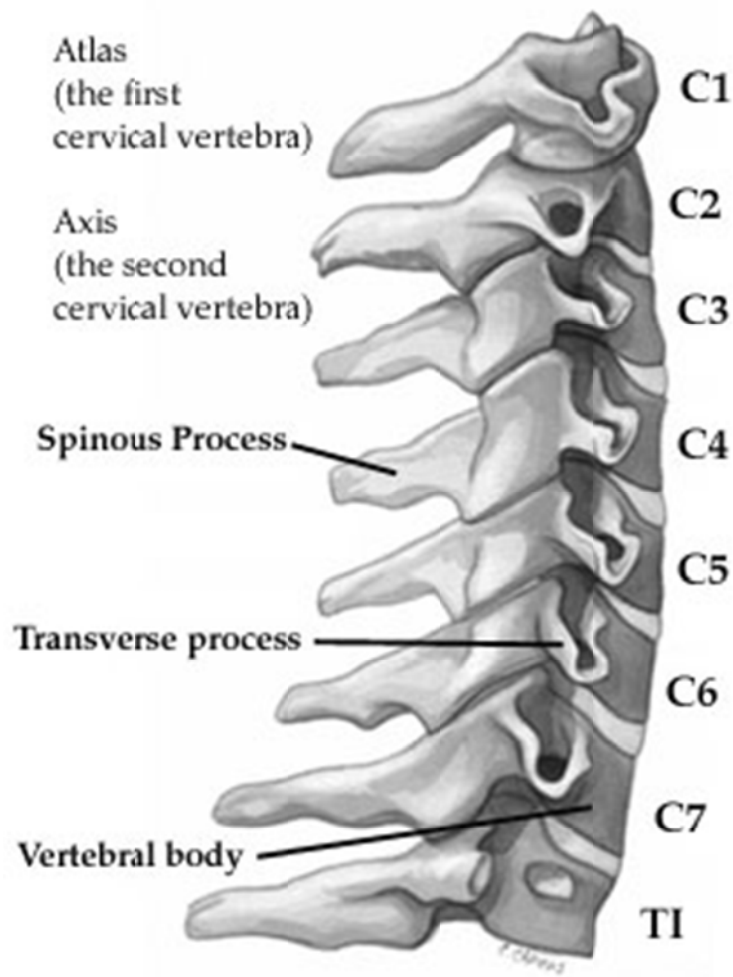


Figure 2. Anatomy of cervical spine highlighting the various bony elements. Atlas and axis differ from the subaxial spine [17].

2.1.1 Cervical Vertebrae

Cervical Spine is classically divided into the upper atypical vertebrae (C1, C2) and the subaxial spine (C3-C7). The atlas (C1) and axis (C2) differ from all other vertebrae. There is a diarthrodial articulation between the anterior articular surface of the dens of C2 and the posterior surface of the anterior arch of C1 where the majority of the rotation in the cervical spine occurs. A typical vertebra consists of an anterior body and a posterior ring made of articular, transverse, and spinous processes. The vertebral body is a cylindrical structure containing the outer cortical and the inner cancellous bone. The vertebrae of the subaxial spine have a consistent osseous anatomy, with slight variations in size and orientation of the lateral mass, lamina and a relative consistency to the size of the vertebral bodies (Figure 3). The bifid spinous processes of the upper cervical vertebrae, excluding C1, changes into a single prominent spinous process of C7. The vertebral bodies of the subaxial cervical spine articulate with one another through the unique joints of Luschka also known as uncovertebral joint.

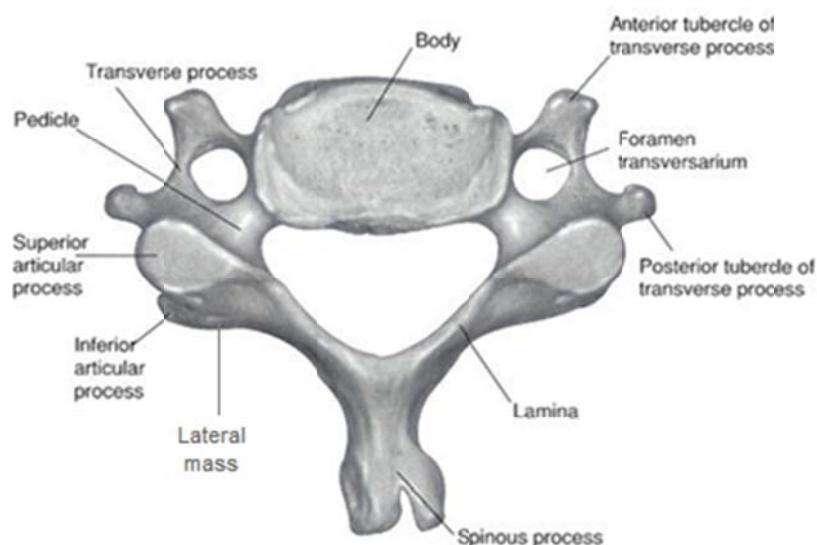


Figure 3. Anatomy of a typical cervical vertebra (C3-C6) [18].

2.1.2 Intervertebral Disc and Facet Joints

The intervertebral disc is located between the vertebral bodies beginning at the C2-C3 level (Figure 4). The cervical annulus is well developed anteriorly; but it tapers laterally and posteriorly towards the anterior edge of the unciniate process on each side. The disc functions as a shock absorber between their respective vertebral bodies with axial loads. The facet joints of the subaxial spine are true diarthrodial articulations encapsulated in a thick fibrous sheath, the facet capsule. They allow small degrees of flexion and extension, limit rotation and ultimately serve to protect the disc from translational shear stresses [19]. It has been shown in the past that the anterior body carries most of the load placed on the spine with only 18% of the compressive load carried by the facets [20]. Few others have shown that the load carried by the facets can vary from zero to 33% depending on the posture. In certain postures the facets will be unloaded and the capsular ligaments will be under tension [21].

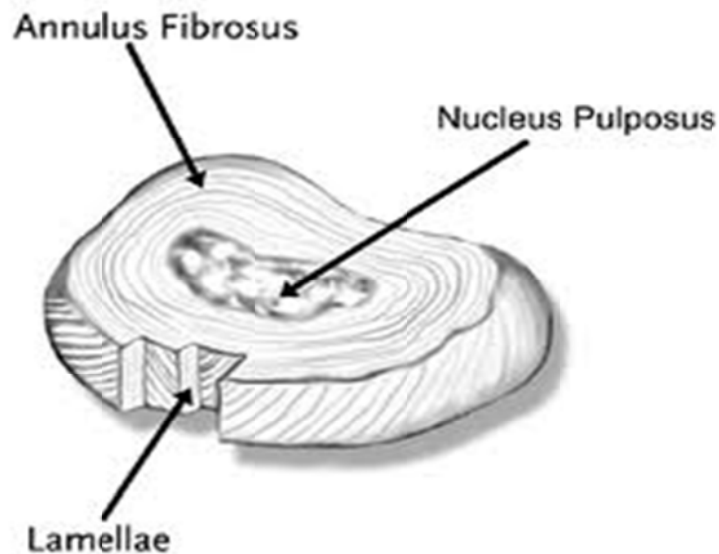


Figure 4. Intervertebral Disc with clearly defined annulus fibrosus and nucleus pulposus [22].

2.1.3 Ligaments

The cervical spine also features a complex arrangement of ligaments to supplement its structure and mobility. Ligaments are uniaxial structures that are mostly effective in carrying loads along the fiber direction. They can resist tensile forces but buckle under compression. The key function of the ligaments is to allow adequate physiologic motion under different directions while limiting excessive motion to protect the spinal cord. The cervical spinal ligaments include mainly anterior longitudinal ligament (ALL) and posterior longitudinal ligament (PLL) that line the anterior and posterior surfaces of disc and vertebral bodies respectively, the capsular ligaments (CL) that are generally oriented in a direction perpendicular to the plane of the facet joints, the ligamentum flavum (LF) that is a thick elastic connective tissue connecting the adjacent laminae together and interspinous (ISL) and intertransverse ligaments that pass between the spinous and transverse process respectively.

2.1.4 Spinal Cord

The spinal canal houses the spinal cord and is surrounded anteriorly by the vertebral bodies, intervertebral discs, and the posterior longitudinal ligaments; laterally and posteriorly by the bony vertebral arch; and posteriorly by the ligamentum flavum. The spinal canal changes in length due to physiologic flexion, extension, and lateral bending. Its effective cross-sectional area also undergoes changes with physiologic axial rotation and horizontal displacement. At the C1 level, the spinal cord occupies just one half of the canal. It occupies three quarters of the canal at the C5-C7 levels, however, which helps to explain why cervical spondylotic myelopathy (CSM) predominately occurs in the lower cervical spine [18].

2.2 Cervical Spondylotic Myelopathy

Cervical spondylotic myelopathy is the most common spinal cord disorder in persons more than 55 years of age in North America and perhaps in the world [23]. As

the number of older persons in the United States increases, the incidence of CSM will most likely increase. Cervical spondylosis is a chronic degenerative condition of the cervical spine that affects the vertebral bodies and intervertebral discs of the neck as well as the contents of the spinal canal. There are three important pathophysiologic factors in the development of CSM: (a) static mechanical; (b) dynamic mechanical; and (c) spinal cord ischemia [24].

Static mechanical factors result in the reduction of spinal canal diameter and thereby compress the spinal cord and the associated nerve roots. Many investigators have reported stenosis based on the diameter of the spinal canal from plain lateral radiographs [1]. With aging, the intervertebral disc loses its water content and elasticity, resulting in loss of disc height, cracks and fissures. The disc subsequently collapses as a result of biomechanical incompetence, causing the bulge in the annulus and nucleus sequestration. This process puts greater stress on the vertebrae and the respective end plates leading to the development of osteophytes that can project posteriorly into the spinal canal and markedly reduce the space available for spinal cord and its blood supply. Some of the other complementary changes include development of osteophytes in the facet joints, arches and thickening and ossification of posterior longitudinal ligament [18], further compromising the spinal canal dimensions and neural foramina (Figure 5). Symptoms are believed to develop when the spinal canal area has been reduced by at least 30 percent [25].

The contribution of dynamic mechanical factors in the development of CSM is related to the fact that the normal motion of the cervical spine may aggravate spinal cord damage precipitated by direct mechanical static compression. This is mainly observed during flexion and extension. During flexion, the spinal cord lengthens and stretches over ventral osteophytes whereas during extension, the ligamentum flavum may buckle into the spinal cord causing a reduction in the available space for the spinal cord (Figure 6).

This circumferential, progressive intrusion into the spinal canal leads to intrinsic changes in the spinal cord.

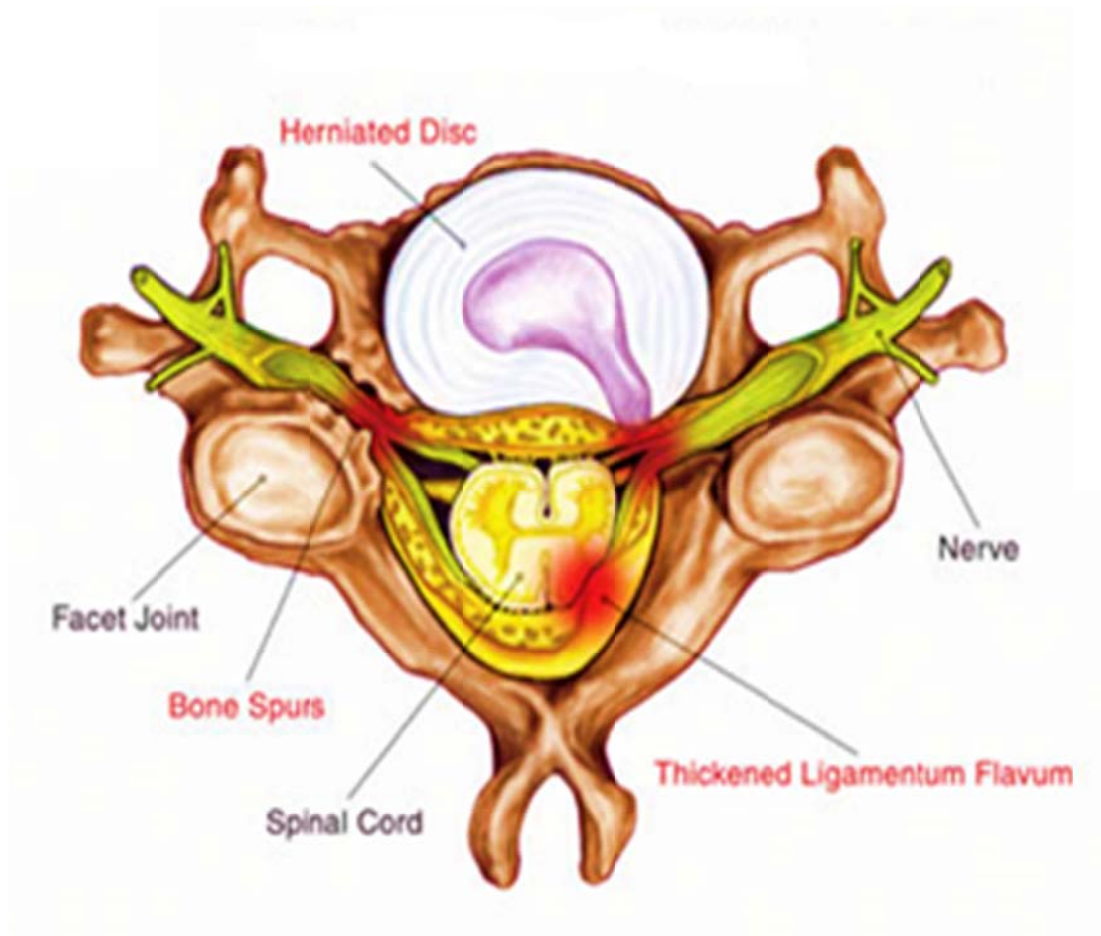


Figure 5. Static mechanical factors in cervical spondylotic myelopathy (Herniated Disc, Bone Spurs and Thickened Ligamentum Flavum) [26].

Although, the precise role of spinal cord ischemia in the development of CSM is not completely understood; patients with CSM have shown histopathologic changes in the spinal cord consistent with ischemia [28,29]. These structural and mechanical changes in the spine result in foraminal and spinal canal stenoses producing

radiculopathy and myelopathy, respectively. Computed Tomography and Magnetic Resonance scans are currently the best available methods for diagnosis as early detection facilitates appropriate intervention before neurological loss becomes irreversible.

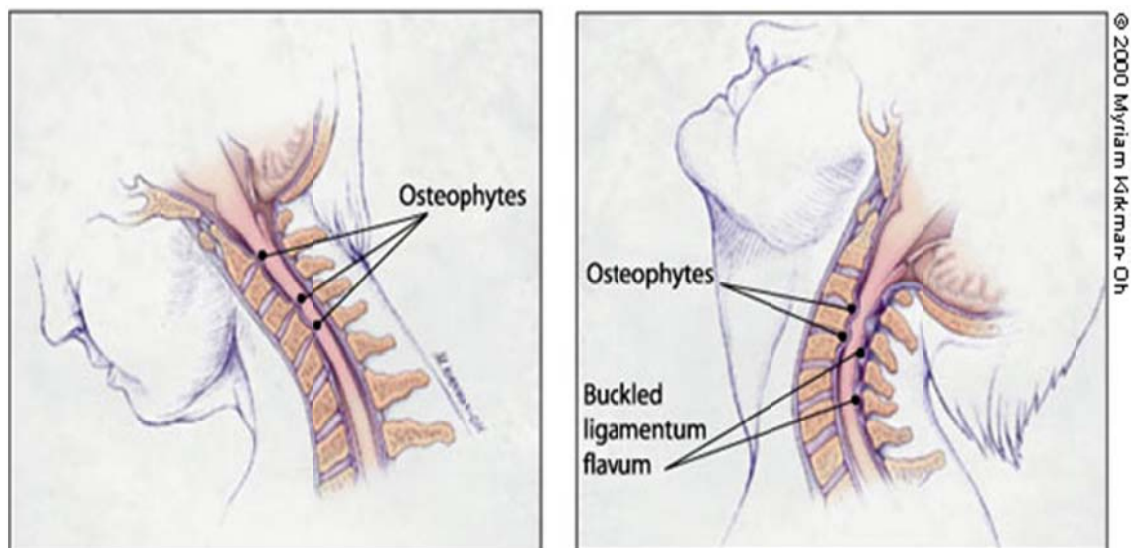


Figure 6. Dynamic mechanical factors in cervical Spondylotic Myelopathy. (Left) During flexion, lengthened spinal cord hits the anterior osteophytes; (Right) During extension, buckled ligamentum flavum decreases the available spinal canal area [27].

2.2.1 Operative Management

The primary goal of any surgical procedure is to decompress the spinal cord, thus providing more room for the neural elements. Surgical options can be broadly classified into two categories namely, anterior and posterior approaches.

2.2.1.1 Anterior Approach

Anterior cervical decompression and fusion remains the traditional approach to symptomatic disc degeneration and disc herniation, although the techniques used to achieve the arthrodesis have evolved over the years. ACDF involves the excision of disc

and bone material causing spinal cord compression and thereafter, stabilizing the spine with autograft /allograft/ or titanium mesh cages with plate fixation (Figure 7). The main advantages of this approach are the ability to directly remove the majority of compressive pathologies encountered in the cervical spine (e.g., disc herniations, ventral osteophytes, or ossification of the posterior longitudinal ligament [OPLL]), and the ability to correct and decompress the cord over kyphotic lesions. The high success rate and long term track record of ACDF in the treatment of cervical spondylosis giving rise to radiculopathy or myelopathy raises the question for the development of alternate procedures.

Although fusion has been proven to be a successful form of treatment at single level, fusion of a relatively mobile multiple segment is not an ideal reconstruction and can potentially lead to deleterious long-term iatrogenic effects [4]. Biomechanical studies have shown that spinal levels adjacent to a fusion experience increased intradiscal pressure, increased motion, high facets loads and higher shear stresses compared to normal [3,30]. Hilibrand et al. [2] reported the occurrence of adjacent segment degeneration at a rate of 2.9% per year after the initial operation, with a cumulative rate of 25% by 10 years. Further potential morbidities include the possibility of decreased cervical range of motion, pseudoarthrosis, graft donor site morbidity and instrumentation-related complications [31]. In an attempt to limit these deleterious effects associated with fusion, cervical disc replacement is an evolving technique that has been proposed as another option for the surgical treatment of degenerative spinal conditions. However, the multi-level application of the device is not yet known. To summarize, anterior based approach is considered when myelopathy is caused by anterior compression and only one or two levels are involved.

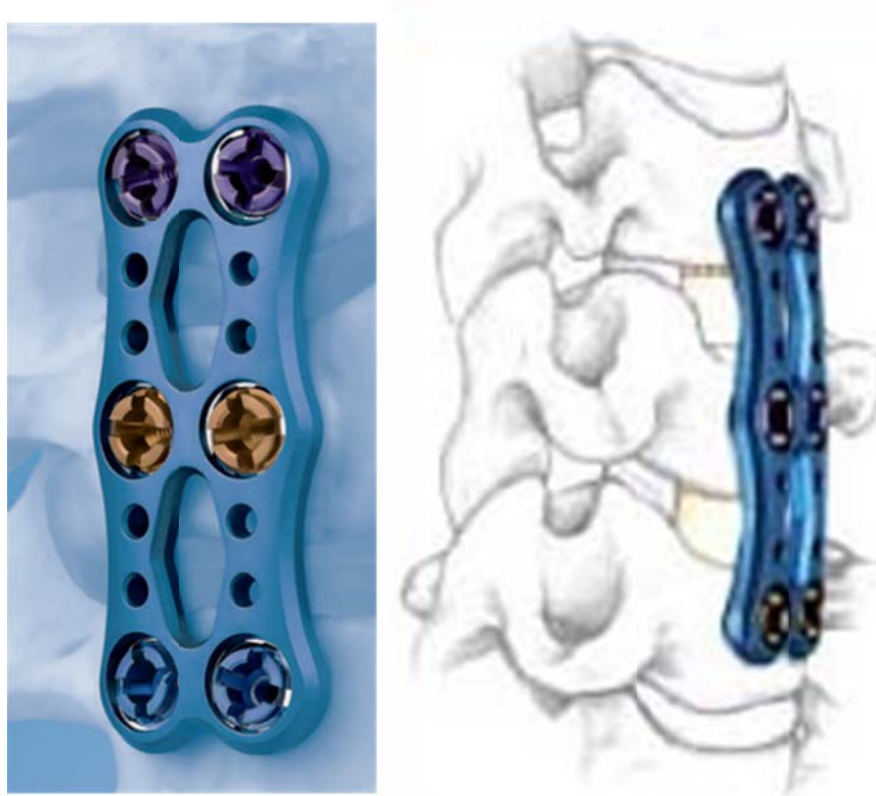


Figure 7. Anterior Cervical Decompression and Fusion; anterior plating for stabilization [32].

2.2.1.2 Posterior Approach

A posterior based approach involving laminectomy or laminoplasty is considered when multiple levels of spine have to be decompressed or when most of the cord compression results from posterior pathological conditions. Posterior surgery may not be appropriate for all myelopathic patients and it clearly has its own drawbacks. The approach involves extensive posterior muscle denervation and hence may alter the loading on the spine. Secondly, since most of the pathology compressing the spinal cord lies on the anterior side, posterior procedures decompress the spinal cord by allowing the cord to drift posteriorly. This drifting of spinal cord occurs in a lordotic or neutral cervical spine, but may not occur in a kyphotic spine. Hence, posterior decompression is

limited to the cases in which the overall sagittal alignment is favorable to cord drift-back [33].

2.2.1.2.1 Laminectomy

Cervical laminectomy is a standard procedure that has been employed for over a century to treat conditions of the cervical spine [34-36]. The earliest recorded use of laminectomy has been detailed by Sir Victor Horsley of University College London, who as early as 1887 used the posterior approach to decompress the cervical spine of a patient with progressive cervical spondylotic myelopathy [37]. By 1935, cervical laminectomies became commonplace procedures [38].

Decompressive laminectomy alleviates the pain and discomfort of nerve impingement by removing a small portion of the bone over the nerve root to provide the nerve root with increased space. The lamina arch along with the ligamentum flavum is removed to create more room for the spinal cord within the spinal canal. (Figure 8). However, the results of the procedure were universally unsuccessful with complications such as segmental instability, postoperative kyphosis, the vulnerability of the unprotected spinal cord, formation of the laminectomy membrane, perineural adhesions, and late neurologic deteriorations [5,6].

2.2.1.2.2 Laminoplasty

Because of the concerns over the complications of laminectomy, laminoplasty was developed in Japan in 1970s. It is considered an alternative to laminectomy, and is intended to relieve pressure on the spinal cord while maintaining the stabilizing effects of the posterior elements of the vertebrae. Being a motion-preservative technique, it eliminates fusion and its associated complications.

Different techniques of laminoplasty have been described which vary by where the hinge and opening of the lamina are developed. They can be broadly classified into two types namely open door (ODL) and double door laminoplasty (DDL) (Figure 9).

Open-door laminoplasty includes opening of the lamina from either left or right side with the contralateral side acting as hinge. In double door laminoplasty, the door is opened in the midline and the hinges are created bilaterally thereby resulting in symmetric opening.



Figure 8. Cervical Laminectomy of C4, C5 and C6 levels. It shows the removal of lamina and spinous process [39].

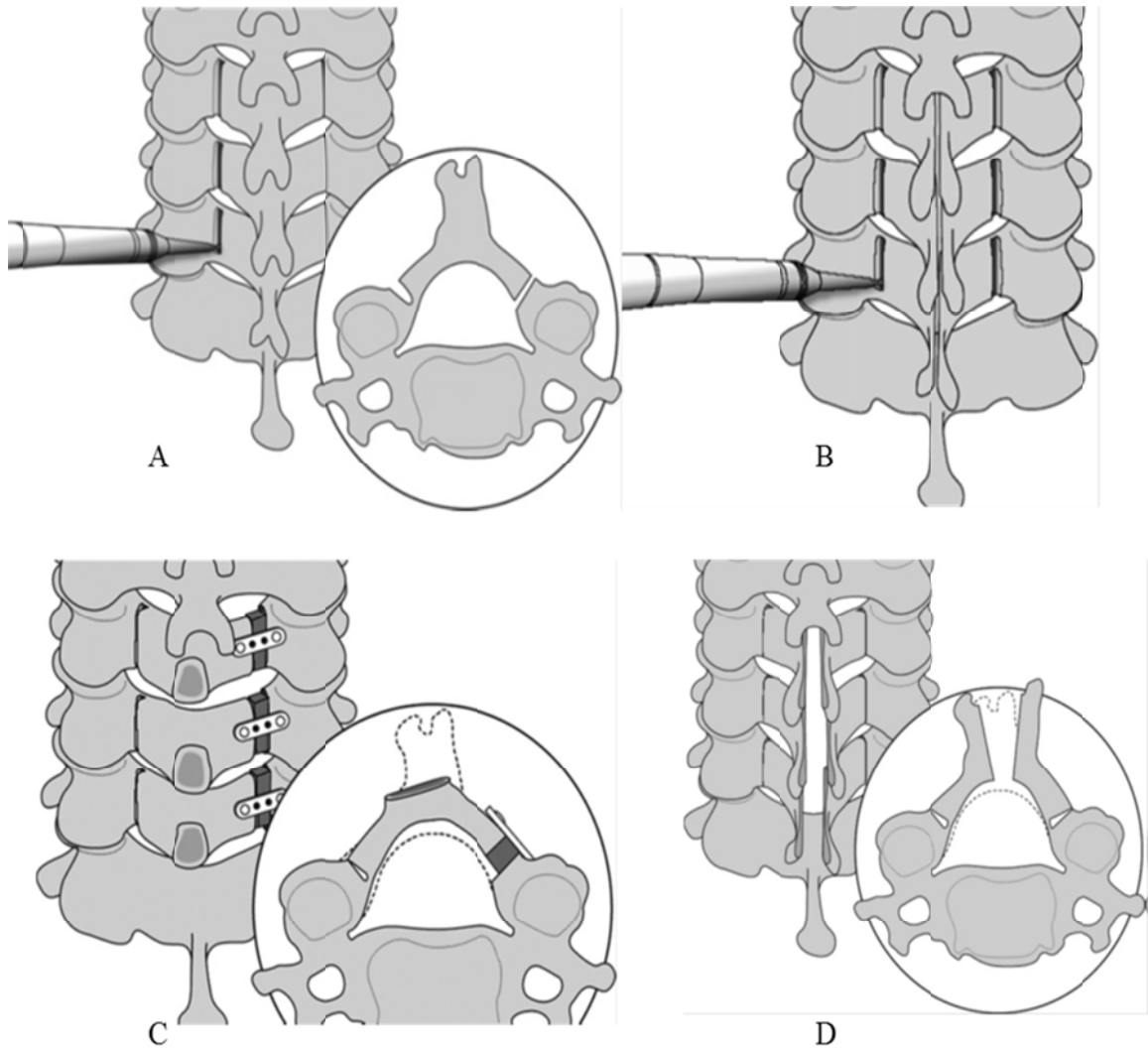


Figure 9. Types of Laminoplasty: (A) Creation of open and hinge side with the use of a high speed burr for open door laminoplasty (B) Creation of bilateral hinges for double door laminoplasty with the use of a high speed burr. Spinous process are split in the midline (C) Open door laminoplasty: Lamina stabilized with plates and screw after open door laminoplasty (D) Double door laminoplasty: Spinous process are spread in the midline and held open with either sutures or spacers [40].

Edwards et al. [41] reported significant reduction in myelopathic progression after multi-level corpectomy and laminoplasty; however, higher prevalence of complications was observed in the corpectomy group. In a recent study Koakutsu et al. [42] did not

observe any critical difference between the ACDF and laminoplasty groups with regard to the neurological recovery and cervical range of motion post 12 months; nevertheless, laminoplasty has the advantage of providing multilevel decompression simultaneously avoiding secondary myelopathy. Although the short-term results after 1 year look promising, long term results may help in demonstrating the superiority of one technique over the other. Few studies have shown contradicting results where anterior cervical decompression and fusion has best results for multi-level cervical radiculopathy compared to laminoplasty that resulted in significant reduction in motion during lateral bending and rotation. The etiology for this reduced motion may be due to the bone graft placement on the hinged side [43].

CHAPTER 3: FINITE ELEMENT MODELS OF INTACT AND SURGICALLY SIMULATED CERVICAL SPINE

Finite element analysis is an essential part of today's engineering activities. The first application of finite element was reported in 1972 by Brekelmans et al. [44]. Since then the number of applications have grown enormously. The irregular geometry of vertebral bodies, complex nature of the disc, and facet contact between the adjacent vertebrae, all make the spine a very complex structure. Hence, an enormous effort has been put in over the years to generate accurate models that provide a true representation of the spinal behavior. The earliest two-dimensional model of the vertebral column was developed by treating vertebrae as rigid masses [45]. Later three-dimensional models using simplified representations of bone geometry, with planar posterior facet joints and identically shaped vertebrae were developed [46]. Many other models used geometrical structures generated using Computer-Aided Design (CAD) packages, while most of the current models are being developed using CT image data.

The models should be capable of predicting the stress distribution in the discs and vertebrae and give very detailed motion data. Today, the finite element method is an ideal tool to assess the biomechanical efficacy of surgical treatments while supplementing the *in vitro* and clinical studies. Recent years have seen vast growth in the development of patient-specific finite element models; hence efforts are underway to develop accurate subject-specific models of spine for the proper evaluation of spine problems. Following the model development, validation is of significant importance. The validity of the finite element models depends on the model input parameters namely, geometry, material properties, boundary and loading conditions.

3.1 Modification of the Existing Intact C2-C7 Finite

Element Model

In this study, a detailed subject-specific 3D finite element model of the cervical spine (C2-T1) was used. The vertebral bodies were segmented from the CT images of the cadaveric spine while the MR images provided the approximate boundaries of the intervertebral disc. The model includes clearly defined annulus and nucleus regions, five major spinal ligaments namely anterior longitudinal ligament, posterior longitudinal ligament, ligamentum flavum, interspinous and capsular ligaments. Additionally, the facet gap was modeled using the tabular pressure-overclosure relationship in ABAQUS finite element software (Simulia, Providence, RI). Validation of the model is essential but extremely difficult due to the varying material properties along the length of the specimen. One of the best available methods for validation is to compare it with the experimental data under similar loading and boundary conditions. In this study, we extended our previously reported validated C2-C7 model [47,48] of the human cervical spine and presented a modified finite element model that provides more robust predictions of kinematic data after surgical simulations.

3.1.1 Addition of T1 to C2-C7 model

Although, the initial C2-C7 model was capable of predicting the spinal behavior correctly, in order to eliminate the boundary effects on the adjacent unaltered level (C7), T1 was added to the model. The external contours of T1 of the same specimen were segmented from CT slices using the Brains2, multipurpose image-processing software [49]. Thereafter the regions of interest were converted into a triangulated surface as explained elsewhere by DeVries et al. [50]. The resultant surface was meshed with hexahedral elements using multi-block meshing technique (IA-FEMesh). The meshing technique used is similar to the one described by Kallemeyn et al. [51]. The vertebral body was divided into cortical and cancellous regions and a Young's modulus of 10GPa

and 450MPa was assigned respectively. All 5 major spinal ligaments (PLL, ALL, LF, ISL, CL) from C2-C7 were extended to the C7-T1 level and were defined as 3D Truss elements acting in tension only using the hypoelastic material definition in ABAQUS. A finite-sliding surface interaction was used to model the facet joints with a tabular pressure-overclosure relationship used to simulate the cartilage layers. The interaction works towards increasing the contact pressure with the narrowing initial gap distance between the facet surfaces. The intervertebral disc was divided into the annular and nucleus regions and was modeled with hybrid linear hexahedral elements. The annulus region of the disc which included ground substance and fibers was modeled with hexahedral and rebar elements respectively. The annular grounds were further divided into anterior, lateral, and posterior regions for better control of the material properties in these regions as represented in Figure 10. The annular fibers were oriented at approximately $\pm 25^\circ$ from the transverse plane and were assigned a nonlinear hypoelastic material definition based on experimental collagen fiber studies [52]. The nucleus was represented by 3-dimensional fluid elements. The intact C2-T1 model consisted of 177,070 nodes and 167,702 elements.

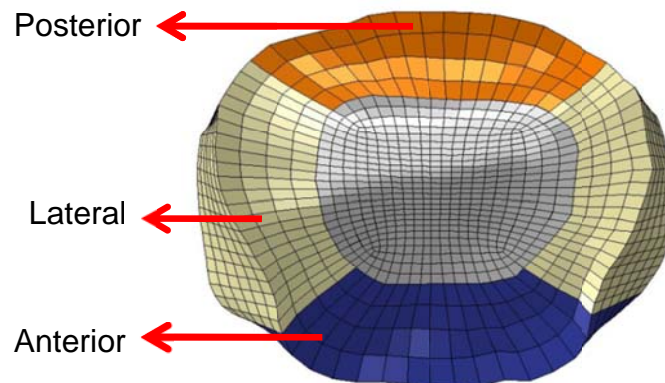


Figure 10. Intervertebral disc showing the annulus and nucleus. Annulus was further divided into anterior, lateral and posterior regions.

3.1.2 Updating the Model to 2Nm

As mentioned earlier, the original C2-C7 model was validated with the specimen-specific experimental data in all the three loading modes at 1Nm. However, when analyzing cervical spinal instrumentation, it is necessary to test the models at higher moments to induce measurable differences in motion response. Hence, the model was run under a physiologic non-destructive moment of 2Nm.

The intervertebral disc is the major component of the entire model that deserves precise modeling due to its complex nature and has a significant effect on major rotations. The grounds substance of the annulus was initially modeled as linearly elastic. But with the original material properties, the model did not converge at higher moments and as a result, changes were made to the material definition. In order to account for the large motion resulting from higher moments, the material properties of the grounds were changed from linearly elastic to hyperelastic definition. Hyperelastic materials are described in terms of a “strain energy potential, which defines the strain energy stored in the material per unit of reference volume as a function of the strain at that point in the material. Material models predicting large-scale material deflection and deformations can be broadly classified into two types a) Incompressible (Mooney-Rivlin, Yeoh, neo-Hookean, Ogden etc.) b) Compressible (Blatz-Ko, Hyperfoam). The posterior annulus may experience strains of up to 50% when in full flexion [53]. Such large strains require nonlinear analysis in the finite element solution. Moreover, the collagenous fibers in the disc have nonlinear behavior with the stiffness changing with increasing strain [54]. Therefore, we used the Mooney–Rivlin formulation, to allow computation of large displacements and strains.

The hyperelastic definition of the annulus grounds was modeled using the isotropic, incompressible, hyper-elastic Mooney–Rivlin (c1, c2) formulation as described below [55].

$$W = c_1 (I_1 - 3) + c_2 (I_2 - 3) + 1/d (J - 1)^2, \text{ where}$$

c_1, c_2 : Material constants characterizing the deviatoric deformation of the material

I_1, I_2 : First/second invariants of the deviatoric strain tensor

$d = 2/K$ material incompressibility parameter,

$J = V/V_0$ local volume ratio and

$K =$ initial bulk modulus of the material.

The initial shear modulus is given by (ABAQUS Documentation)

$$G = 2(c_1 + c_2)$$

Hence, the relationship between Young's modulus 'E' and material constants c_1 and c_2 , for the annulus ground substance can be approximately written as:

$$E \approx 6 (c_1 + c_2) \text{ with } c_2 \approx 0.25c_1.$$

The input parameters for ABAQUS are c_1 and c_2 . Initial baseline properties were taken from literature and subsequently calibration was performed to validate the motion response with the experimental data. The final values of Young's modulus at all the levels for all three regions of the intervertebral disc are provided in Table 1. Figure 11 shows the intact C2-T1 finite element model.

Table 1. Young's Modulus of Annulus fibrosus for different levels

Segment	Anterior (MPa)	Posterior (MPa)	Lateral (MPa)
C2-C3	4.2	2.25	3.5
C3-C4	2.25	2.25	1
C4-C5	1.5	1.5	1
C5-C6	1.5	1	1
C6-C7	1.5	1	2.25
C7-T1	6	6	2.25

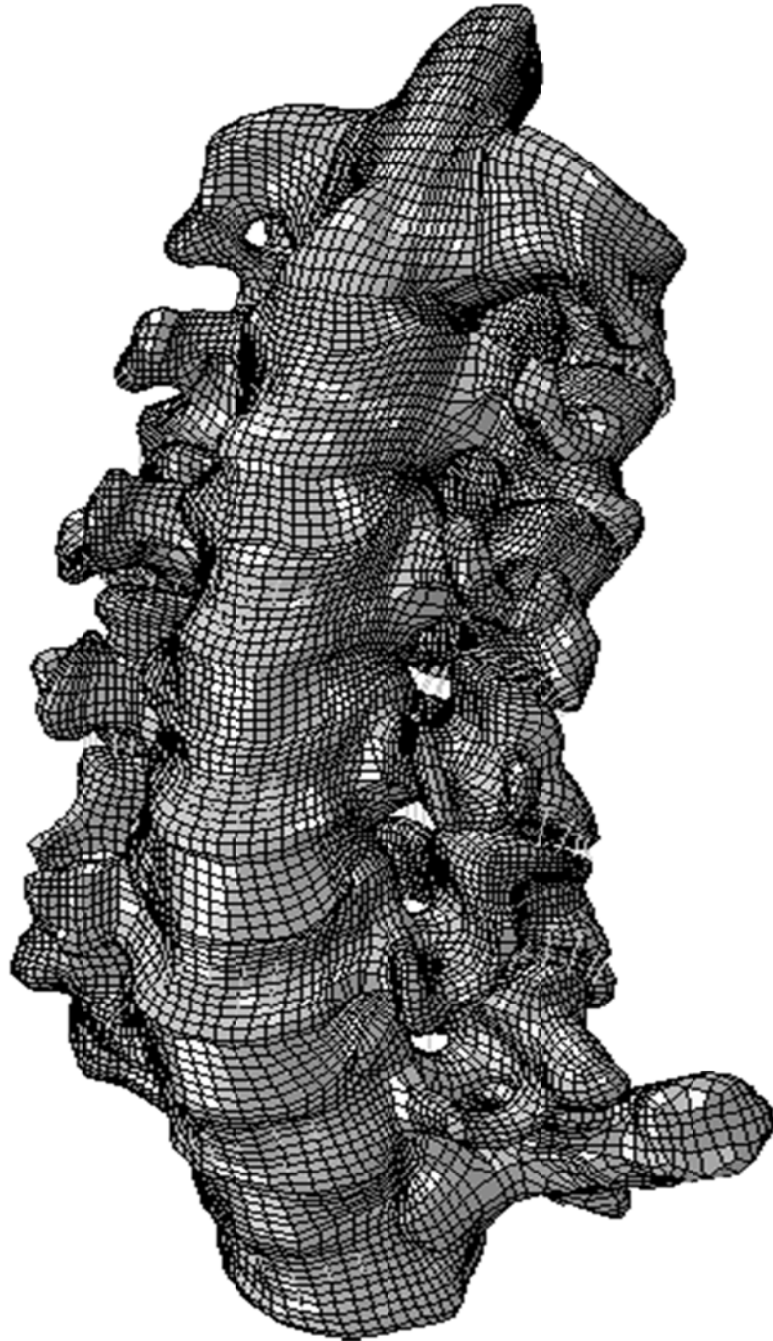


Figure 11. C2-T1 Intact finite element model of cervical spine.

3.1.2.1 Boundary and Loading Conditions

The intact model was tested under physiologic flexion/extension (\pm MX), right/left lateral bending (\pm MZ), and right/left axial rotation (\pm MY) modes. The inferior nodes of T1 vertebra were fixed in all directions and a pure moment of 2Nm was applied on superior surface of C2. The analysis was performed using the finite element software ABAQUS 6.9.

3.1.2.2 Flexibility Testing

The goal of the flexibility tests was to obtain three-dimensional physical properties of the spine under pure moments and measuring the intervertebral rotations. The main advantage of the flexibility test is that it captures the natural behavior of the spinal column by allowing complete freedom of movements. The tests also serve as a standardized comparison of biomechanical results among various researchers by measuring the capability of the spinal device to provide multi-direction stability under physiological loading conditions [56].

3.1.2.3 Validation of the Intact Finite Element Model

In addition to the geometric and material complexities, validation of the finite element model is itself a challenge. Validation of a finite element model is crucial to correctly predict the biomechanical responses of spine to complex loading conditions. Most of the reported validation studies have been undertaken by comparing it with multi-specimen experimental data. Any number of permutations of material properties in a finite element model would lead to the same overall stiffness, and hence emphasis should be placed on comparing as many parameters as possible. Since, a complete validation of a model is not possible due to the limitations involved in the physical measurement of all parameters, it must be viewed more as a representation of an *in vitro* model rather an absolute proof. Hence, there is a need to represent this *in vitro* environment more closely to the *in vivo* conditions.

The updated intact model was validated against subject-specific experimental and literature data. Most of the existing models in literature have been validated via only end points responses to applied moments [57-59]. Since the spine exhibits a complex nonlinear behavior due to the nature of the soft tissues involved, it is essential to look at the entire loading curve rather than just the end points.

The model validation was divided into two parts. We first compared the C2-C7 motion data of C2-T1 model with the subject specific experimental data in flexion/extension, right/left lateral bending, and right/left axial rotation for a moment of 1Nm. The model was validated along the entire length of the loading curve rather than just the end points. The final calibrated model followed the experimental data extremely well during flexion/extension as shown in Figure 12. The red curves represent the loading and unloading curves for the experimental data while the blue triangular dots denote the finite element predictions for the C2-C7 motion in a C2-T1 model.

During lateral bending, the finite element model predicted an approximately 14% lag in left and right lateral bending at the end points (Figure 13). The major difference between the experimental and finite element prediction occurred at the C3-C4 level. Although, the exact reason is not known, the unusually large amount of motion at this particular level during experimental testing may be due to the pathological changes at intervertebral disc and facet joints.

There was a good agreement between the finite element predictions and experimental data during left/right axial rotation (Figure 14). The nonlinear behavior exhibited by the spine during the flexibility tests was well captured by the model.

Because of the limited motion data pertaining to C2-T1 motion segments, we could compare the C2-T1 model data with the literature data in flexion/extension only. Figure 15 shows the comparison of the segmental motion at C7-T1 with the literature data in flexion/extension [60].

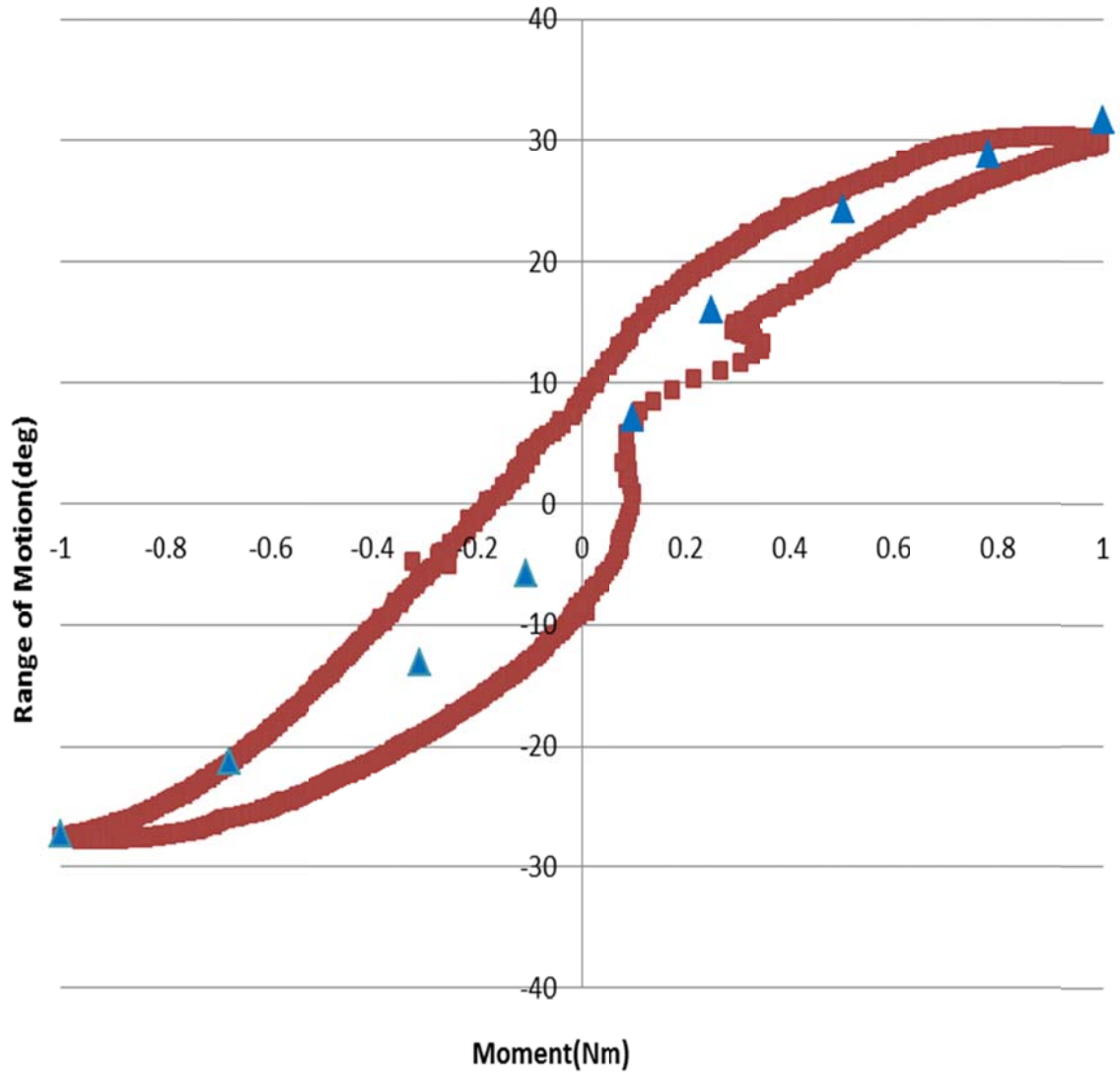


Figure 12. C2-C7 Model Validation in Flexion/Extension. Experimental data is represented red in color and blue triangular dots denote the finite element predictions.

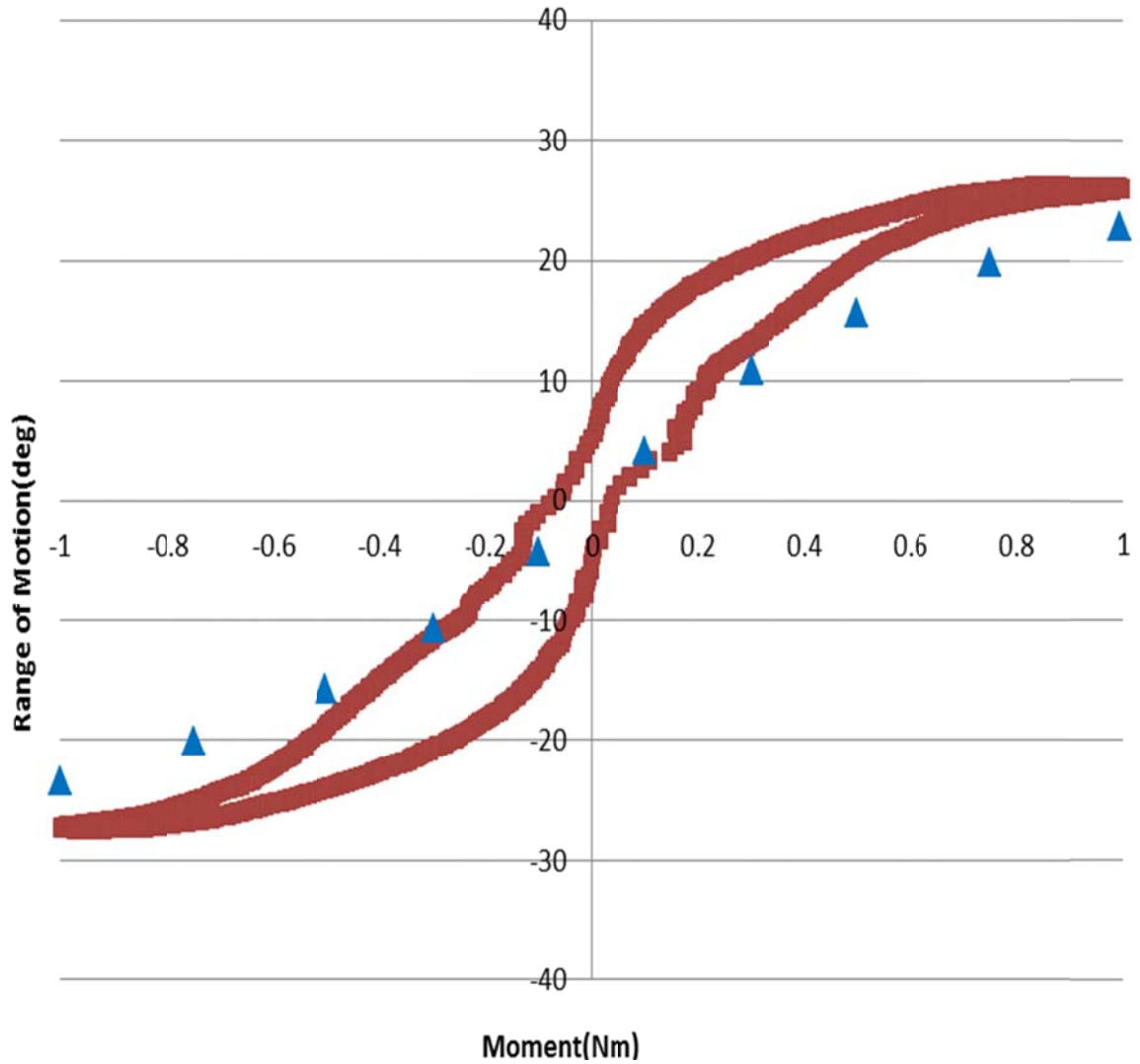


Figure 13. C2-C7 Model Validation in Right/Left Lateral Bending. Experimental data is represented red in color and blue triangular dots denote the finite element predictions.

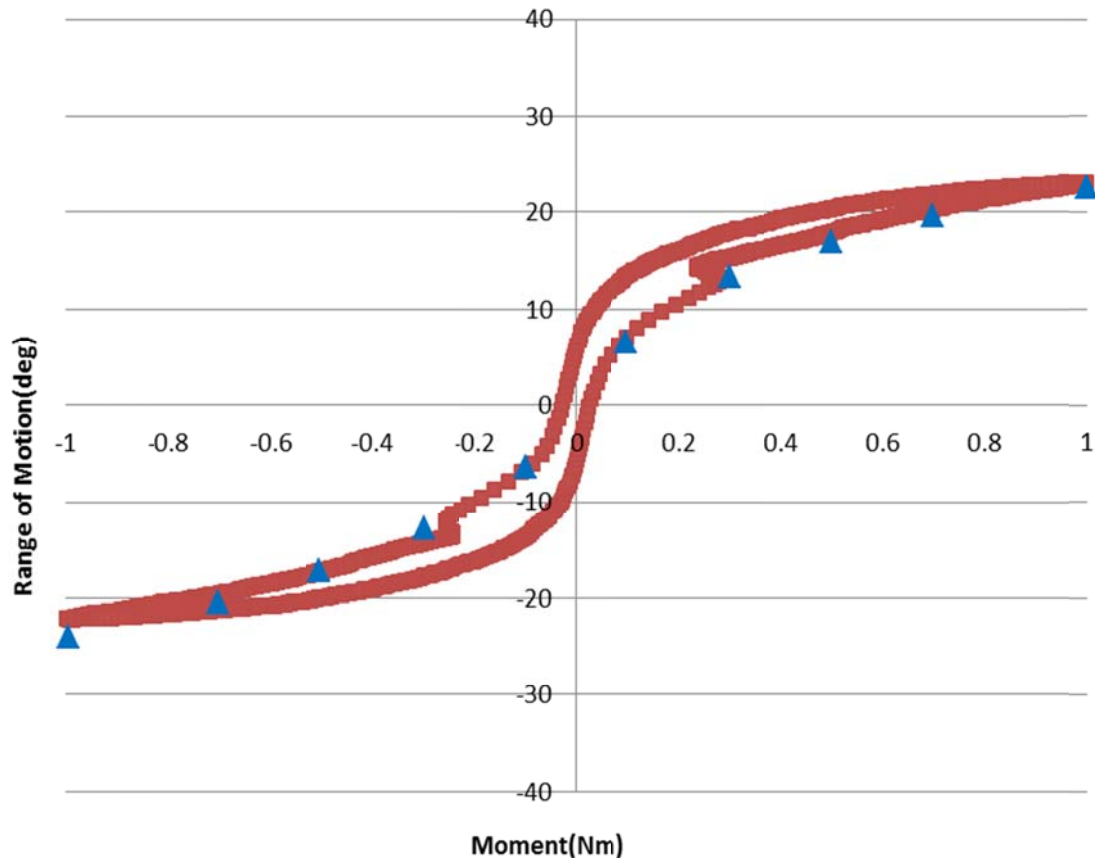


Figure 14. C2-C7 Model Validation in Left/Right Axial Rotation. Experimental data is represented red in color and blue triangular dots denote the finite element predictions.

3.1.2.4 Results

The results from the intact finite element model include range of motion, intervertebral disc and cortical body stresses in all the six loading modes. Figure 16 shows the range of motion data for all the loading modes. The model resulted in asymmetric flexion/extension data with a flexion of 48.8° and an extension of 44.3° . Lateral bending was symmetric and was approximately 34° , whereas axial rotation was around 35° . Wheeldon et al. [60] tested seven relatively young normal human cadaveric cervical spine specimens (C2-T1) under a moment of 2Nm in flexion/extension only. These experimental results correspond well with our finite element predictions.

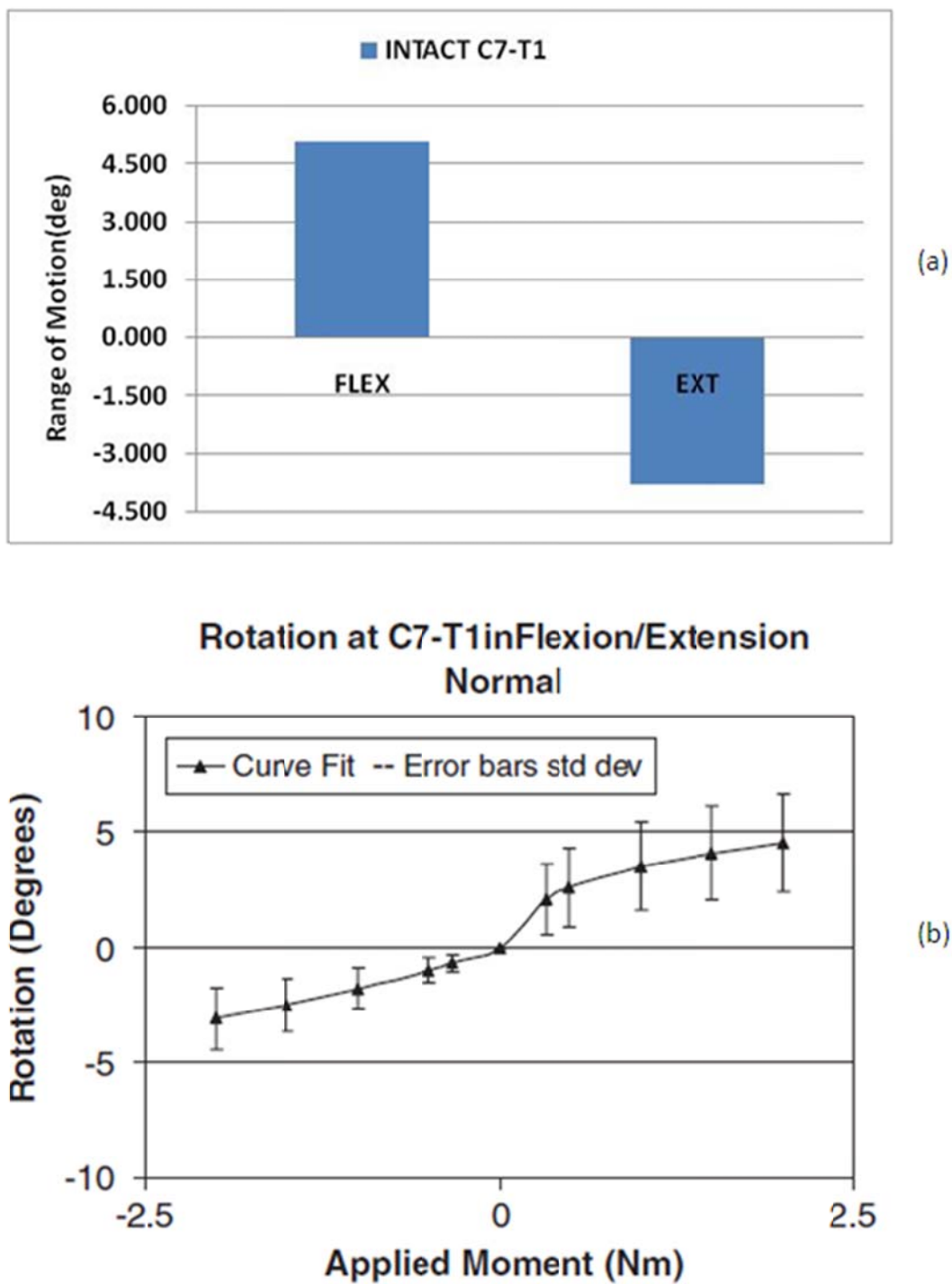
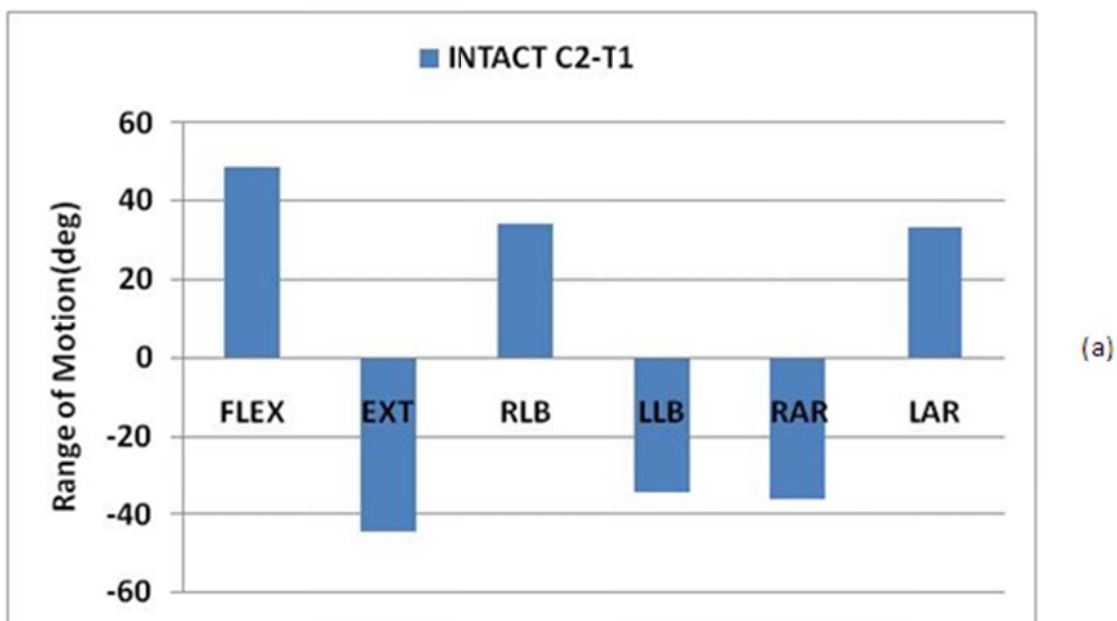
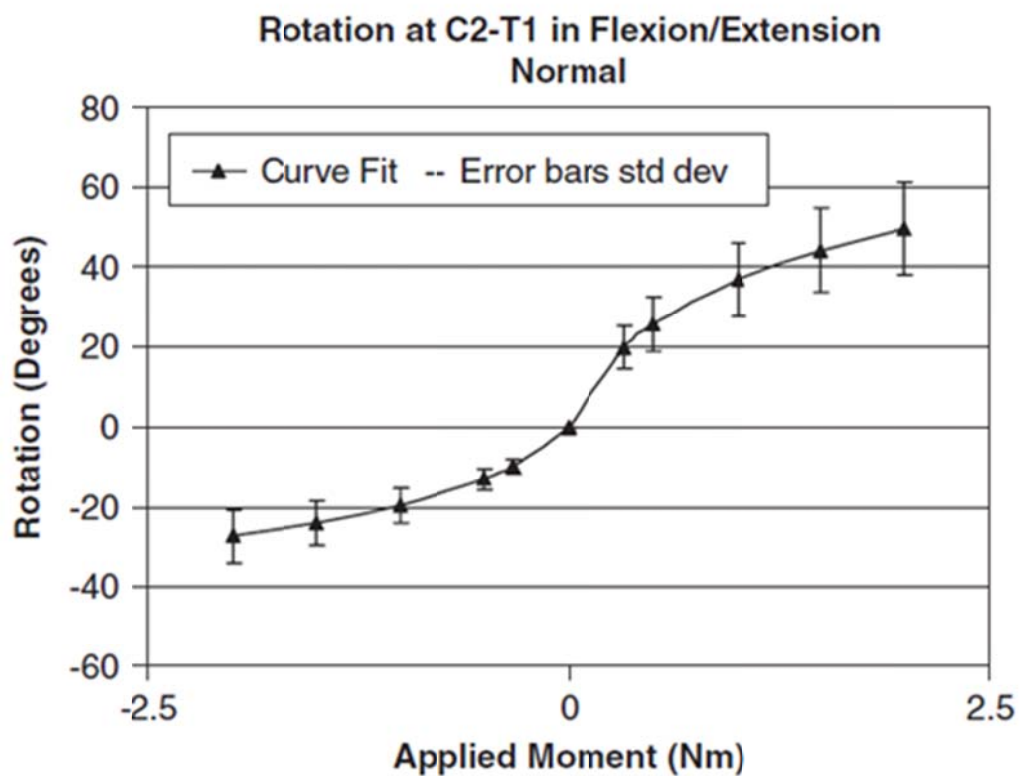


Figure 15. C7-T1 Range of motion obtained from (A) Finite element model (B) Experimental study in flexion/extension [60].



(a)



(b)

Figure 16. C2-T1 Range of motion obtained from (A) Finite element model (B) Experimental study in flexion/extension [60].

3.2 Laminectomy in the Cervical Spine

Absolute stenosis of the spine, defined by a canal measuring less than 10mm in anterior/posterior dimension, develop radicular or myelopathic complaints [61]. Posterior approaches for decompression of spinal cord were reported between the sixteenth and eighteenth centuries, and laminectomy for intraspinal tumors was first performed in the nineteenth century. One of the primary indications for cervical laminectomy is the cervical spinal stenosis with preserved lordotic curvature. The technique involves creation of laminectomy margins at the junction of lamina and lateral mass and then removing the lamina en bloc by detaching the interspinous ligament and ligamentum flavum (Figure 17). Advantages of laminectomy include the familiarity of the procedure, ability to decompress multiple neural foramina, and fusion is an option rather than a necessity, an attribute that helps in preservation of motion. And, the disadvantages include the tendency to produce segmental instability, postoperative kyphotic deformity and late neurologic deterioration in certain patients.

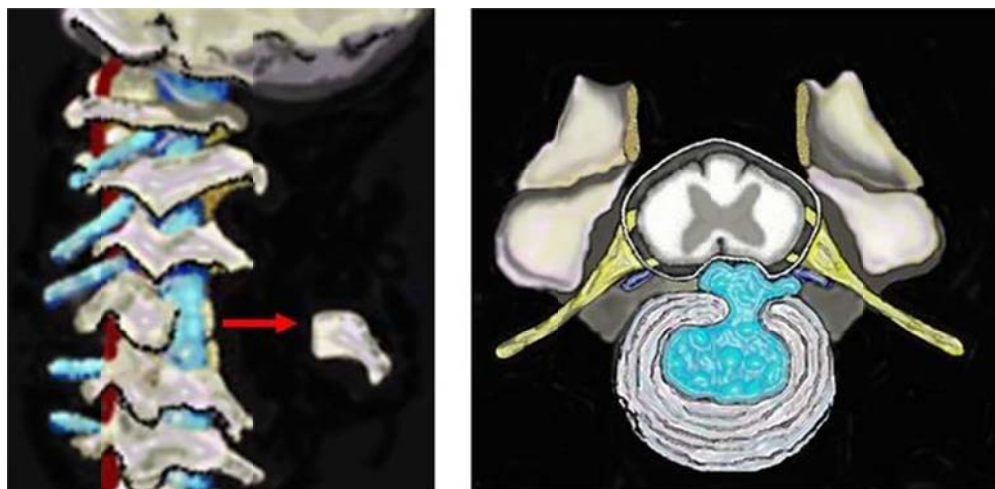


Figure 17. Cervical decompressive laminectomy [62].

3.2.1 Background and Literature Review

Post laminectomy kyphosis of the cervical spine has been associated with worsening myelopathy, debilitating postural deformity, and intractable pain. In a study done by Kaptain et al. [63], kyphosis was observed in 21% of patients who have undergone laminectomy for CSM with the progression of deformity twice as likely if preoperative radiological studies demonstrate a straight spine. Interestingly, the authors did not observe any correlation between postoperative kyphosis and functional outcome. Spontaneous dislocation or subluxation of cervical vertebrae can occur as a result of extensive laminectomy involving facet resection. The vertebral displacement may thereby result in progressive swan-neck deformity. This is more prominent in younger individuals due to the greater elasticity and laxity of cervical ligaments compared to old people. One of the other disadvantages with complete laminectomy is the vulnerability of the unprotected spinal cord and the instability of the spine due to the loss of posterior structures [64]. Baisden et al. [5] used a goat model to show the significant increase in the cervical kyphosis and sagittal plane slack motion at 6 months post laminectomy while no significant differences were observed with laminoplasty when compared to the intact groups. Hence, radiographic studies should be undertaken beforehand to determine if patients have sufficient lordosis to undergo laminectomy.

Posterior stabilization technique involving facet fusion may prevent or treat instability. This could be achieved by using either lateral mass plates or pedicle screw fixation [65]. Heller et al. [66] did an independent matched cohort analysis between patients treated with laminoplasty and laminectomy with fusion. Laminoplasty group reported significant improvement in strength, dexterity, gait, pain with no major complications; while laminectomy with fusion resulted in complications such as progression of kyphosis and myelopathy, nonunion and instrumentation failure. In another comparative study between ACDF, laminectomy and laminoplasty; laminectomy

resulted in the least favorable clinical results especially in people with bilateral radiculopathy [43].

To date, most of the *in vitro* and clinical studies are limited to the global biomechanical outcome of the surgical procedure. However, in order to obtain a better idea about the long term results, there is a need to look at the internal responses of the spine. This can be best obtained from the mathematical models that are thoroughly validated for their accuracy and have the capability to predict the biomechanical behavior of the human spine in response to the surgical procedures.

3.2.2 Simulation of Laminectomy in a Finite Element

Model

The intact C2-T1 finite element model was modified to simulate the surgical procedure of laminectomy at levels C3-C6. The spinous process and lamina on both the sides of the vertebra were resected, while the facet joints were kept intact. Figure 18 shows a laminectomy of the C5 vertebra. The procedure was repeated at levels C3, C4 and C6.

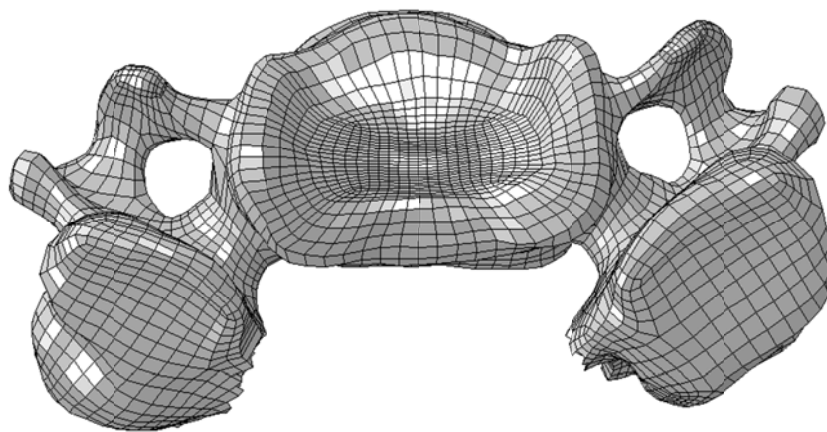


Figure 18. Laminectomy of C5 vertebra.

Additionally, the associated ligaments (interspinous ligaments, ligamentum flavum) were removed. The final laminectomy model was comprised of 165,865 nodes and 158,957 elements Figure 19 shows the final C2-T1 model with Laminectomy performed at levels C3-C6.

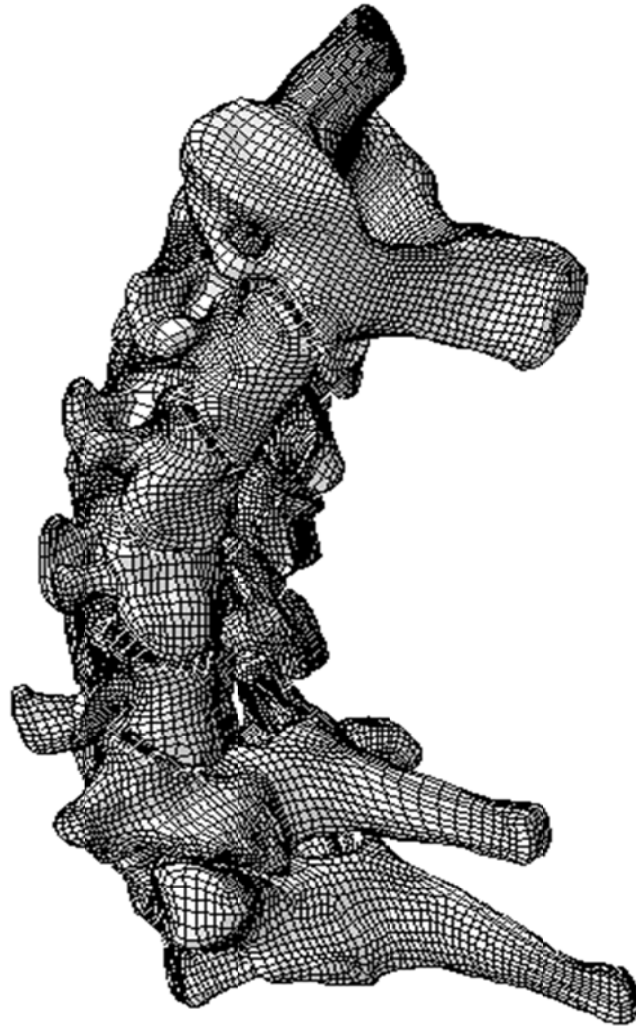


Figure 19. C2-T1 model with laminectomy at C3-C6.

3.3 Open Door Laminoplasty in the Cervical Spine

3.3.1 Background and Literature Review

Until the 1970s, laminectomy has been the sole therapeutic option for posterior decompression of the spinal cord. However, the complications associated with wide laminectomy of the cervical spine led to the development of alternate posterior surgical procedures [67]. The open door laminoplasty procedure involves “hinging” one side of the lamina and cutting the other side to form a door. The side of the canal to be opened is chosen for a number of reasons. If subsequent foraminotomies are planned, the open side should be ipsilateral to them; in case of asymmetric myelopathy, the surgeon chooses to open the more involved side and finally the choice may also be influenced by the surgeon’s dominant hand [68]. A trough is prepared initially to remove all three layers of bone (dorsal cortex, followed by the cancellous layer and then the ventral cortex) along the junction of the lamina and the lateral mass. A hinge of approximately 3-4mm is created along the contralateral junction of the lamina and lateral mass by removing the dorsal cortex and the unicortical layer. The laminar hinge should yield slightly with a reasonable bending force.

The number of lamina to be opened to fully release the spinal cord has always been a question, C3-C7 or C3-C6. In anatomical terms, Pal and Routal [69] demonstrated the significance of C7 in maintaining the stability of the cervical spine. Hosono et al. [70] compared the clinical outcomes of patients with C3-C6 and C3-C7 laminoplasty. The results favored C3-C6 laminoplasty in terms of postoperative axial neck pain, operating period, and length of the operative wound.

Restenosis owing to postoperative closure of the lamina in laminoplasty is a well-known complication. To decrease the incidence of this complication, several modifications to Hirabayashi’s original methods have been proposed including the use of anchor screws adjacent to facet joint on the hinge side and the use of bone graft spacers

and titanium plates bridging the lamina and the facet joints in the open side (Figure 20). Few studies have shown the successful maintenance of increased sagittal diameter for cervical laminoplasty using small suture anchors [71,72]. However, Matsumoto et al. [73] reported laminar closure in 34% of patients with the only significant factor being the presence of preoperative cervical kyphosis. Hence, additional procedures involving the use of laminar spacers and plates to prevent laminar closure may be necessary in patients with cervical kyphosis.

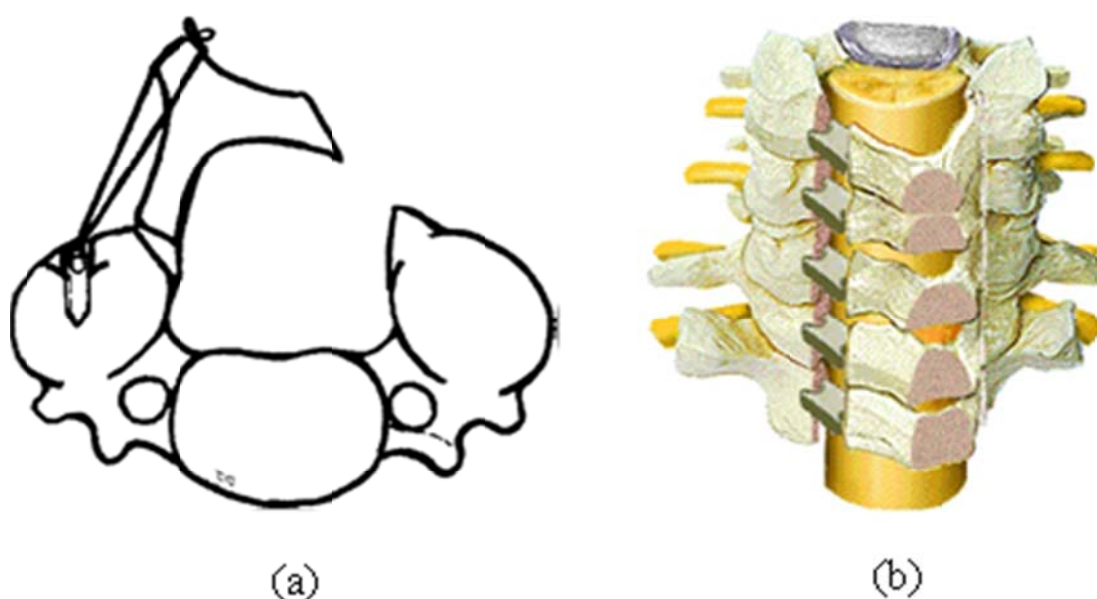


Figure 20. Open door Laminoplasty stabilized by (A) Anchor system [71] (B) Spacer [74].

Moreover, dissatisfaction with the results of multilevel corpectomies and laminectomies for multilevel cervical spinal stenosis led to the development of laminoplasty techniques. Studies that compared the clinical outcomes of patients treated with corpectomy versus laminoplasty, and patients treated with laminectomy and fusion versus laminoplasty proved laminoplasty to be a better outcome in terms of lesser

complications and functional improvement in strength, dexterity, sensation, pain and gait [41,66].

Achieving and maintaining an increased sagittal diameter after open-door cervical laminoplasty is probably one of the most important changes in anatomic parameters to facilitate neurological recovery. O'Brien et al. [75] reported 105% and 88.9% increase in the anterior posterior and sagittal canal diameter respectively after open-door laminoplasty with titanium plates. The worsening of cervical alignment was observed in approximately 35% and the development of kyphosis in 10% of patients who went for long term follow-up post laminoplasty. This development of kyphosis or loss of cervical alignment can be related to the extent to which the facet joint is disrupted and preoperative curvature of the spine [76].

Several clinical studies have been performed to determine the cervical range of motion post laminoplasty. A two-year follow up study showed the gradual decrease in the range of motion during flexion/extension by 31.66%, but the rate of reduction slowed with time. Interestingly, no correlation was found between the postoperative axial pain and decreasing cervical range of motion. However, a positive correlation was observed with extension motion. Though the exact cause of this decreased range of motion remains unclear, spontaneous laminar fusion, degeneration of adjacent segments, posterior muscle condition could contribute to it [77,78]. A decrease in range of motion due to fusion at the hinge side may stabilize the spine and maintain favorable long-term results, while it may sometimes become a source of axial complaints. However, it is important to notice that most of the literature pertains to patients undergoing decompression for ossification of posterior longitudinal ligament which itself relates to increased rigidity, and thus may overestimate the restricted range of motion linked to laminoplasty procedure [79]. Contradicting to these clinical results, several *in vitro* studies have shown preservation of range of motion in all directions after multi-level laminoplasty [13,14].

The use of titanium miniplates for maintaining the lamina in the open position arose from the complications with other techniques of stabilization like sutures and bone blocks. The use of miniplates from cranial fixation systems for cervical laminoplasties was first described by Frank et al. [80] and later O'Brien et al. [75] quantified the increased the spinal canal area using this technique. Deutsh et al. [81] performed open door laminoplasty using a new Titanium Mesh LP miniplate and screw system with a claw positioned on the trapdoor lamina and a flat plate on the lateral mass (Figure 21). No intraoperative and postoperative complications were observed. A retrospective study performed on 104 patients with instrumented ODL proved the technique to be a safe and reliable method for preventing progression of myelopathy with multilevel involvement. There was no sign of fatigue failure or loosening of plates in this large series of patients, thereby avoiding the revision for fixation failure which could have led to the closure of lamina [82]. Shaffrey et al. [83] performed a modified open door laminoplasty with allograft bone and titanium miniplates and reported good short-term results in terms of neurological outcome in younger patients with congenital and spinal stenosis. Hence, with the increasing laminoplasty market, there is a need to evaluate the effect of these implants on the biomechanical stability of the spine.

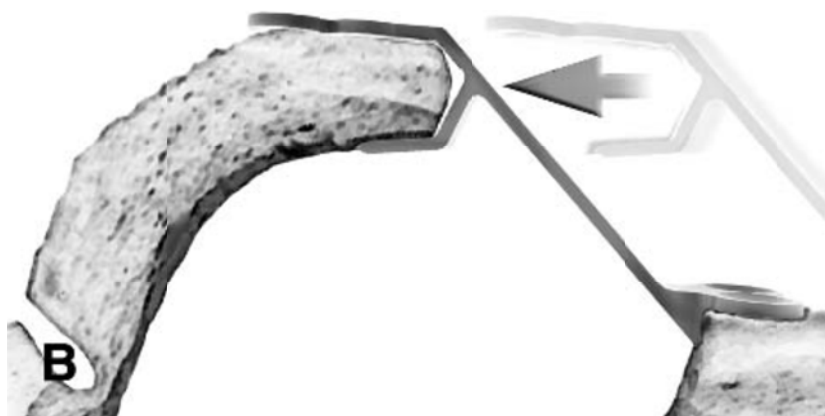


Figure 21. Axial CT image of plate in situ [68].

3.3.2 Simulation of ODL at Levels C3-C6

The intact mesh (C2-T1) was modified to simulate a multi-level open door laminoplasty procedure. As an example, the procedure is explained clearly for the C5 vertebra below.

- A bicortical cut was simulated along the junction of the lamina and the lateral mass of the intact vertebral mesh by completely removing a layer of elements. Care was taken to preserve the facet surfaces.
- On the contralateral side, a hinge of approximately 3-4mm was created along the junction of the lamina and lateral mass by removing elements representing the unicortical layer. The hinge was further smoothed with a cylinder using in-house code (C++) to simulate the shape of a burr. Care should be taken to prevent two things: Creation of the hinge too laterally or medially and removal of excessive bone. Figure 22 shows the vertebra with the hinge and open side of the lamina.
- The choice of ligament resection for laminar opening varies with the surgeon and the technique. The spinous processes of the involved vertebrae (C3-C6) along with the interspinous ligaments were excised. Additionally, the ligamentum flavum at the adjacent levels (C2-C3 and C6-C7) was partially cut on the open side of the lamina to allow for the laminar opening.
- The lamina of each vertebra, C3-C6, was opened towards the hinge by applying a uniform load until a laminar opening space (LOS) of 10mm was obtained as illustrated in Figure 23. Our previous studies on single level laminoplasty have shown an increase of 56% in spinal canal area and 35% increase in the sagittal canal diameter at level C5 [11]. During the surgical procedure, as the door is opened, stresses build in and around the hinge region. Consequently, the stresses at the centroid of each element were recorded to be used as initial conditions.

These stresses tend to close the lamina and must be resisted by some stabilization technique.

- Two screw holes in the lateral mass and one hole in the lamina were created based on the desired plate position (Figure 24). Care was taken to angle the screws away from the facet joints.

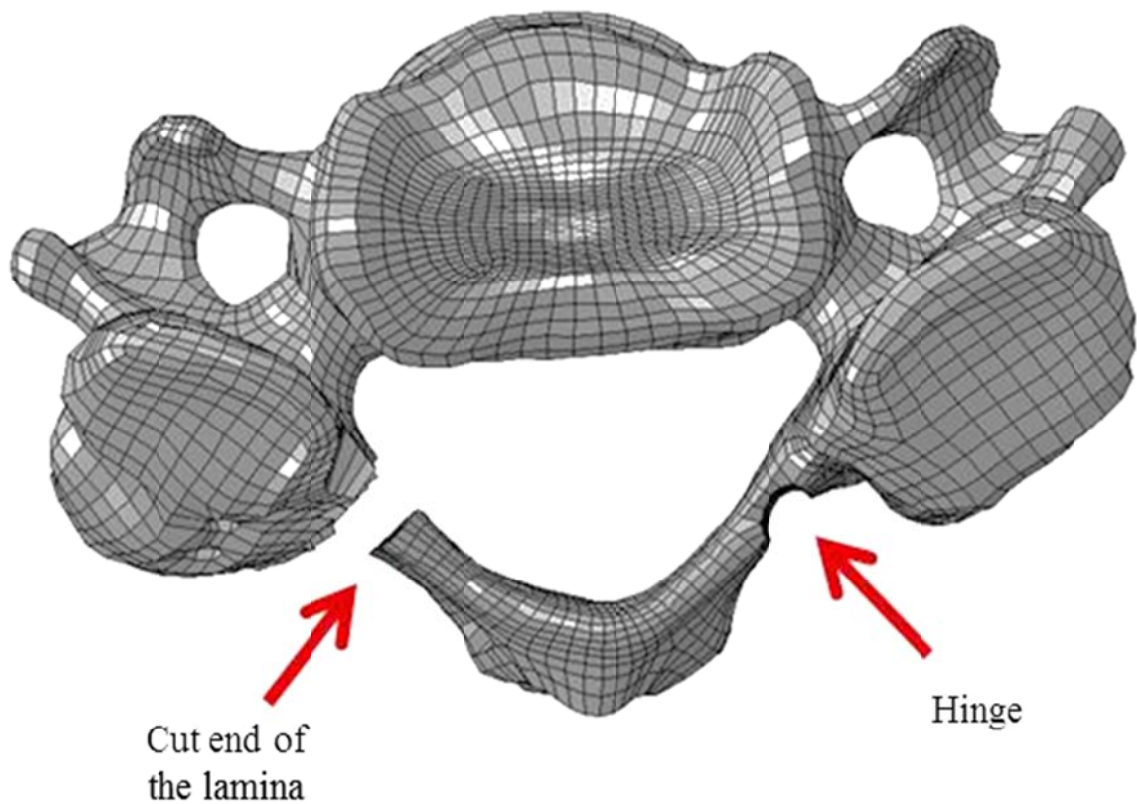


Figure 22. Superior view of a vertebra showing the hinge and cut end of the lamina.

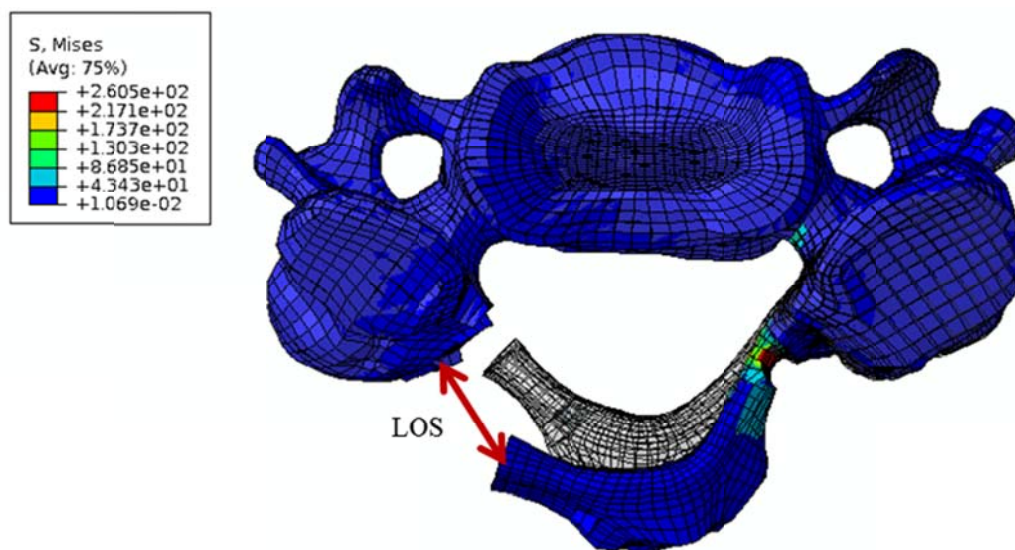


Figure 23. Superior view of C5 vertebrae showing laminar opening.

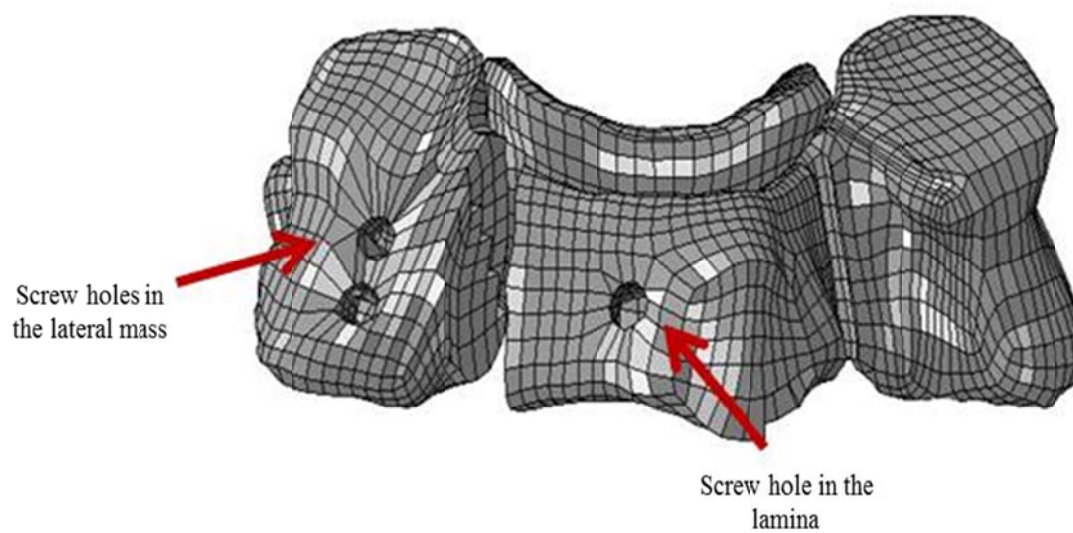


Figure 24. C5 vertebra showing holes in lateral mass and lamina.

- As these stresses tend to close the lamina, different techniques have been used to stabilize the lamina in the open position. In this study, we employed a stable plate and screw system. CAD models (Pro/ENGINEER; Parametric Technology Corporation, Needham, MA) of the plates and screws were generated from the physical dimensions. (Figure 25).

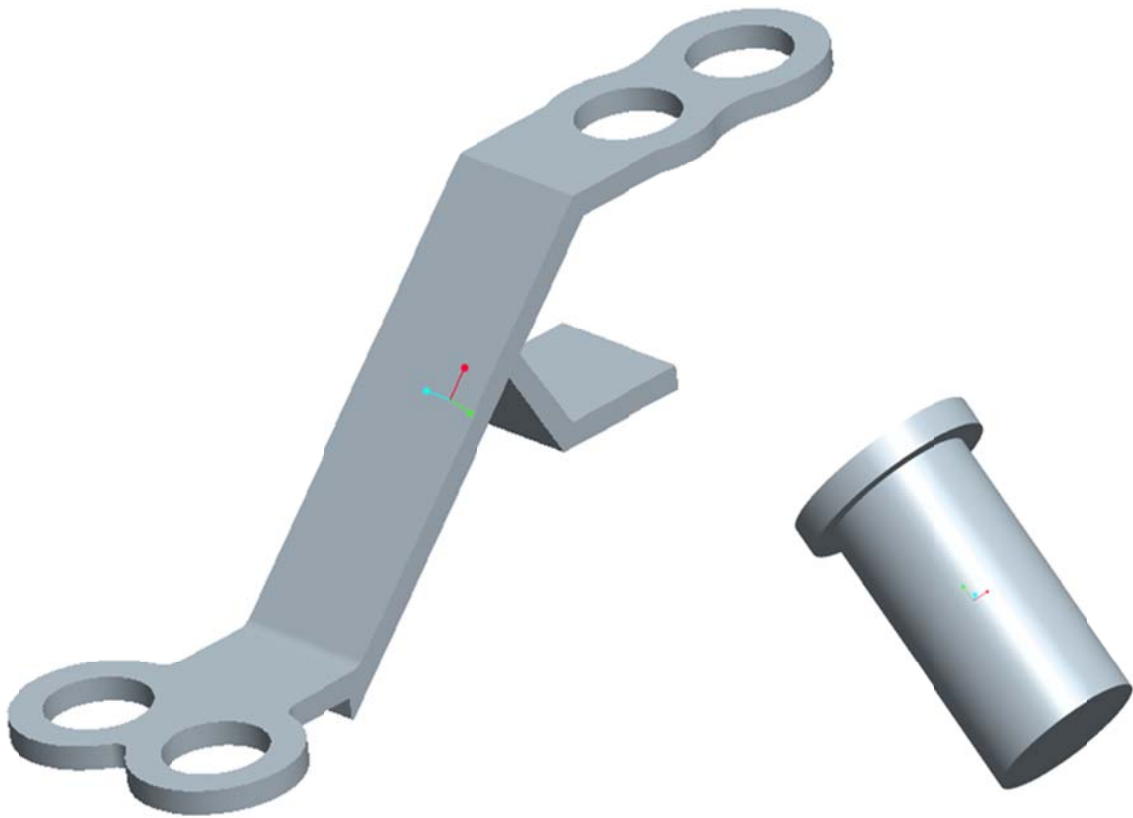


Figure 25. ProE Model of the laminoplasty plate and screw.

- Figure 26 shows the plate and screw meshed with hexahedral elements using IA-FEMesh [84]. Each component was assigned an elastic modulus of 116 GPa and Poisson's ratio of 0.3. Our previous studies on single level laminoplasty using one or

two screws on the laminar side showed no significant differences in stress distribution. Hence, each vertebra was stabilized with a single plate and three screws. During surgery the plate is often bent to ensure proper fixation. Consequently the finite element mesh of the plate was deformed to accommodate screw placement on the laminar side.

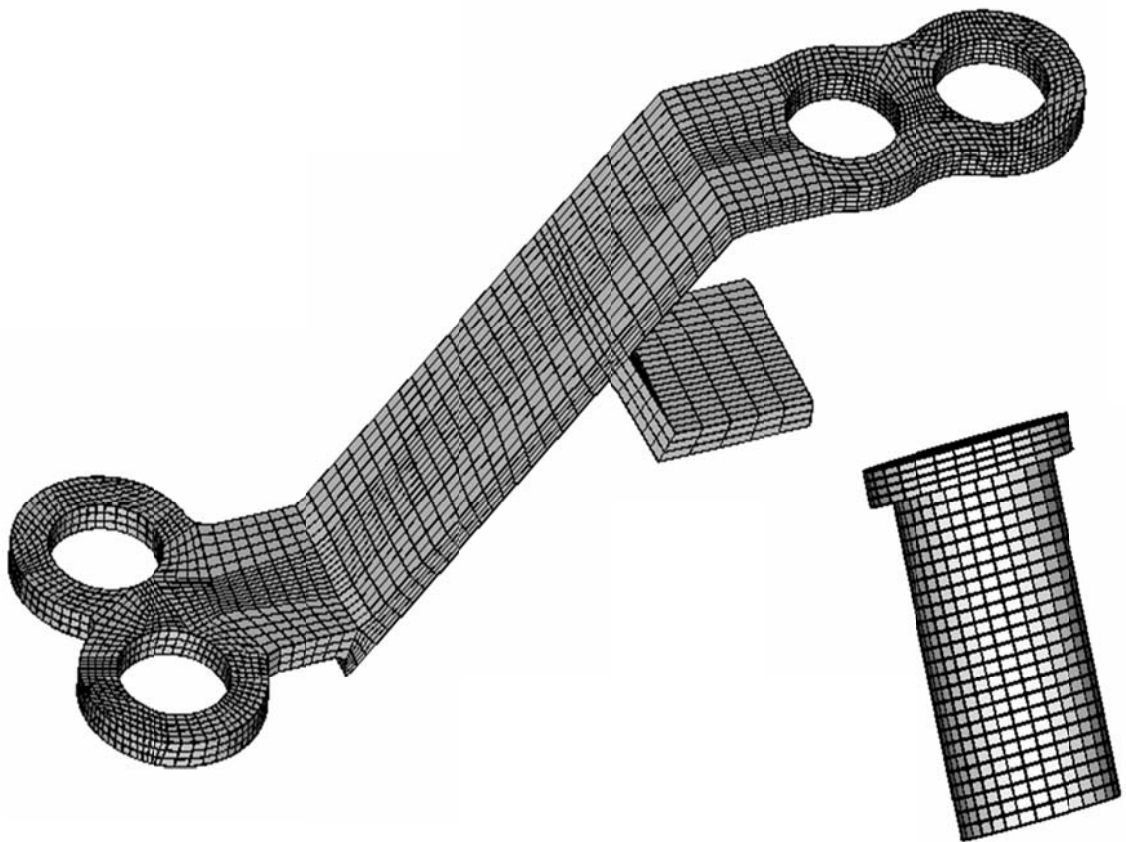


Figure 26. Finite element mesh of the plate and screw.

- In order to simulate a realistic interaction between components, different contact pairs have been defined. These contact pairs differ depending on the involved components and were modeled by means of the master-slave technique implemented by the finite

element code ABAQUS. Small sliding contact was formulated at the interface of the bone and the laminoplasty plates with a friction of 0.37 where the contacting surfaces can undergo only relatively small sliding relative to each other. Additionally, the surfaces of the bone/screw and the screw/plate were tied as they were assumed to remain in contact throughout the analysis (Figure 27). Such contact formulations have been used previously to model the contact between the screw and bone [85].

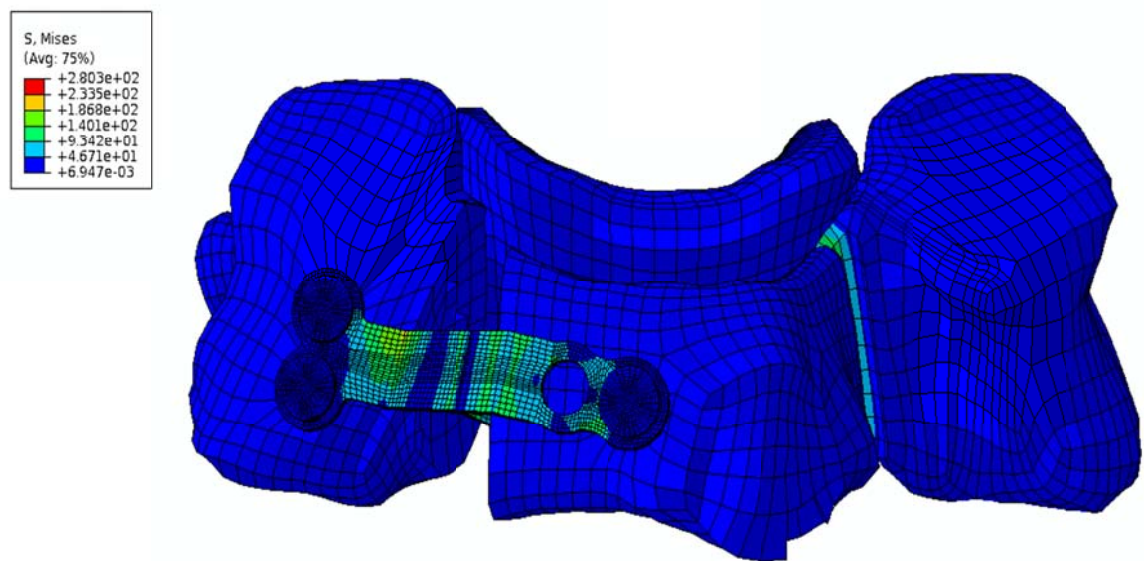


Figure 27. von Mises stress (MPa) distribution in C5 vertebra stabilized with plate and screws.

- Figure 28 shows the final C2-T1 laminoplasty model with open door laminoplasty performed at C3-C6 levels. The final ODL model contained 306,662 nodes and 273,609 elements.

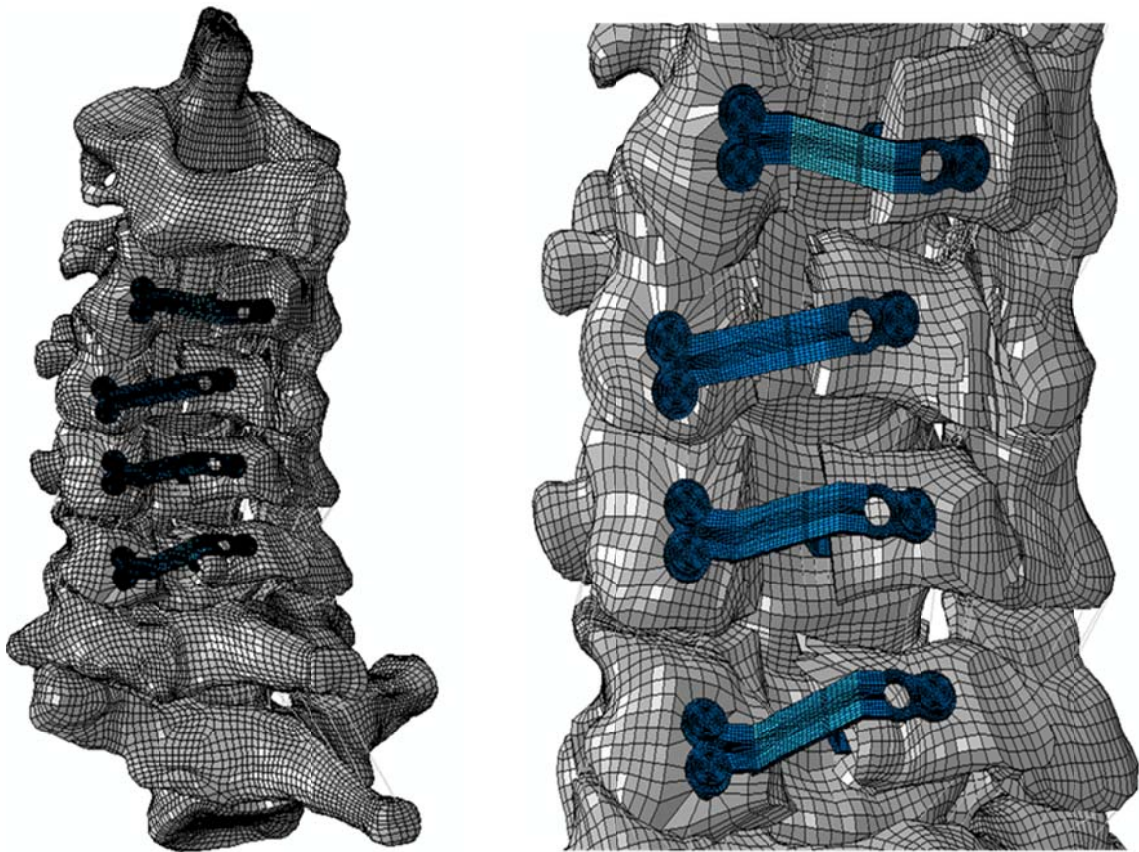


Figure 28. C2-T1 finite element model with open door laminoplasty performed at levels C3-C6. (Left) Full model; (Right) Local zoom.

3.4 Double Door Laminoplasty in the Cervical Spine

3.4.1 Background and Literature Review

Kurokawa et al. [86] in 1982 developed double-door laminoplasty also known as French-door laminoplasty. The procedure involves drilling of two troughs on either side of the lamina/lateral mass junction. The spinous process are cut in the midline and then lifted off to expand the spinal canal area. One of the potential advantages of this technique is the preservation of long spinous processes that act as potential stabilizers of the neck. Compared to the open door laminoplasty, double-door laminoplasty has some

theoretical advantages like symmetrical expansion of the spinal canal, and the potential for posterior fusion with a bone graft bridge between the spinous process. Variations have been described to stabilize the lamina in the opened position and to re-create the posterior arch. The lamina are supported in the open position using sutures through the facet capsules and the lamina, suture anchors, autografts, HA spacers or plates [87,88]. Grafts or Spacers are held in space with either sutures or screws. Of all the available methods for stabilization, spacers are beneficial as they reduce the operating time and the intraoperative bleeding.

Ueyama et al. [89] observed that the group with HA spacers effectively maintained the range of motion compared to the group with autogenous iliac grafts. While using the HA spacers, the authors recommended cutting the edge of spinous process without fracturing the lamina and taking proper care while pulling the suture thread to stabilize the spacer as it may destroy the lateral gutter. However, inadequate contact between the spacer and bone was one of the initial problems, resulting in the instability of the spacer and restenosis of the spinal canal. Hirabayashi et al. [90] investigated the shape of the widened space created by the split spinous processes during a double-door laminoplasty. They concluded that the optimal shape of a spacer adapting to the resulting space is trapezoidal, in both the axial and frontal sections. The study also reported increased lateral deviation of the spinous process with the hinge than without the hinge; suggesting the importance of creation of hinge during laminar opening. Hence, most of the currently available spacers are trapezoidal in shape to accommodate the contour of the spinous process (Figure 29). Nevertheless, surgeons still use autogenous iliac bone graft for an unstable segment instead of a HA spacer, and bone chips on the bilateral gutters. Few others have considered using spacers made from the base of spinous process thereby avoiding harvesting bone blocks from the iliac crest and good bony union was observed using this technique [91].

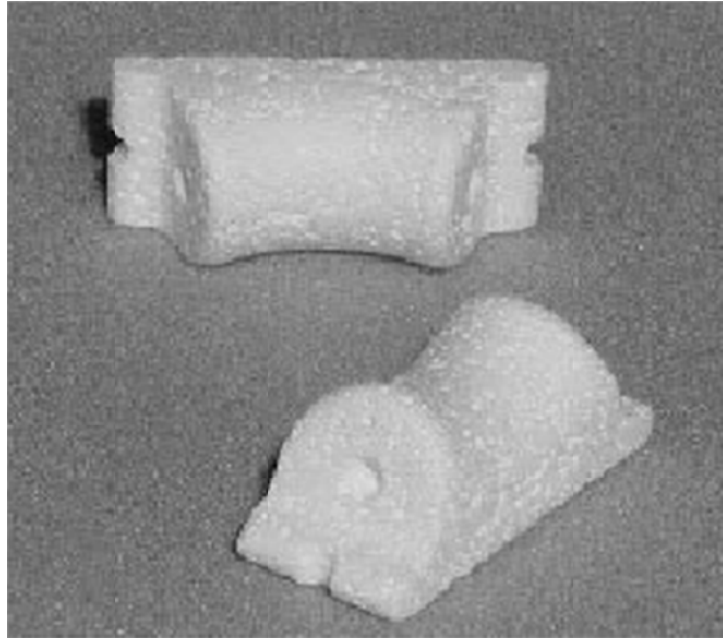


Figure 29. Hydroxyapatite Spacer [10].

Postoperative displacement of HA spacers has been a problem with double door laminoplasty when compared to open door laminoplasty. The biomechanical properties of the reconstructed posterior arch may play a key role in the migration of the spacer. In ODL, the triangular construct provides enough resistance to both shear and lateral forces along with the spring effect of the hinge to keep the spacer in situ. Whereas in DDL, the square construct formed is susceptible to the smallest shear forces from the lateral or dorsal direction, thus displacing the spacers. Kaito et al. [92] reported postoperative dorsal migration $>2\text{mm}$ in 42% of patients implanted with HA spacers and fixed with non-absorbable sutures. In addition 38% of the spacers rotated 10° . However no correlation was observed between the displacements of HA spacers and neurological complications. The authors suggest placing the HA spacers at the base of spinous process close to the dura matter, but further prospective studies should be conducted to determine

this. Figure 30A and Figure 30B show the spacer stabilized with sutures and screws respectively.

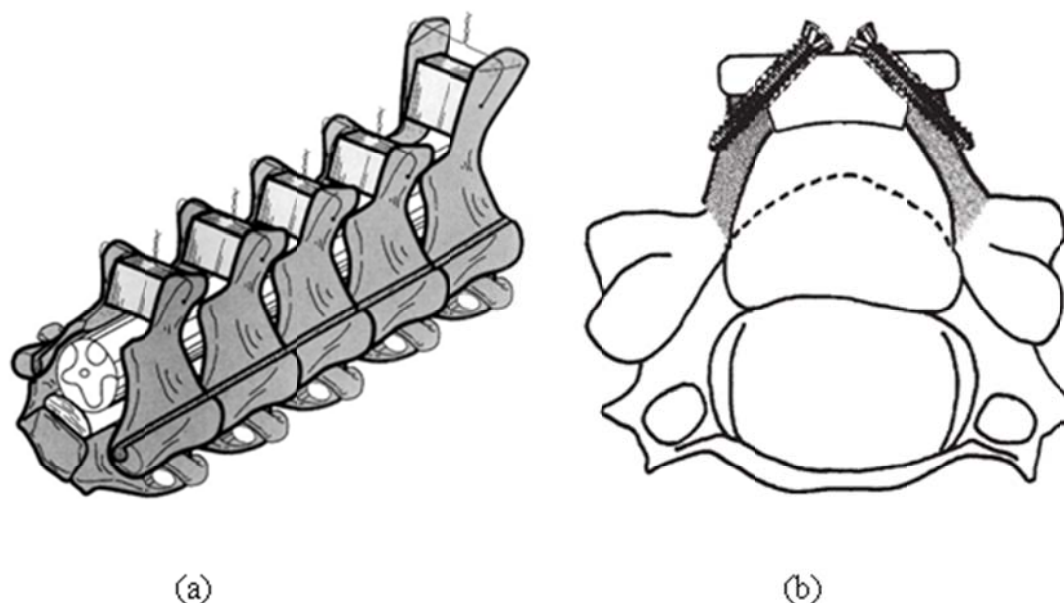


Figure 30. DDL with HA spacer stabilized with (A) sutures [93] and (B) screws [94].

Several clinical studies have been performed by various authors to compare the neurological outcomes, ranges of motion, cervical alignment post DDL. Double door laminoplasty has been effective in achieving good neurological outcomes in people with different spinal alignments over a period of 5 years [95]. Most authors report the clinical outcome based on the Japanese Orthopaedic Association scoring system (JOA). The mean recovery rate for double door laminoplasty and its modifications was around 50-70% and most of them accounted the results to the degree of preoperative myelopathy and not the surgical technique [94,96,97]. Neither of the surgical techniques namely open or double door laminoplasty procedure was shown superior to another. The short term results with improved JOA scores of double door laminoplasty for cervical stenotic

myelopathy were maintained over 10 years in 78% of patients with OPLL and in most of the patients with myelopathy [98]. Goto et al. [99] reported the clinical outcome of a new surgical technique for cervical laminoplasty where the lamina on both the sides, spinous processes and various attached ligaments are removed. Trapezoid-spaced HA spacers are placed between the cut ends of the lamina and lateral masses bilaterally at each level. Malleable titanium mini plates and screws were used for fixation of the spacers. At the end of 12 months, fusion was seen around the HA spacers and spinal alignment and range of motion was well preserved. The spacers helped in reducing the force to miniplates and the malleability of miniplates reduced the force to which the screws are subjected.

Puttlitz et al. [100] compared the kinetics after Open-door (ODL) and French door laminoplasty (FDL), where they noticed that both FDL and ODL resulted in significant decrease in the range of motion 6 months postoperatively. But, no significant differences between the two techniques were observed after 6 months. They also showed that ODL produces a significant reduction in motion 6 months postoperatively compared with the immediate postoperative condition. Hence, the authors recommended early physical therapy to preserve a more physiological pattern of cervical range of motion.

However, currently there exists no computational study that compares the biomechanical effects of the two laminoplasty techniques.

3.4.2 Simulation of DDL at Levels C3-C6

The intact mesh (C2-T1) was modified to simulate a double door laminoplasty procedure at levels C3-C6.

- Two bilateral hinges at the junction of each lateral mass and lamina were created as described for the single hinge of the ODL procedure (Figure 31). Hinges should not be too medial or too lateral as too medial may result in insufficient enlargement of the spinal canal, and too lateral makes opening the split lamina difficult and may also cause facet fusion.

- The spinous process was split along the sagittal plane and opened until a laminar spacing of 10mm was obtained. The laminar opening was defined as the distance between the basal region of spinous process as shown in Figure 31.

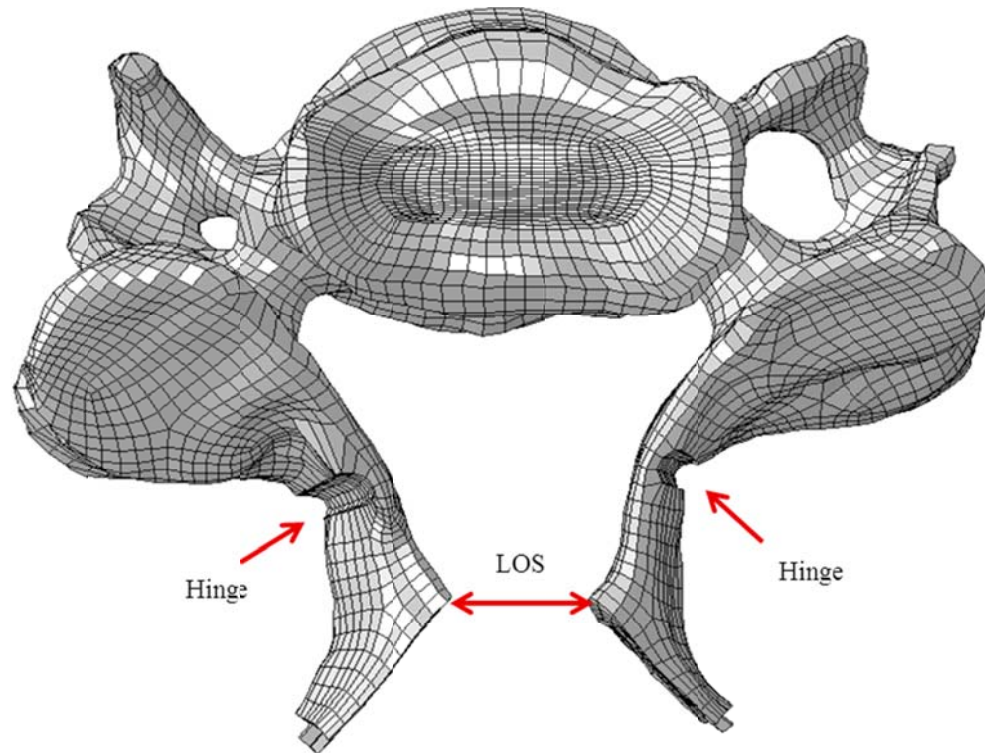


Figure 31. Superior view of a vertebra following laminar opening for DDL ; highlighting the bilateral hinges and Laminar Opening Space (LOS) of 10 mm.

- The tip of the spinous process was removed, preserving enough bone to hold the spacer. The technique also involved resection of the interspinous ligaments at each of the involved levels and partial removal of the ligamentum flavum at the midline from C2 to C7 to allow for the laminar opening.
- The initial stresses developed during laminar opening were fed back into the model as initial conditions. As these stresses tend to close the lamina back, a 10mm trapezoidal

shaped HA spacer (Elastic modulus of 26GPa [101] and Poisson's ratio of 0.27), meshed with hexahedral elements, was used to stabilize the lamina in the open position (Figure 32). A convergence study was performed by applying compressive loads on the lateral sides to determine the minimum number of elements required for accurate solution.

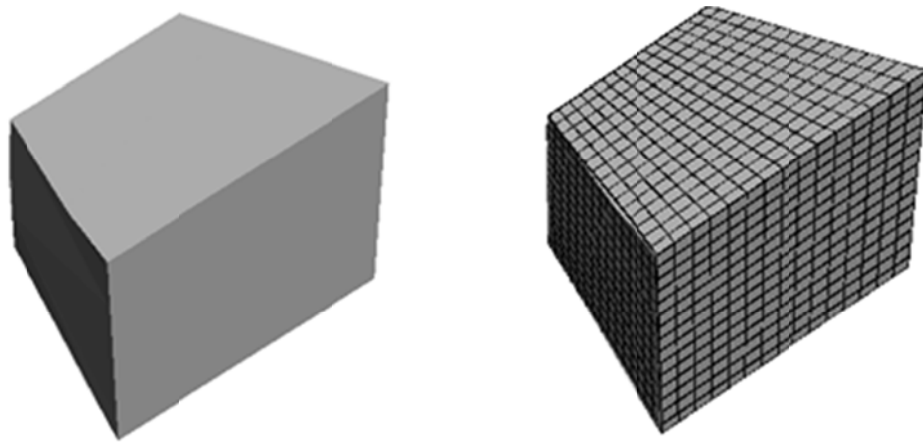


Figure 32. Trapezoid shaped spacer. (Left) Solid model; (Right) Finite element mesh.

- Several studies have hinted towards bony union between the HA spacers and spinous process. Iguchi et al. [102] evaluated 33 patients who underwent HA-spacer assisted laminoplasty and were followed for at least 1 year. They reported bone regrowth around the spacer in 91% of patients and rigid bonding of the spacers to the bone in 61% of the cases. Hence, the spacers were thought to remain in contact throughout the analysis, and this was simulated by using the TIED command in ABAQUS that holds the surfaces of spacer and bone together (Figure 33) [91,102].

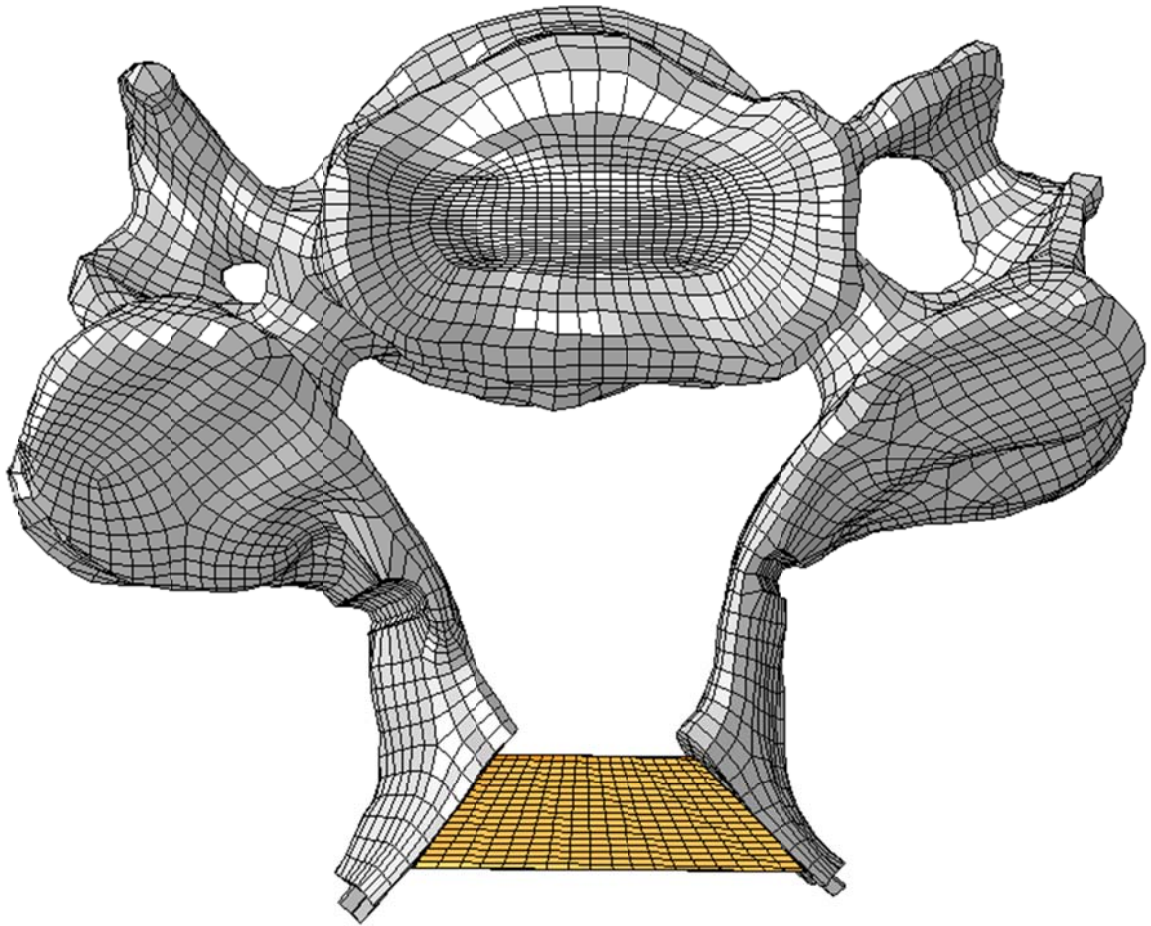


Figure 33. C6 Vertebra stabilized with spacer.

- The technique was implemented at all the levels C3-C6 and Figure 34 shows the final C2-T1 double door laminoplasty model. The final C2-T1 double door laminoplasty model consisted of 202,400 nodes and 188,866 elements.

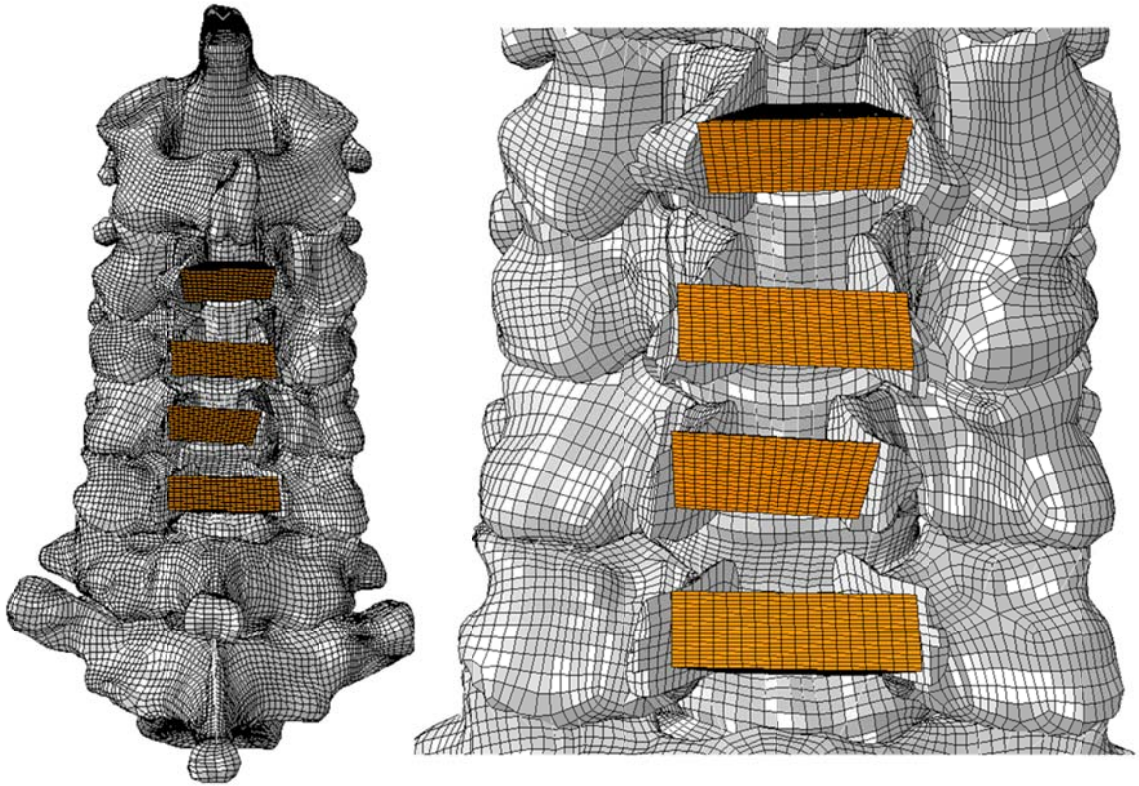


Figure 34. C2-T1 finite element model with double door laminoplasty performed at levels C3-C6. (Left) Full model; (Right) Local zoom.

3.5 Results

3.5.1 Comparison of Spinal Canal Area

Both open and double door laminoplasty aim to increase the spinal canal area and decompress the spinal cord. ImageJ software was used to measure the spinal canal area for each of the levels C3-C6 after open and double door laminoplasty [103]. The spinal canal area for each model was averaged across the four levels. The mean spinal canal area for the intact model was approximately 243mm^2 . The open door and double door laminoplasty techniques resulted in a 46% and 37% increase in the spinal area compared to the intact model. No significant differences in the spinal canal area were observed between the two techniques of laminoplasty for the current 10mm laminar opening. This

increase in canal space is sufficient for posterior migration of spinal cord. Wang et al. [104] did a computer simulated comparison study between single and double door techniques. The authors reported significant differences in the postoperative spinal canal area between the two techniques when the lamina was opened by more than 12mm; while no significant differences were observed when the lamina was opened by less than 12mm. Similar results were obtained from a cadaveric study that showed a 43% increase in spinal canal area after open door laminoplasty [105]. Figure 35 shows the comparison of the spinal canal area of the three models (intact, open door and double door laminoplasty) with the literature data [104].

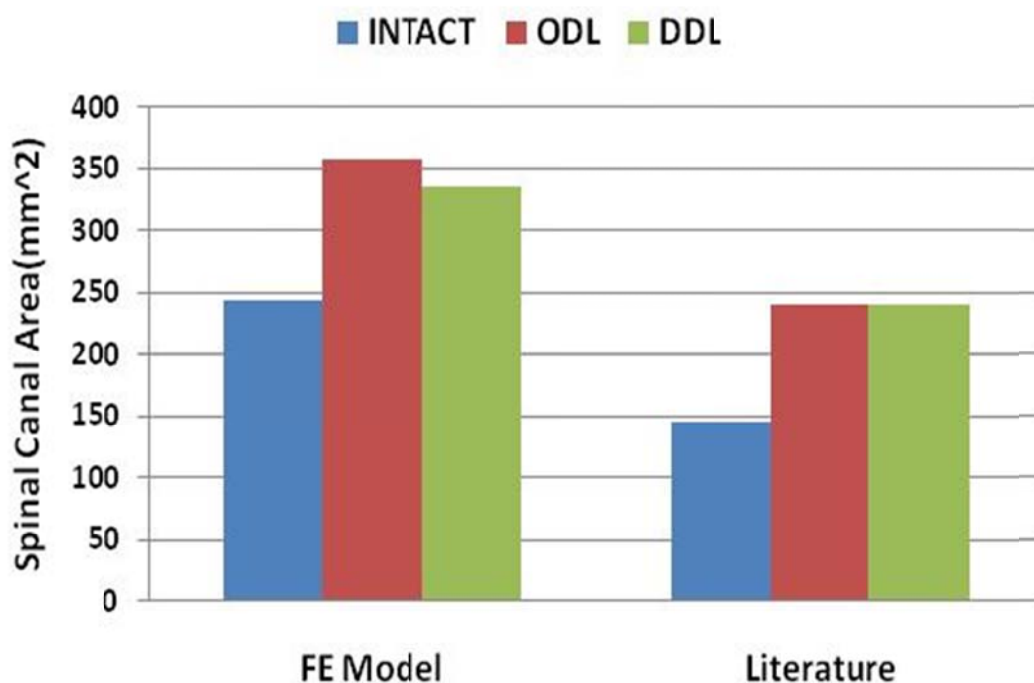


Figure 35. Comparison of spinal canal area of the three models (intact, open door and double door) with the literature data [104].

3.5.2 Stress Distribution in the Cortical Bone

To understand the iatrogenic changes that occur as a result of surgical procedures, the stresses in the cortical regions of the vertebral bodies were evaluated. The maximum von Mises stresses during the laminar opening (open and double door laminoplasty) was recorded in both the anterior and posterior cortical regions of the vertebral bodies. Figure 36 shows the von Mises stress distribution in C3-C6 after the laminar opening. Compared to open door laminoplasty, the stress distribution in the vertebral bodies after double door laminoplasty was found to be more symmetrical. This is due to the splitting of the spinous process in the midline for DDL. The stresses recorded were also slightly higher with unilateral laminar opening than midline laminar opening. Compared to the anterior regions, posterior regions of the altered levels (C3-C6) showed a marked increase in the stress after both open and double door laminoplasty. Figure 37 compares the maximum von mises stresses in the cortical regions of vertebral bodies after laminar opening.

3.5.3 Stress Distribution in Laminoplasty Constructs

The main objective of the laminoplasty technique is to hold the lamina in the open position without failure to successfully decompress the spinal cord. The laminoplasty constructs namely the screws and plates of ODL and the HA spacer of DDL were evaluated for their stability. During all the six loading modes, the von Mises stresses in the plate and screw were within the yield strength of the Ti implant i.e.917MPa. Figure 38 shows the von Mises stress distribution in the plate where the maximum von Mises stress was approximately 250MPa.

Figure 39 shows the von Mises stress distribution in the HA spacer with peak stresses at the corners due to the TIED contact constraint introduced in the model to stabilize the lamina. Nevertheless, the stresses within the spacer were within the failure strength and were found to be approximately 200MPa.

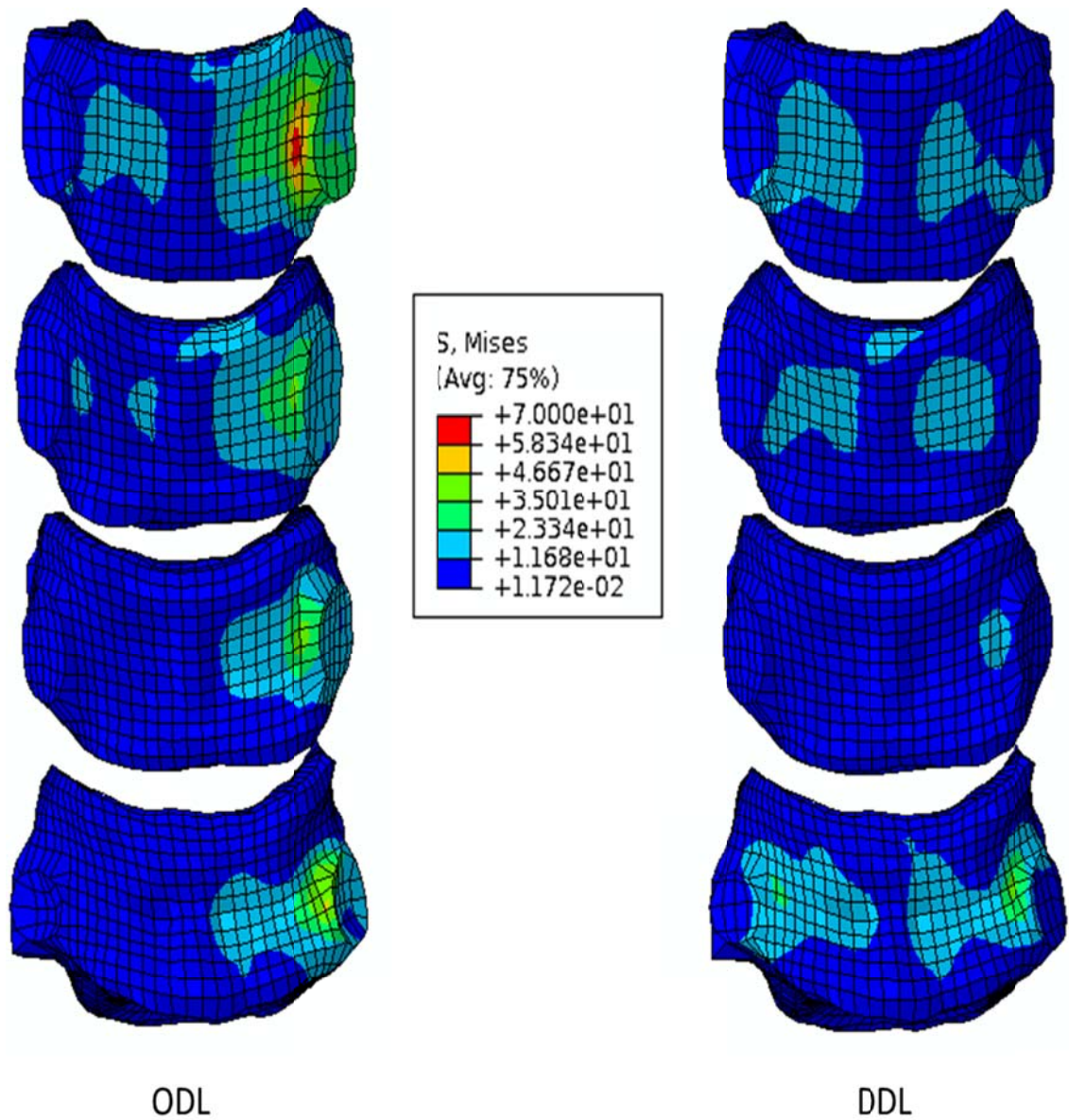


Figure 36. Posterior view of the von Mises stress distribution in the vertebral bodies (C3-C6) after open and double door laminoplasty.

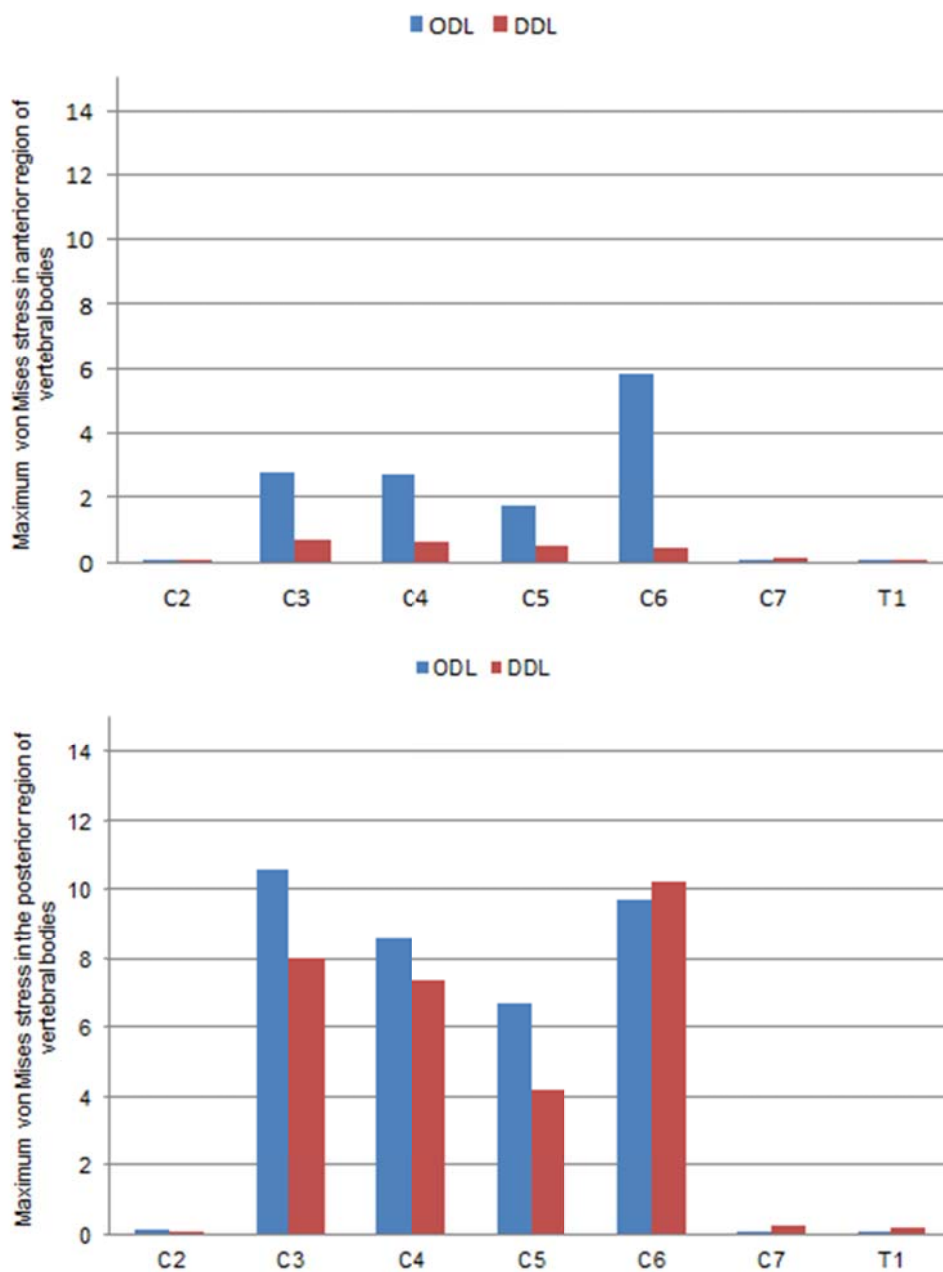


Figure 37. Maximum von Mises stress in the (Top) anterior and (Bottom) posterior regions of the vertebral bodies after the laminar opening for open and double door laminoplasty.

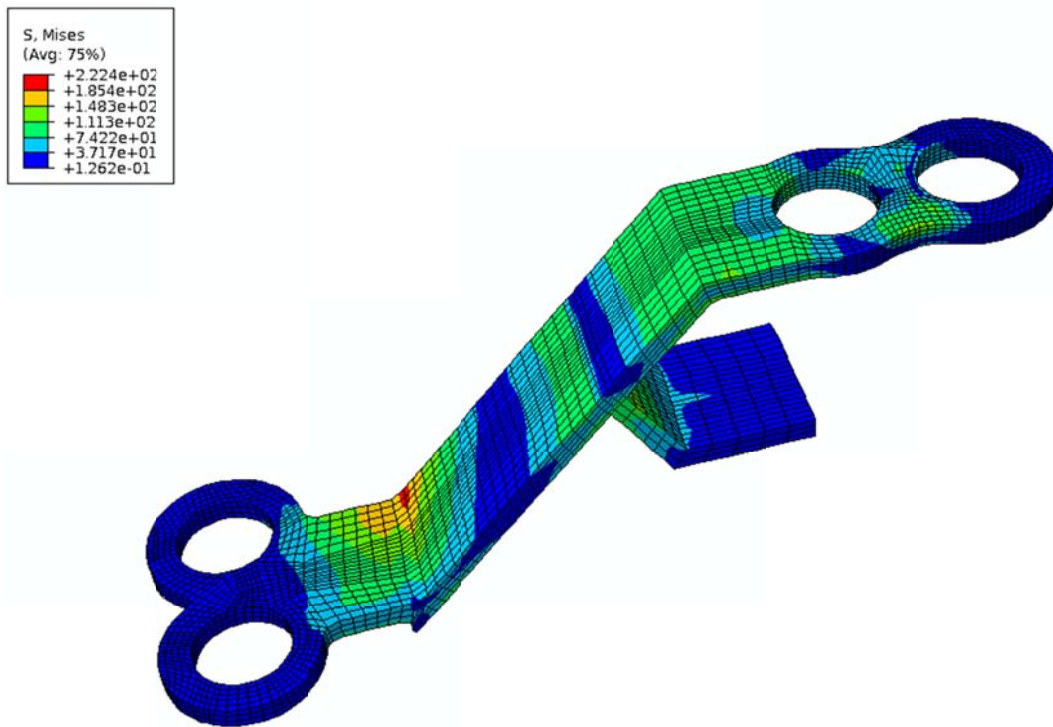


Figure 38. von Mises Stress (MPa) distribution in the laminoplasty plate.

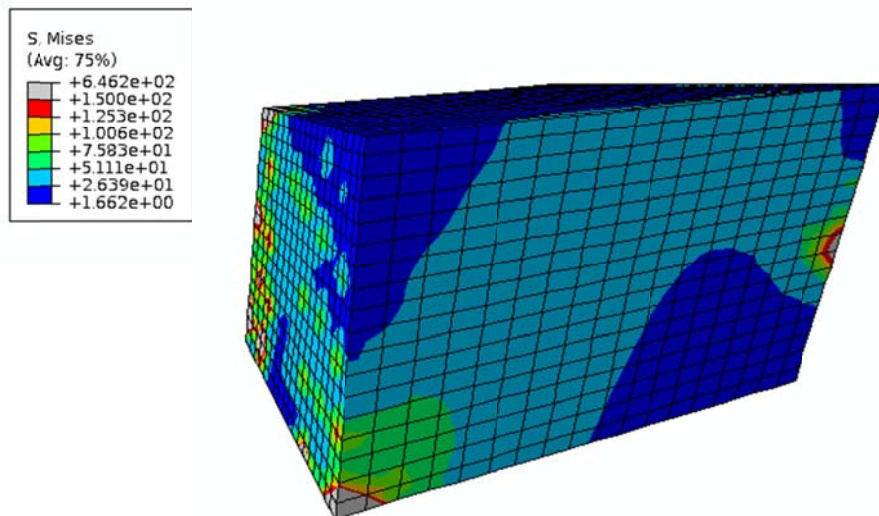


Figure 39: von Mises Stress (MPa) distribution in the spacer.

3.5.4 Flexibility Test

The intact and all three surgically simulated models (ODL, DDL and laminectomy) were tested in flexion/extension (\pm MX), right/left lateral bending (\pm MZ), and right/left axial rotation (\pm MY). The inferior nodes of the T1 vertebra were fixed in all directions and a moment of 2Nm was applied on the superior surface of C2. The analysis was performed using the finite element software ABAQUS 6.9; enabling the biomechanical response of the intact, laminectomy, and both laminoplasty procedures to be compared. The ranges of motion, stresses in the annular regions of the intervertebral discs, and the stresses in the cortical regions of the vertebral bodies were analyzed for all four models (intact, laminectomy, open door laminoplasty, double door laminoplasty).

Figure 40 compares the percent changes in the C2-T1 range of motion after laminoplasty and laminectomy. The ODL and DDL resulted in a 5.4% and 20% increase in C2-T1 range of motion respectively, while the laminectomy resulted in a substantial 57.5% increase in the C2-T1 motion during flexion, with only minimal changes in the other directions.

The intersegmental motions in response to the six loading modes were compared following the simulated surgical procedures Figure 41. During flexion, after ODL the adjacent levels C2-C3 and C6-C7 showed a 39% and 20% increase in the motion respectively; while no substantial changes were observed at the altered levels. The percent increase in motion after DDL varied from 4.3% to 34.6%. Compared to the intact model, laminectomy at C3-C6 led to a profound increase (37.5% to 79.6%) in motion across the levels C2-C3 to C6-C7. During extension, the superior adjacent level C2-C3 showed an increase in motion of 8.5% and 28.8% after ODL and DDL respectively. For left lateral bending, a decrease of 11.7% and 20.3% in motion was observed at the inferior adjacent level C6-C7 after ODL and DDL respectively. Similarly, left axial rotation resulted in 13.2% and 15.08% decrease in motion at C6-C7 after ODL and DDL

respectively. After laminectomy, both lateral bending and axial rotation led to minimal changes in the motion (<5%).

Figure 42 shows the percent changes in the annular stresses of the intervertebral disc after the simulated surgical procedures. Stresses were recorded in the anterior and posterior regions during flexion and extension, respectively. The left region of annulus was examined during left lateral bending and left axial rotation, while the right side was monitored during right lateral bending and right axial rotation. After ODL, the adjacent discs (C2-C3 and C6-C7) showed an increase in the stress values while DDL and laminectomy resulted in increase in the stresses across the surgically altered levels (C2-C3 to C6-C7) during flexion. Minimal changes in the disc stresses were observed at most of the levels during other loading modes.

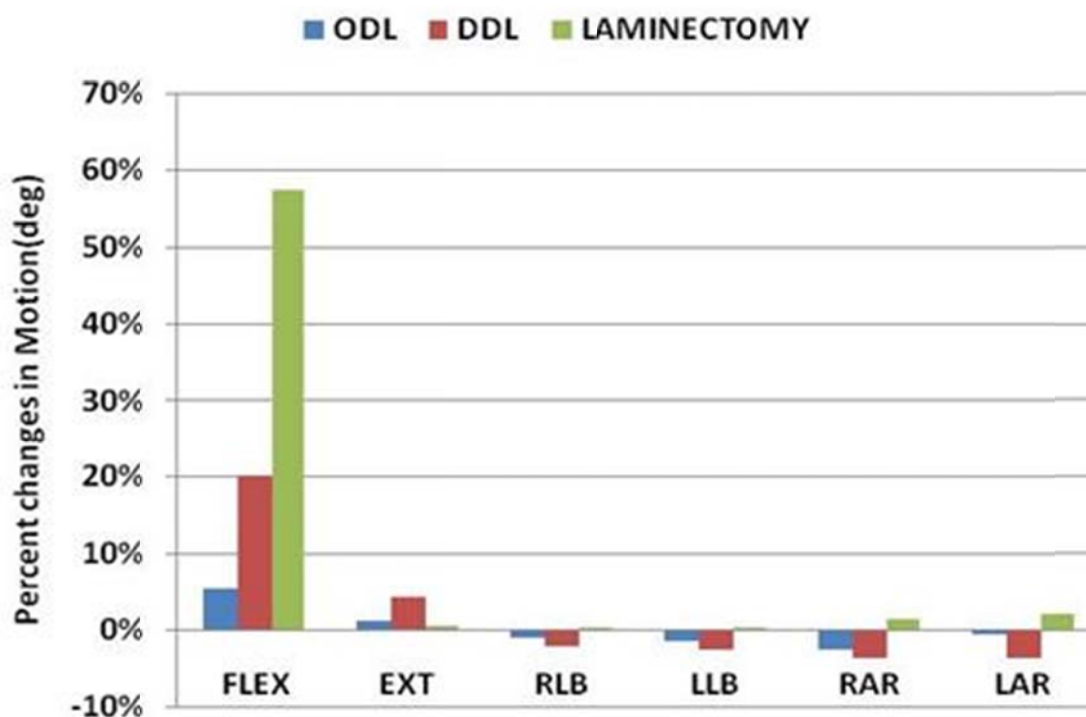


Figure 40. Percent changes in C2-T1 range of motion after ODL, DDL and laminectomy.

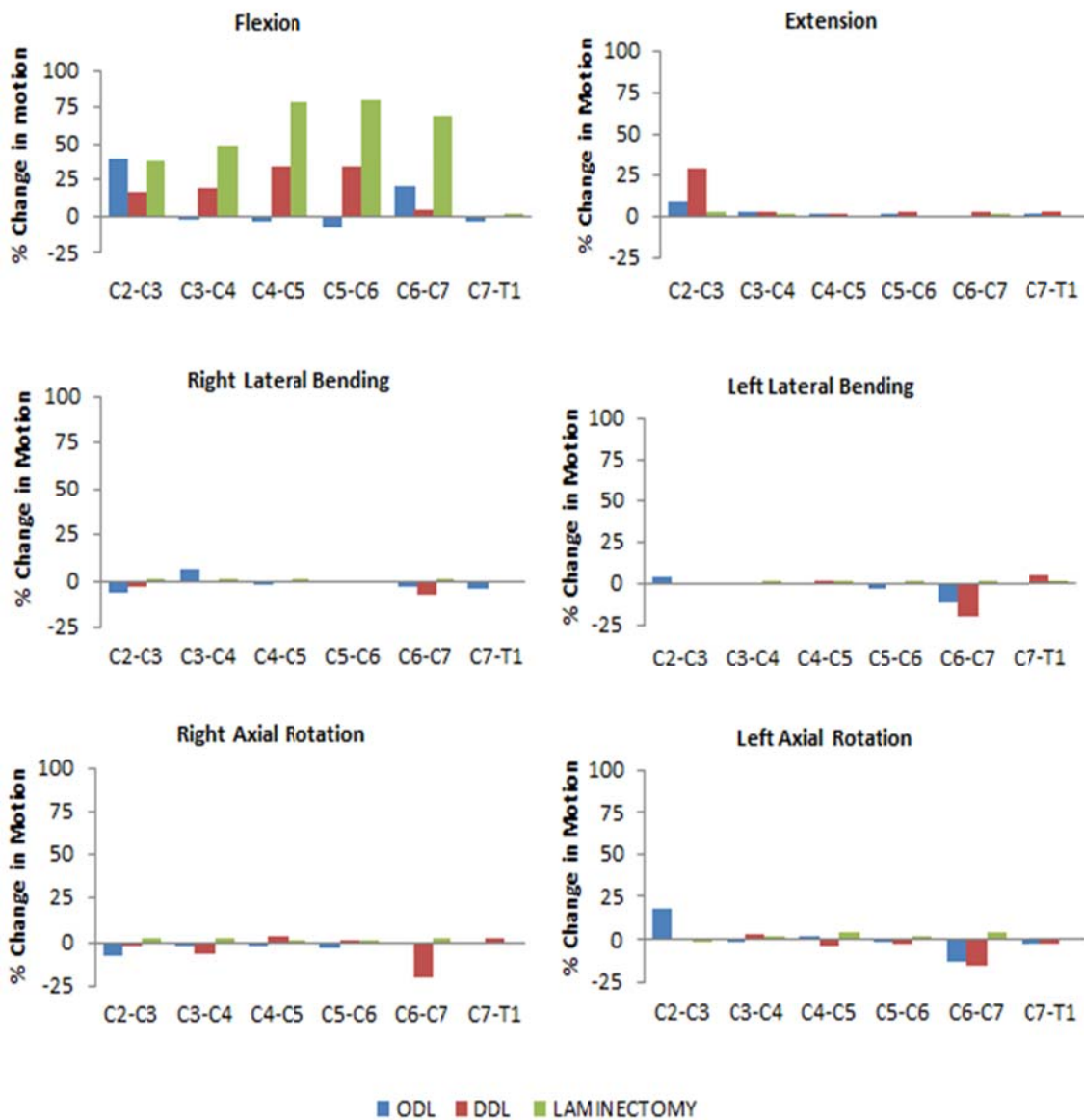


Figure 41. Percent change in intersegmental motion after the three surgical techniques for the six loading modes.

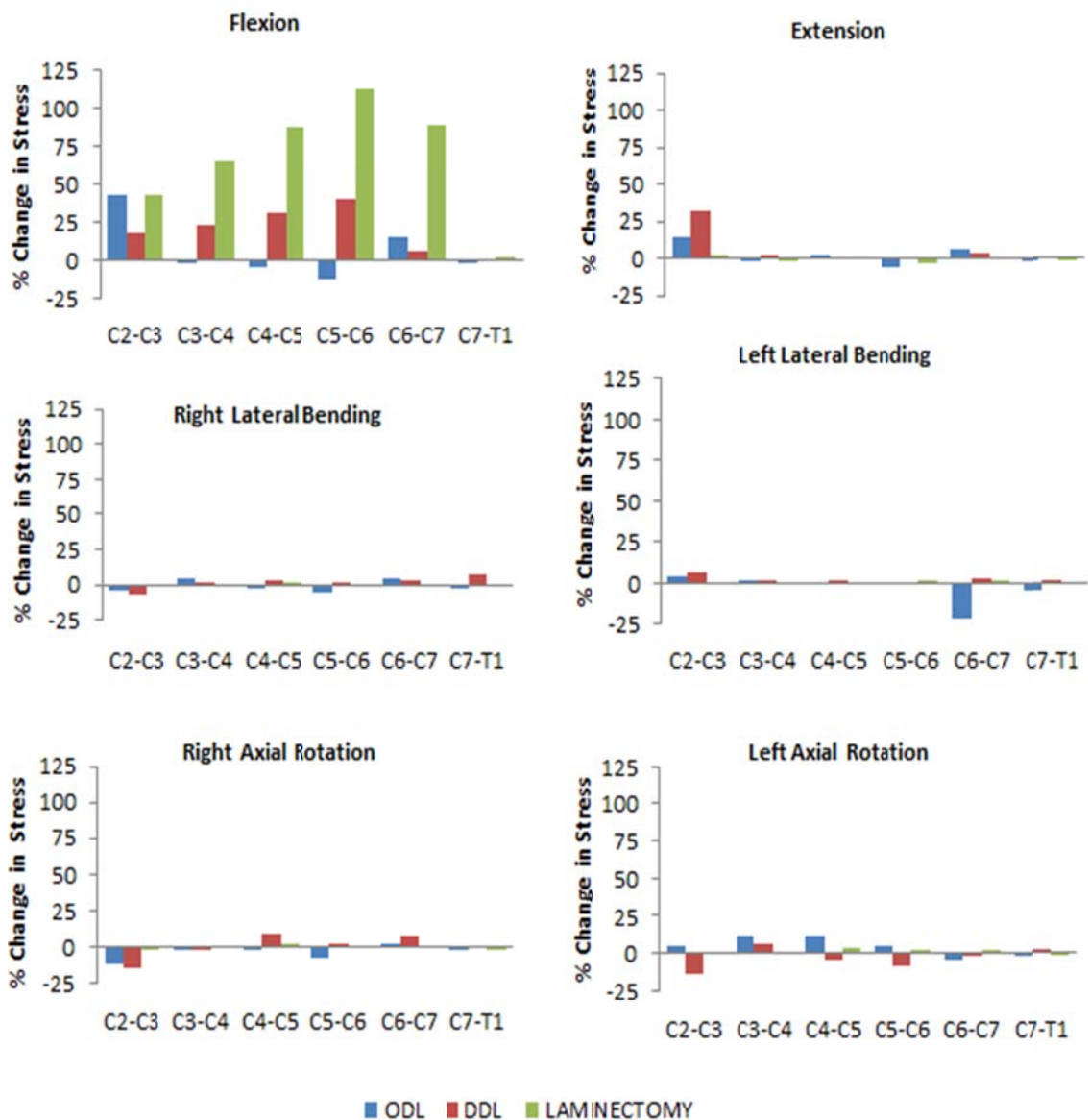


Figure 42. Percent change in stresses in the annular regions of the intervertebral discs after the three surgical techniques during the six loading modes.

The facet contact forces were analyzed for the intact and the three surgically simulated models (open door laminoplasty, double door laminoplasty and laminectomy). No major differences were observed between the four models in the six loading modes.

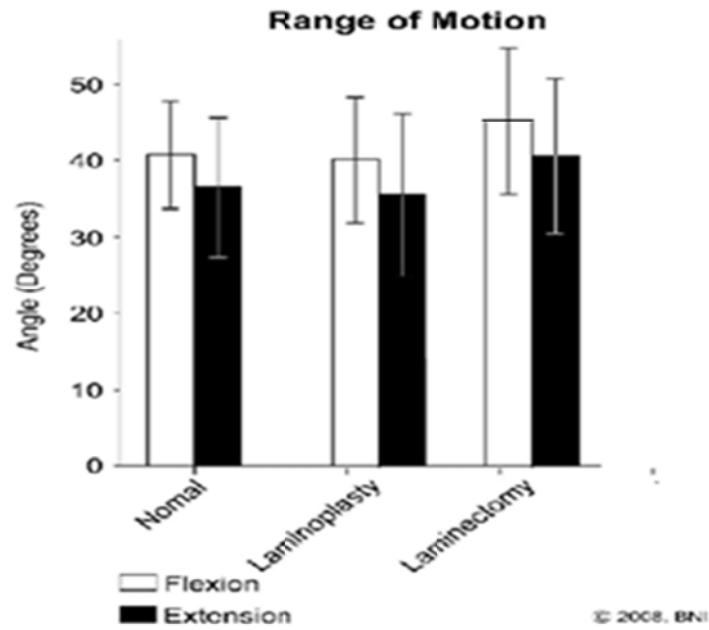
3.6 Discussion

A C2-T1 validated finite element model of spine that is capable of providing robust kinematic predictions after surgical simulations was used in this study. Many experimental and very few finite element studies have been done in the past to look at the effect of single to multi-level laminectomy on the biomechanics of spine. Kumaresan et al. [106] used a 3D validated finite element model of the lower cervical spine to study the biomechanical effects of single-level laminectomy with and without graded facetectomy. Results indicated that laminectomy led to increased motions and stresses on adjacent levels under flexion compared to other loading modes. In order to rule out the possibility of the effect of loading and boundary conditions on the results, Wan et al. [107] used a validated C2-C7 model with C5 laminectomy to show significant increase in the range of motion, intervertebral disc and cortical shell stresses at C4-C5 and C5-C6. Goel et al. [108] tested cadaveric cervical spines (C2-T2) after two-level laminectomy to observe a significant increase in the sagittal rotation. Ding et al. [109] used four human cervical spine specimens (C2-T1) to report a 15% increase in axial rotation after two-level laminectomy. Clearly, most of the studies have shown instability of the spine post laminectomy which is very well seen in our model with an approximate 58% increase during flexion. The increased disc stresses seen at the altered and adjacent levels after multi-level laminectomy correspond well with the earlier biomechanical studies and may be clinically correlated to the process of disc degeneration. Since no facet injury was simulated in the current study, laminectomy did not have a major effect on lateral bending and axial rotation [110].

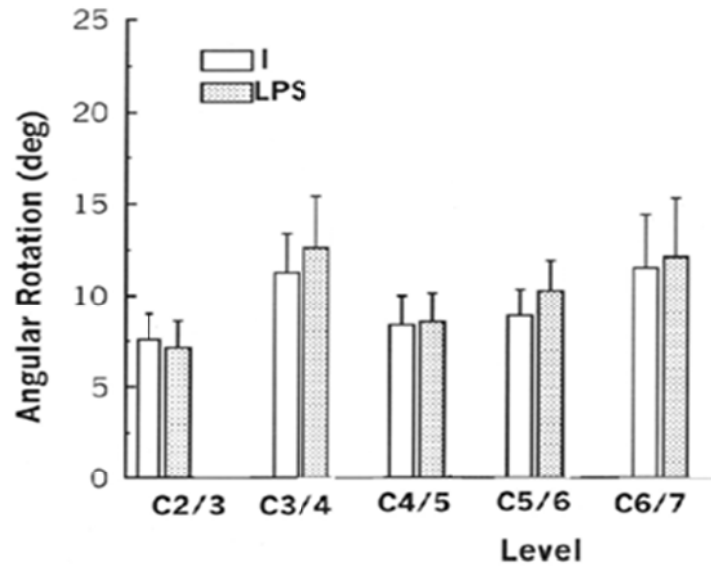
In vitro studies performed on cadaveric cervical spines after open door laminoplasty which utilized either plates or sutures showed preservation of motion [9,10,13,14], while laminectomy resulted in an increase of $12\% \pm 9\%$ in flexion and $17\% \pm 13\%$ in extension when compared to laminoplasty (Figure 43A) [13]. Nonetheless, most of the studies did not report the effect of the surgical procedures on intersegmental

rotations. Hence, to further augment/validate the current finite element results we performed *in vitro* studies on cadaveric cervical spines after multi-level laminoplasty and laminectomy at C3-C6. Open door laminoplasty stabilized with titanium miniplates led to insignificant ($p>0.05$) changes in motion while laminectomy led to a significant ($p<0.05$) increase in motion during the three loading modes [111]. As observed in the current finite element study, laminoplasty preserved the motion except for slight changes in the intersegmental rotations during flexion. Kubo et al. conducted an *in vitro* study after DDL where no significant differences in the external responses of spine were observed, but the intersegmental rotations showed an inclination towards increased motion at all levels (Figure 43B) [10]. The current DDL finite element model predicted an approximate 20% increase in C2-T1 range of motion, thereby explaining the role of lamina-ligamentum flavum complex in the stability of spine.

This study has the general limitation associated with most of the previous studies where the effect of muscles on the stability of spine has been ignored. The resection of the spinous processes and interspinous ligaments is at the discretion of the surgeon and the laminoplasty technique employed. After open door laminoplasty, during flexion, the increased motion at C2-C3 and C6-C7 could be attributed to the resection of interspinous ligament and unilateral ligamentum flavum at those levels, while the resection of ligamentum flavum at the midline and interspinous ligaments from C2 to C7 after double door laminoplasty led to the increased motion at all the operated levels. The decreased motion observed during lateral bending after laminoplasty could be due to pre-stress in the ligaments that developed during laminar opening. The increased motion, annular stresses and cortical stresses seen after the surgical procedures could accelerate the process of degeneration and may result in the formation of osteophytes.



(a)



(b)

Figure 43. Experimental data (A) C2-T1 motion after Open Door Laminoplasty and Laminectomy [13] (B) Intersegmental motions after Double Door Laminoplasty [10].

The current study showed laminoplasty as superior to laminectomy in terms of range of motion at the altered and unaltered levels. Finite element predictions suggest the preservation of range of motion after open door laminoplasty. It also addressed the role of ligaments in maintaining the stability of the cervical spine as extensive ligament resection could substantially affect the motion as seen after DDL. Significant changes in the von Mises stresses of the intervertebral disc were observed after laminoplasty and laminectomy during flexion and correlated to the changes in the intersegmental motions.

CHAPTER 4. EXPERIMENTAL TESTING OF CADAVERIC CERVICAL SPINE SPECIMENS AFTER LAMINOPLASTY AND LAMINECTOMY

4.1 Introduction

Posterior-based surgical approaches (i.e., laminectomy or laminoplasty) are considered when multiple levels of the spine are to be decompressed or when the source of the cord compression results from posterior pathological conditions [112,113]. A variety of laminoplasty techniques have been described and typically differ based upon the location of the “hinge” and the “opening” of the lamina. Methods also vary in part in the manner of the laminar reconstruction following the laminoplasty and can be broadly classified into two types, namely open door and double door laminoplasty.

A limited number of *in vitro* studies have been performed on cadaveric cervical spine specimens after open door laminoplasty and laminectomy. Moreover, there exist discrepancies in the literature regarding the type of stabilization technique used for ODL and the testing system itself. Nowinski et al. [9] used sutures for stabilization where the facet capsule was damaged. It has been shown that altering the facets affects the stability of the spine [110]. There is also lack of literature data on the segmental rotations. Such information helps determine the effect of the surgical procedure on the unaltered and altered levels. Most of these studies have compared the total range of motion and tested their spines under moments $\leq 1.5\text{Nm}$. Animal models have also been used to evaluate the effect of laminoplasty and laminectomy on the biomechanics of the cervical spine [5,114].

Moreover, little information other than experiential expertise exists regarding the number of lamina (C3-C7 or C3-C6) to be opened for complete decompression of the spinal cord. Pal and Routal [69] demonstrated the significance of C7 in maintaining the stability of the cervical spine. Hosono et al. [70] compared the clinical outcomes of

patients with C3-C6 and C3-C7 laminoplasty. The results favored C3-C6 laminoplasty in terms of postoperative axial neck pain, operating period, and length of the operative wound.

The current chapter presents an experimental investigation, addressing the multidirectional flexibility of the cervical spine in response to both open door laminoplasty and laminectomy (LT_C3456) procedures. Both two-level (LP_C56) and multi-level laminoplasty (LP_C3456) procedures were considered.

4.2 Materials and Methods

4.2.1 Specimen Preparation

Five fresh-frozen human cadaveric cervical spine (C2-T1) specimens (Mean Age \pm Standard Deviation: 70.5 \pm 15.16) were procured, thawed to room temperature, and denuded of all residual musculature, with care taken to preserve the intervertebral disc and supporting osteoligamentous structures. Each specimen was scanned using CT to ensure the absence of pathological defects. In preparation for mounting the specimens for testing, C2 and T1 were potted using Bondo (*Bondo Corp, Atlanta, GA*). The transverse plane of the C4-C5 intervertebral disc was made horizontal while potting the specimens to represent the neutral position. The specimens were then wrapped in saline soaked gauze and placed in a labeled double plastic bag and kept frozen at -20°C.

4.2.2 Biomechanical Testing

Flexibility of the spine is a measure of the physical characteristic of a spinal construct, where the motion of the vertebrae is measured in response to the applied load. There has been controversy surrounding the use of load-controlled or displacement-controlled testing for measuring the flexibility of spine. While each has its own share of advantages, pure moment loading ensures that the load experienced by a specimen remains constant along its length independent of its geometry, motion or stiffness. One of

the major advantages of applying a pure bending moment is that it allows an unbiased comparison of the biomechanical properties of different spinal constructs [115].

4.2.2.1 Test Setup

The different kinds of systems used to apply pure bending moments include suspended deadweights attached to the rods of loading frame or indirectly through the use of pulleys [116], cable driven systems where the forces are applied by cables driven over the pulleys [115,117] and spine simulators. [118-120] In a study done by Grassmann et al. comparing constrained and unconstrained testing system, it was observed that unconstrained setup allowing coupled motions resulted in the movement of spinal segments in a more physiologic manner [121]. Hence, more emphasis should be placed towards designing the testing systems in a way to reduce the artifacts that result in impure moments.

Based on the advantages and disadvantages of the various available testing systems, we chose a servo hydraulic Materials Testing Machine (MTS) (858Bionix II, MTS Corporation, Eden Prairie, MN) retrofitted with 2 spine fixtures to apply pure, unconstrained multidirectional loads. As seen in Figure 44, the spine loading simulator consisted of 2 gimbals with a 6DOF load cell attached to the top gimbal. In our testing setup, the bottom gimbal acted as a slave and followed the motion of top gimbal to which the moments were applied. Preliminary studies on sheep cervical spines indicated large shear forces resulting from the fixed bottom gimbal. The resulting shear forces either led to impure positive or negative moments being generated for a given rotation. DiAngelo et al. [119] loaded the spine eccentric to the load axis of the actuator while allowing the shaft to move relative to the actuator, thus minimizing the shearing forces. Equizabal et al. [122] redesigned their fixed ring cable driven experimental apparatus with a sliding ring to avoid non-trivial anterior-posterior shear forces and non-uniform loading conditions. Hence, in order to account for this high shear forces in our testing system, we

added a passive XZ table below the bottom gimbal that would ultimately offset the high shear forces by translating in the required direction.

On the day of testing, the specimens were thawed to room temperature and mounted to the servo hydraulic materials testing machine. Custom made rigid body sensors consisting of 3 infrared light emitting diodes (IREDs) were rigidly attached to the anterior of each vertebra and the upper and lower gimbals (Figure 44). The motion of the sensors was tracked with an optical motion capture system (Optotrak 3020, Northern Digital Inc., Waterloo, Ontario, Canada).

4.2.2.2 Test Protocol

Each test included pure moment loading ($\pm 2\text{Nm}$) in flexion/extension, right/left lateral bending and right/left axial rotation at a loading rate of 4Nm/min . To precondition the specimen and to minimize the viscoelastic effects, each loading cycle was repeated three times, with the data from the third cycle used for analysis. The specimens were copiously moistened using 0.9% sodium chloride irrigation solution throughout the study.

Subject to the aforementioned protocol, each specimen was tested in the following sequential order as shown in Figure 45: (a) Intact; (b) Laminoplasty at C5-C6 (LP_C56); (c) Laminoplasty at C3-C6 (LP_C3456); and (d) Laminectomy at C3-C6 (LT_C3456). In an effort to start each test from the same neutral position, surgeries were performed without removing them from the materials testing machine.

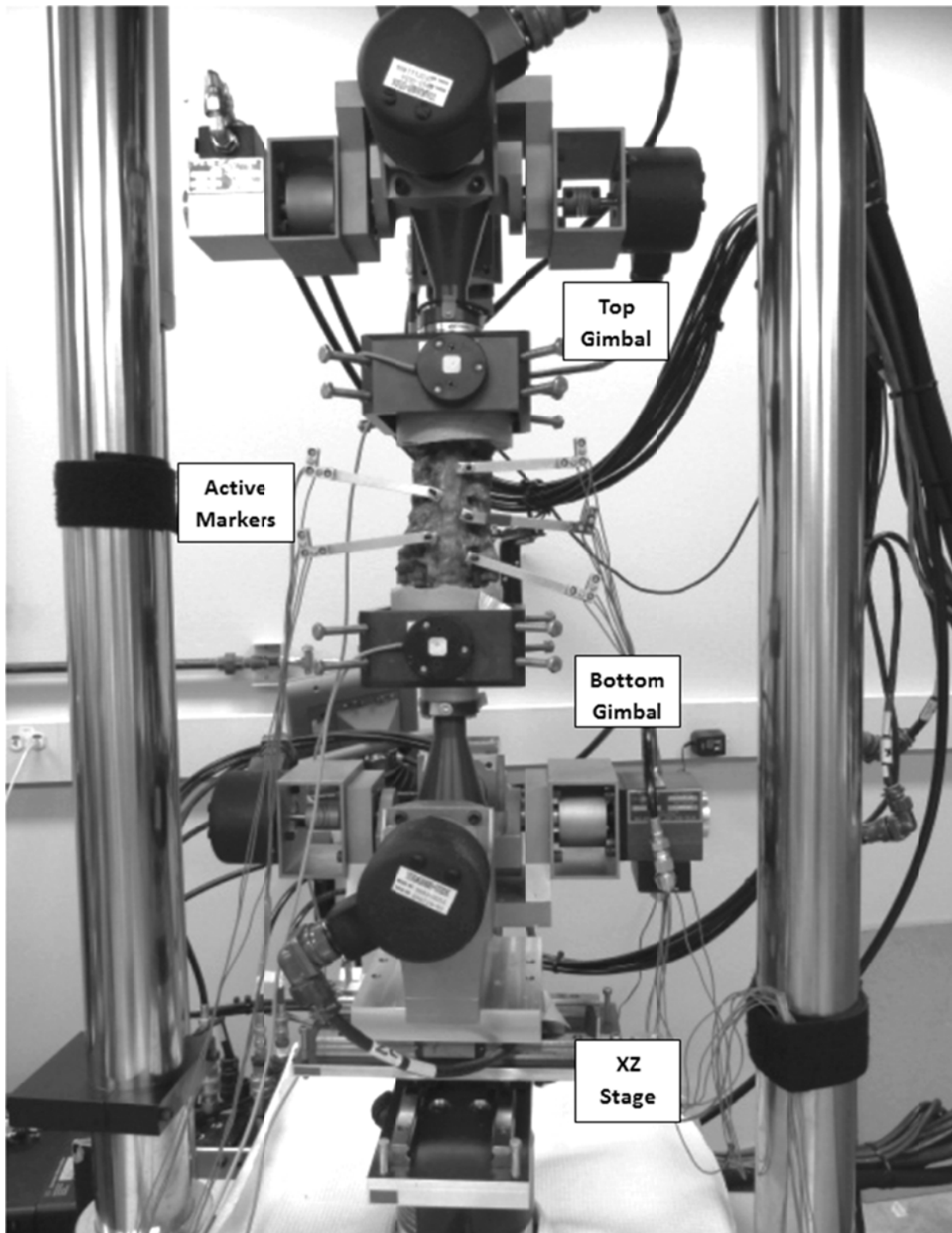


Figure 44. Photograph of a specimen mounted for testing on servo hydraulic materials testing machine (858Bionix II, MTS Corporation, Eden Prairie, MN). XZ table was placed below the bottom gimbal to offset any shear forces by translating in the required direction. Rigid body markers (IREDS) were attached to the vertebral bodies of spine.

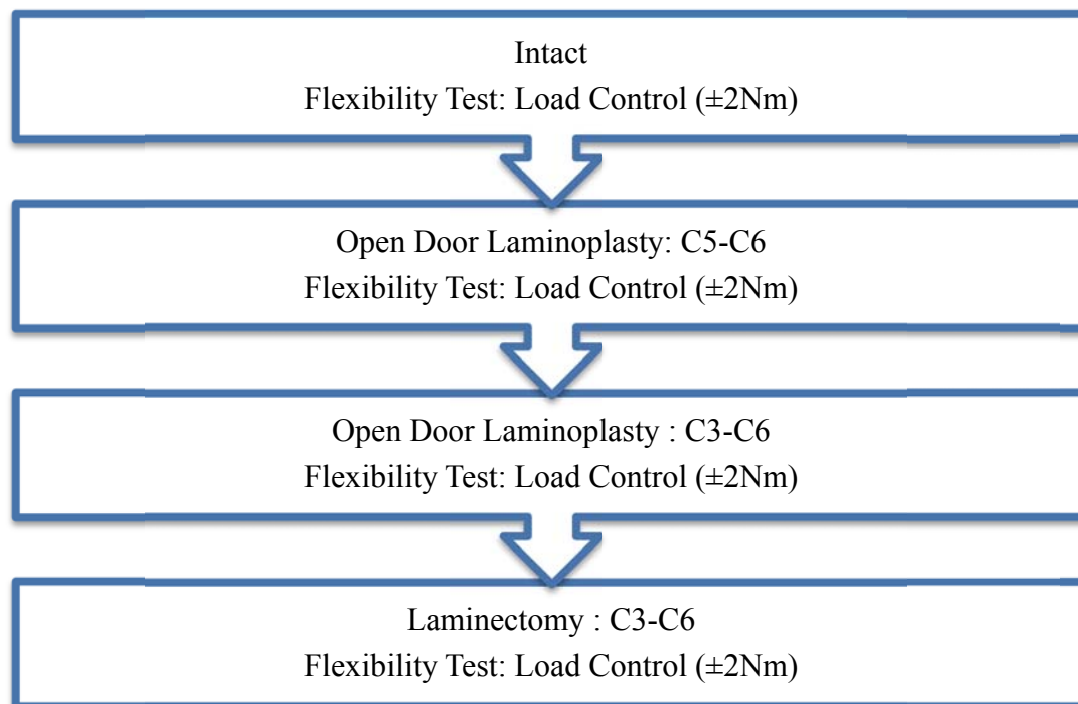


Figure 45. Flowchart showing the sequential order of biomechanical testing.

4.2.3 Surgical Techniques

4.2.3.1 Laminoplasty (C5-C6)

After testing the specimen in the intact condition, an open door laminoplasty was first performed at the C5 and C6 levels. A 3mm high speed burr was used to create a hinge on the right lamina and lateral mass junction by removing the dorsal cortex and cancellous layer. A cut of approximately 4-5mm was made on the contralateral side by using the same high speed burr. Thereafter, the spinous processes of C5 and C6 were resected. Interspinous ligaments (C4-C5, C5-C6 and C6-C7) and unilateral ligamentum flavum on the open side (C4-C5, C6-C7) were resected with a scalpel to aid in laminar opening. The lamina of the involved vertebrae were then opened gently towards the hinge and stabilized with plates and screws (*Medtronic Sofamor Danek*, Memphis, TN). A 10

mm plate was secured with 2 screws on lateral mass and one on the open end of lamina (Figure 46). Care was taken to preserve the facet capsules throughout the procedure.



Figure 46. Photograph showing a 10mm open door laminoplasty plate and screw. The left end of the plate sits on the lateral mass while the U-shaped slot holds the lamina via screws.

4.2.3.2 Laminoplasty (C3-C6)

After the C5-C6 laminoplasty was tested, the procedure was extended to the C3 and C4 levels. The additional ligaments resected included the interspinous ligaments (C2-C3, C3-C4) and unilateral ligamentum flavum on the open side at C2-C3 (Figure 47A).

4.2.3.3 Laminectomy (C3-C6)

Following the laminoplasty study at C3-C6, a laminectomy was performed (levels, C3-C6) by cutting through the hinge on the right lamina and lateral mass junction (Figure 47B). The plates and screws on the contralateral side were removed. The preserved ligamentum flavum at C2-C3 and C6-C7 was then resected for the complete removal of posterior elements.

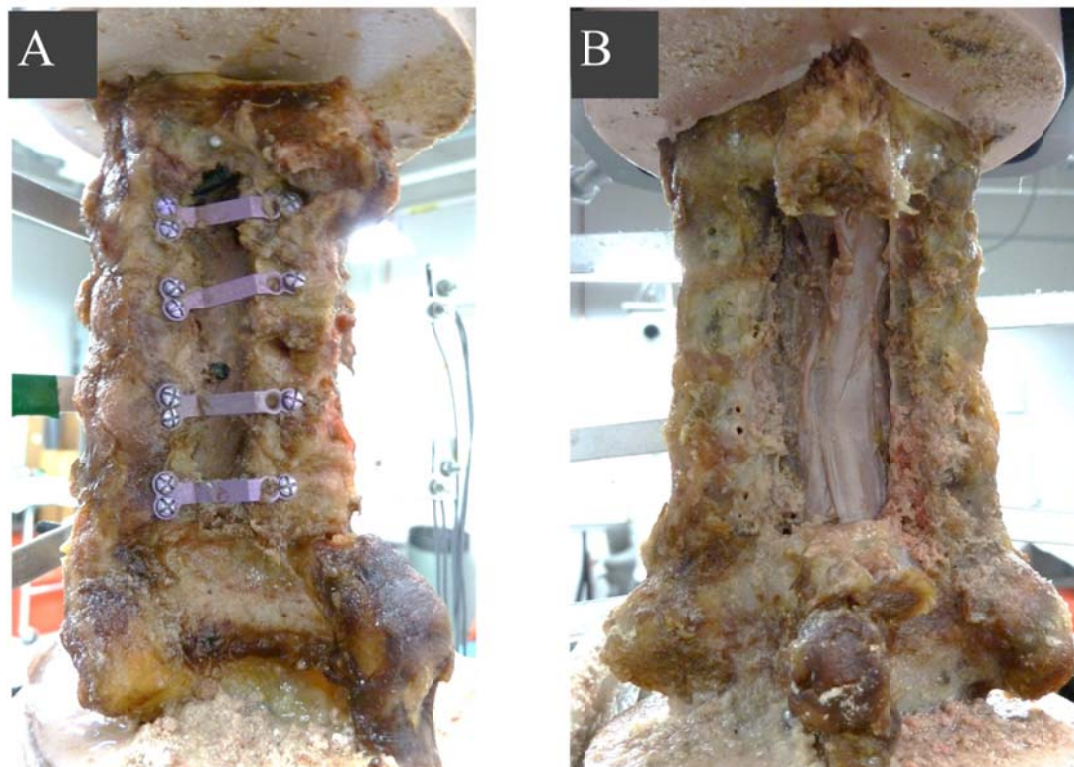


Figure 47. Photograph depicting the procedures of (A) Open door laminoplasty performed on the left side at C3-C6; the laminae were held open with plates and screws and (B) Laminectomy with the complete resection of lamina and associated ligaments at C3-C6 levels.

4.2.4 Data Analysis

A three-dimensional coordinate system was used where the positive X axis was defined towards the left, the positive Z axis anteriorly and the positive Y axis superiorly [56]. The total and segmental rotations for all the specimens after each test were exported using the Euler angle sequence which was dependent on the primary and secondary motion of interest. For example, during a flexion/extension test, the Euler sequence chosen was XZY (flexion/extension - lateral bending - axial rotation) since the dominant off axis motion was lateral bending [48]. Statistical analysis was performed using repeated measure analysis of variance and the significant differences were further

analyzed with multiple comparisons Tukey adjustments. Significant p values were defined as <0.05 for the current study.

4.3 Results

For each flexibility test, the range of motion was determined as the range of maximum rotation for a moment of $\pm 2\text{Nm}$. A sample moment-rotation curve showing the segmental rotations plotted against moment for an intact specimen during flexion/extension is shown in Figure 48. The moment-rotation (C2-T1) curves of the intact, two-level laminoplasty (LP_C56), multi-level laminoplasty (LP_C3456), and multi-level laminectomy (LT_C3456) for a specimen during flexion/extension are shown in Figure 49.

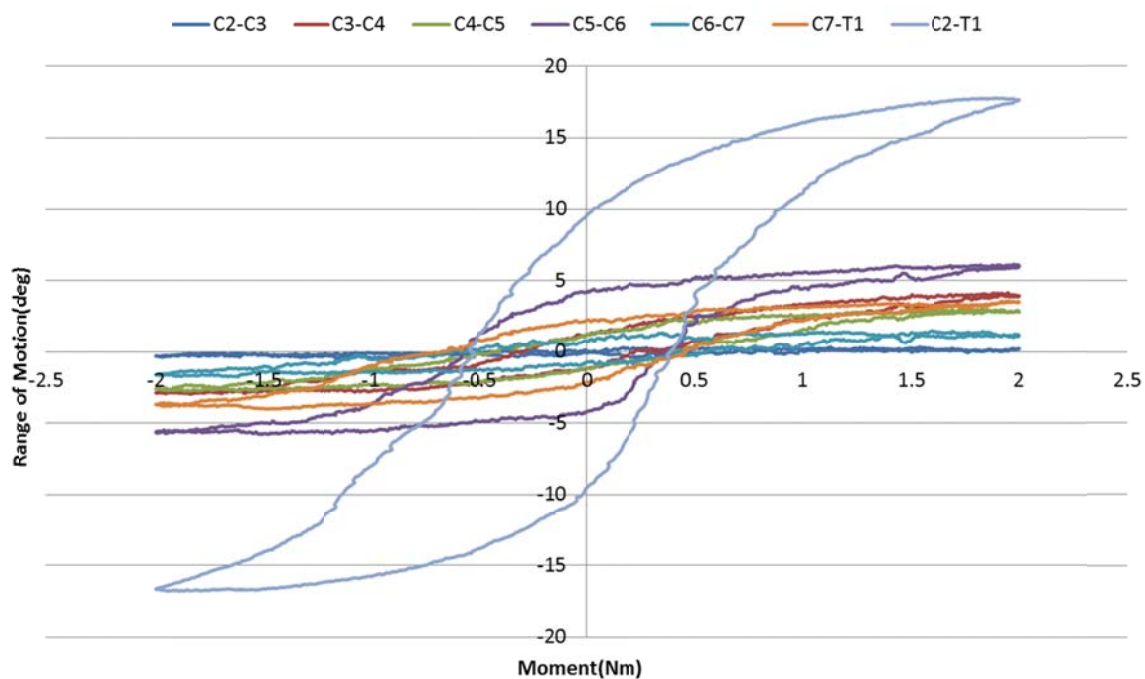


Figure 48. Sample Moment-Rotation curve from the three-dimensional flexibility test. Graph shows the segmental rotations plotted against moment for an intact specimen during flexion/extension.

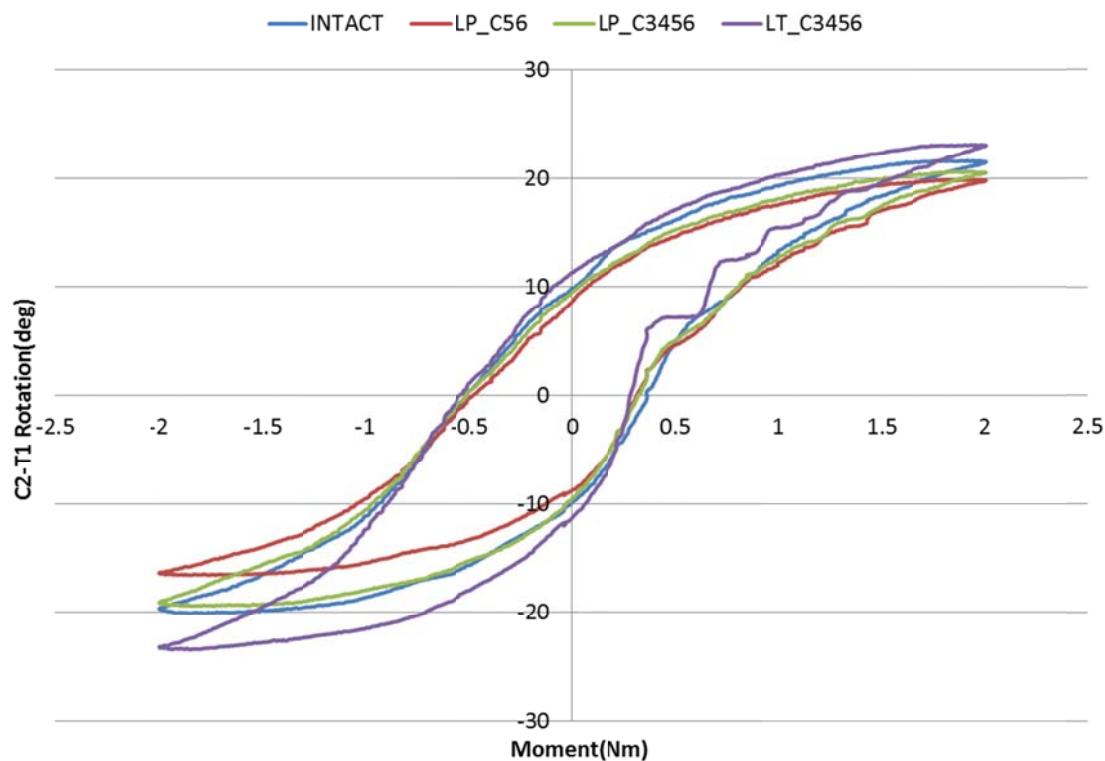


Figure 49. Moment-Rotation curves of the intact, two-level laminoplasty (LP_C56), multi-level laminoplasty (LP_C3456), multi-level laminectomy (LT_C3456) from the three dimensional flexibility test (flexion/extension).

The percent changes in motion (C2–T1; as compared to the intact state) after the laminoplasty (two-level and multi-level) and laminectomy procedures are shown in Figure 50. Compared to the intact state, an insignificant ($p=0.7844$ in flexion/extension, $p=0.8645$ in lateral bending, $p=0.9891$ in axial rotation) decrease in the C2-T1 motion was observed after two-level laminoplasty for each loading mode. Multi-level laminoplasty resulted in a minimal increase during lateral bending (4%) and axial rotation (6%). Laminectomy resulted in a statistically significant ($p<0.05$) increase in the range of motion compared to the intact and two-level conditions during the three loading modes (21% in flexion/extension, 8% in lateral bending and 15% in axial rotation compared to the intact state). Compared to the multi-level laminoplasty, laminectomy showed a 22% increase ($p=0.0369$) in flexibility during flexion/extension.

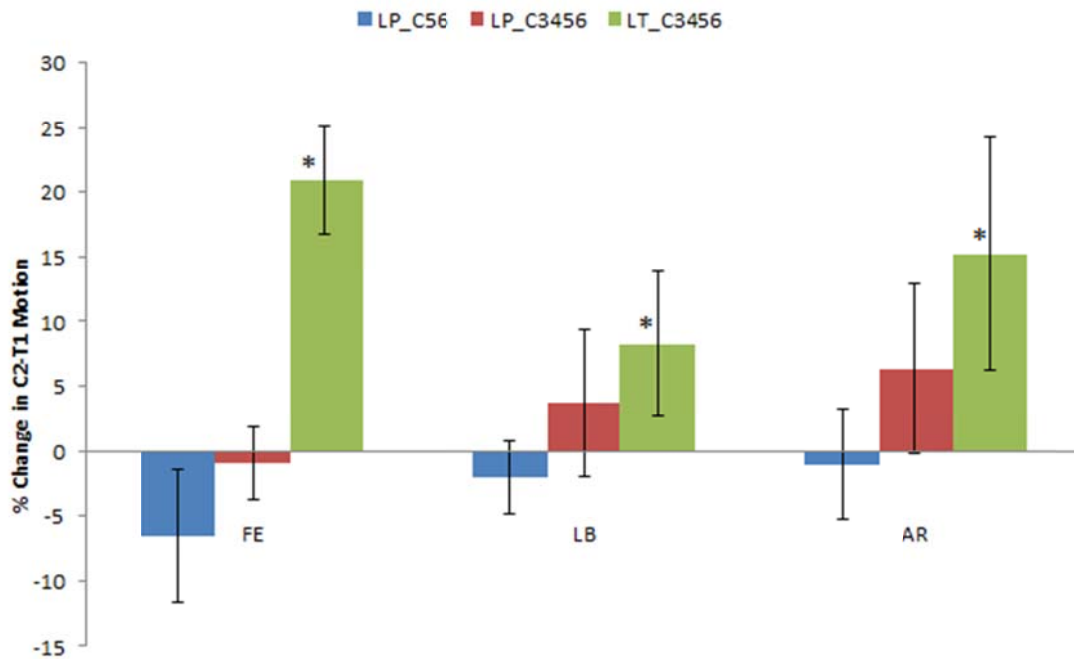


Figure 50. Percent change in C2-T1 range of motion during the three loading modes, FE (Flexion/Extension), LB (Lateral Bending) and AR (Axial Rotation). Laminoplasty (LP_C56 and LP_C3456) resulted in minimal changes while laminectomy reported significant increase in the motion compared to the intact state.

The mean intersegmental rotations for the four tested conditions during the flexion/extension, lateral bending and axial rotation are shown in Figure 51. Most notably, the superior adjacent levels namely C4-C5 and C2-C3 showed changes in motion after two-level and multi-level laminoplasty respectively.

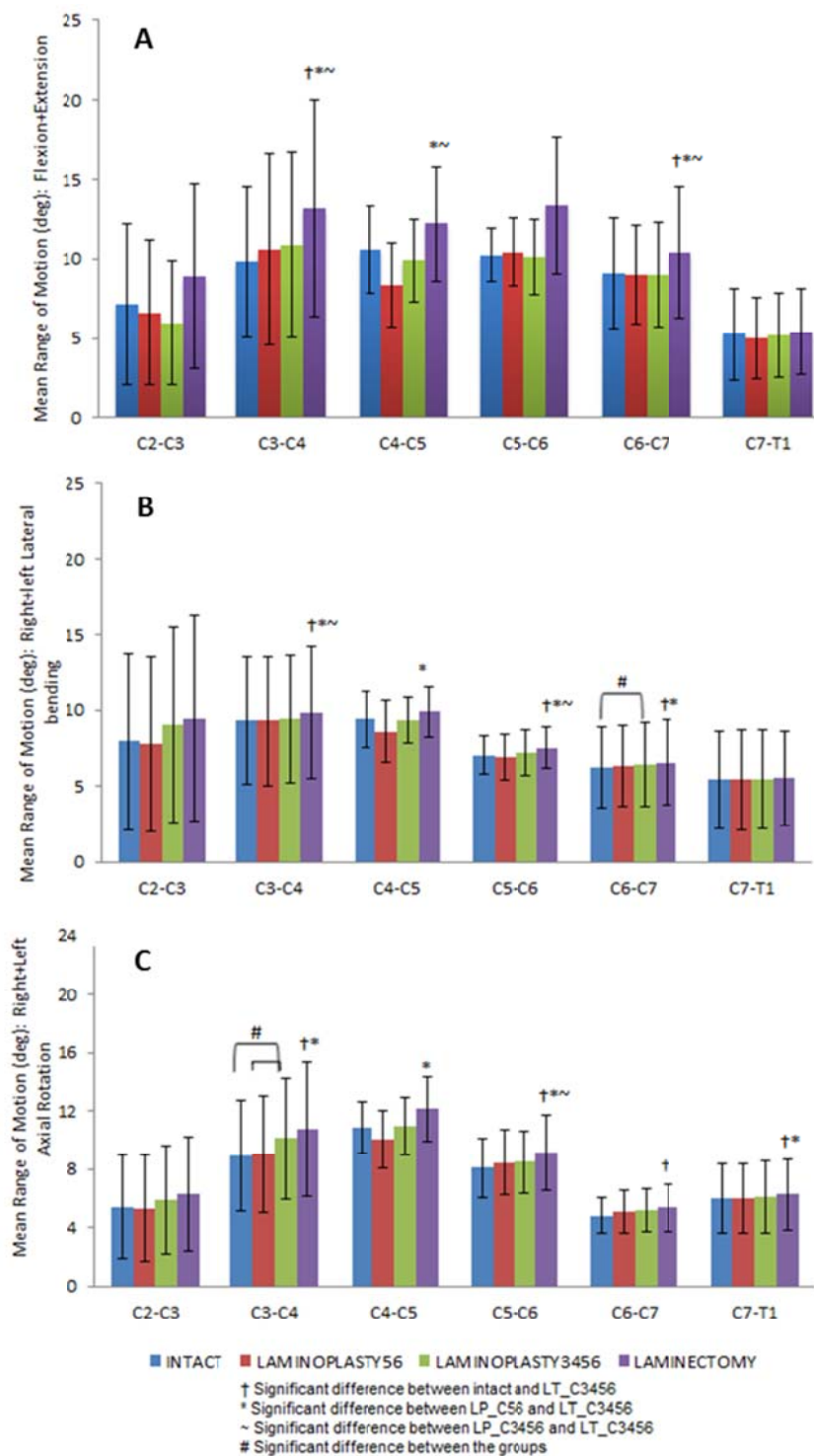


Figure 51. Mean intervertebral rotations (\pm standard deviation) for each level (C2-C3 to C7-T1) during (A) Flexion + Extension; (B) Right + Left lateral bending; (C) Right + Left axial rotation.

The percent changes after laminoplasty and laminectomy for the remainder of the paragraph are reported relative to the intact state. For flexion/extension, two-level and multi-level laminoplasty showed a 21% and 17% decrease ($p>0.05$) in the range of motion at C4-C5 and C2-C3 respectively. The percent increase in flexion/extension at the intersegmental levels (C2-C3 to C6-C7) varied from 14% to 34% approximately after laminectomy when compared to the intact condition. After two-level and multi-level laminoplasty, a 9% decrease ($p=0.117$) and 14% ($p=0.6443$) increase in lateral bending was observed at C4-C5 and C2-C3 respectively. The percent increase in lateral bending after laminectomy varied from 5% to 19% in lateral bending across levels C2-C3 to C6-C7. Axial rotation at C4-C5 decreased 7% ($p=0.4329$) after two-level laminoplasty. Multi-level Laminoplasty resulted in an increase in the axial rotation for levels C2-C3 to C6-C7. The percent changes in axial rotation after multi-level laminectomy diverged from 11% to 20% across the levels C2-C3 to C6-C7.

4.4 Discussion

Posterior surgical techniques such as laminectomy and laminoplasty allow decompression of the spinal cord by allowing the cord to drift posteriorly. Hence, such techniques are typically limited to cases in which the overall sagittal alignment is favorable to cord drift-back [33].

Achieving and maintaining an increased sagittal diameter after cervical laminoplasty is probably one of the most important criteria to facilitate neurological recovery. Clinical studies on laminoplasty with titanium miniplates have demonstrated that the technique is a safe and reliable method for preventing progression of myelopathy with multilevel involvement [81,82,123]. Deutsh et al. [81] performed open door laminoplasty using a Titanium Mesh LP miniplate and screw system with a claw positioned on the trapdoor lamina and a flat plate on the lateral mass. No intraoperative and postoperative complications were observed. Our earlier studies on single-level

laminoplasty have shown increased sagittal diameter and spinal canal area using this technique [11]. The *in vitro* and computational studies done on a single C5 vertebrae gave us the information on the loads taken by posterior bone before the failure of the laminoplasty construct [11,12]. In 2008 the U.S. laminoplasty market was valued at \$65.3 million, representing an increase of 9.5% over 2007. The advantages offered by laminoplasty over its alternatives, markedly, that laminoplasty acts as a motion preserving technique and maintains the spinal alignment will help in the future growth of the market [15]. Hence, with the increasing laminoplasty market; there is a need to critically evaluate the effect of these implants on the biomechanical stability of the spine.

The number of levels to be operated varies from patient to patient and it depends on the number of stenotic levels. Hence, it is necessary to understand the biomechanical significance of decreasing/increasing the number of operated levels. The trough and hinge creation for laminoplasty can be technically challenging. Although extreme care was taken while opening the lamina, 20% (4 vertebrae) of the hinges broke at the lamina/lateral mass junction. This may be secondary to the bony changes involved in acquisition and storage of cadaveric specimens or due in-part to the technique itself. Indeed, such hinge breakage may occur during a typical surgical procedure *in-vivo*. Despite this, the lamina was held open throughout the testing with the help of plates and screws on the contralateral (opening) side without need for plating of the broken (hinge) side. No plate/screw failures or laminar reclosures occurred at any of the levels throughout the testing of these specimens.

The range of motion data showed that both two-level and multi-level laminoplasty resulted in minimal changes while laminectomy resulted in a substantial increase in flexion and axial rotation. These results corroborate well with existing *in vitro* laminoplasty and laminectomy studies. Subramaniam et al. [13] performed open door laminoplasty and laminectomy sequentially on seven spines and tested them in flexion and extension. No significant difference in range of motion was observed between the

intact and laminoplasty specimens; however, compared to laminoplasty, laminectomy reported an increased motion during flexion ($12\% \pm 9\%$) and extension ($17\% \pm 13\%$). Nonetheless, the study lacked the lateral bending and axial rotation data and the spines were tested to a moment of 1.5Nm. Nowinski et al. [9] showed the importance of facet joints on the stability of cervical spine as little as 25% resulted in a significant increase in the range of motion. However, open door laminoplasty where the lamina was stabilized with suture did not show significant difference in the range of motion except a marginal increase in axial rotation. Puttlitz et al. [100] studied the temporal and longitudinal effects of laminoplasty in a caprine model. Both two-level and multi-level laminoplasty demonstrated a statistically insignificant decrease in the motion post-operatively, while a significant decrease in the range of motion was noted at 6 months post-op. Baisden et al. [5] used a goat model to show the significant increase in the cervical kyphosis and sagittal plane slack motion at 6 months post laminectomy while no significant differences were observed with laminoplasty when compared to the intact group. Several studies [9,114,124] have demonstrated instability of the spine post multilevel laminectomy which is evident in our current study with an approximate 20.9% increase in the flexibility during flexion/extension. This statistically significant increase in motion is notable; nevertheless, a greater volume of specimens may be necessary to understand the implications of laminoplasty versus laminectomy on single segment motions with multi-level techniques.

It should be noted that resection of the spinous process is optional during laminoplasty. Some techniques remove the spinous process and interspinous ligaments at the operated segments, while others retain these structures. Ultimately this is at the discretion of the surgeon. Our decision not to resect the spinous process cranial to the two-level laminoplasty lead to encroachment of the C4 spinous process with the opened C5 lamina during extension, thereby resulting in decreased motion at C4-C5; a similar trend was observed at C2-C3 after the multilevel laminoplasty. This decrease in the

motion was statistically insignificant and varied among the specimens. It was found to be more pronounced in older specimens and specimens with the adjacent laminae close to each other; thus leading to the encroachment of the spinous process into the opened lamina. Moreover, both left lateral bending and left axial rotation demonstrated increased ranges of motion (18% and 10%, respectively) following multi-level laminoplasty. This inclination towards an increased range of motion after left lateral bending and left axial rotation can be attributed to opening the lamina on the left side, which involved limiting resection of the ligamentum flavum to the left side. Future studies will address determining the optimal side for hinge placement and addresses the benefits and drawbacks of spinous process resection.

4.5 Conclusion

The current study proved laminoplasty to be a motion preservation technique wherein plates provided additional stability via reconstruction of the laminar arch while laminectomy can cause instability of spine. These kinds of *in vitro* studies help in understanding the effect of *in vivo* surgical procedures on the biomechanics of spine.

CHAPTER 5: APPLICATION OF ADAPTIVE BONE REMODELING THEORY TO CERVICAL LAMINOPLASTY

5.1 Introduction

The main aim of laminoplasty is to recreate a stable laminar arch that preserves the laminar opening. Restenosis owing to postoperative closure of the lamina in laminoplasty is a well-known complication. This may result either from hinge failure due to a greenstick fracture or due to a poor stabilization technique. Hence, it is essential to understand the effect of laminoplasty on the internal architecture of bone and this can be best obtained by quantifying the bone remodeling response. Clinical studies have shown that with the advent of rigid stabilization techniques (i.e. plates and screws) to hold the lamina in the open position, hinge failure has been the only primary concern in reconstructing the laminar arch [123]. Bone remodeling applied to cervical laminoplasty helps in answering certain clinical/biologic questions about the surgical procedure. For example, it helps determine the effect of this posterior based surgical procedure on the anterior vertebral bodies and hinge healing process.

Any changes to the normal architecture of the bone may result in variations of normal stress patterns. As a result, bone may engage in the process of remodeling, thereby adapting itself to the exposed functional mechanical requirements; a principle universally known as Wolff's Law. The purpose of this study is to apply an adaptive bone remodeling theory to the problem of hinge failure observed during laminoplasty. Numerical formulations of adaptive bone remodeling theory integrated with the finite element method are one of the common methods employed to study bone remodeling.

Living bone is continually undergoing processes of growth, reinforcement and resorption. These processes are termed collectively "remodeling". Bone remodeling can only take place by the activity of certain cells embedded in the matrix structure namely osteoblasts, osteocytes and osteoclasts. Mathematical models are based on the assumption

that mechanical load is sensed by osteocytes. These are then thought to stimulate the actor cells in the bone remodeling process. The actor cells, (namely osteoblasts and osteoclasts) organized in a basic multicellular unit [125] play a role in bone formation and bone resorption respectively (Figure 52). Under normal circumstances in the mature skeleton, bone resorption and bone formation are coupled. At any given remodeling site, bone formation predictably follows bone resorption such that resorbed bone is replaced with an equal amount of new bone. In summary, the bone remodeling cycle is initiated and orchestrated by osteocytes, and regulated by the crosstalk between osteoblasts and osteoclasts.

5.1.1 Bone Remodeling Theories

Frost made the distinction between internal and surface remodeling [125]. Internal remodeling is the resorptive and formative processes occurring within the space encompassed by periosteum and endosteum whereas surface remodeling occurs only on periosteal and endosteal surfaces. Literature presents several attempts made by various authors to quantify bone remodeling process. Significant amount of work has been done in the past to mathematically predict the bone formation and resorption. Finite element models serve as an ideal tool to accurately represent the internal mechanical load in terms of stresses and strains. Several authors have worked towards combining mathematical bone remodeling equations with the finite element models for quantitative predictions regarding bone formation and resorption [127-129]. All these mathematical models are based on the principle that bone remodeling is induced by a local mechanical signal that activates regulating cells to adapt accordingly by changing either the internal or external morphology (Figure 53). It is assumed that this stimulus is directly proportional to the local mechanical load in the bone that can be determined from the local stress tensor, local strain tensor or strain energy density. Apparent density or elastic modulus was used

to characterize the internal morphology while nodal surface movement was used for external morphology.

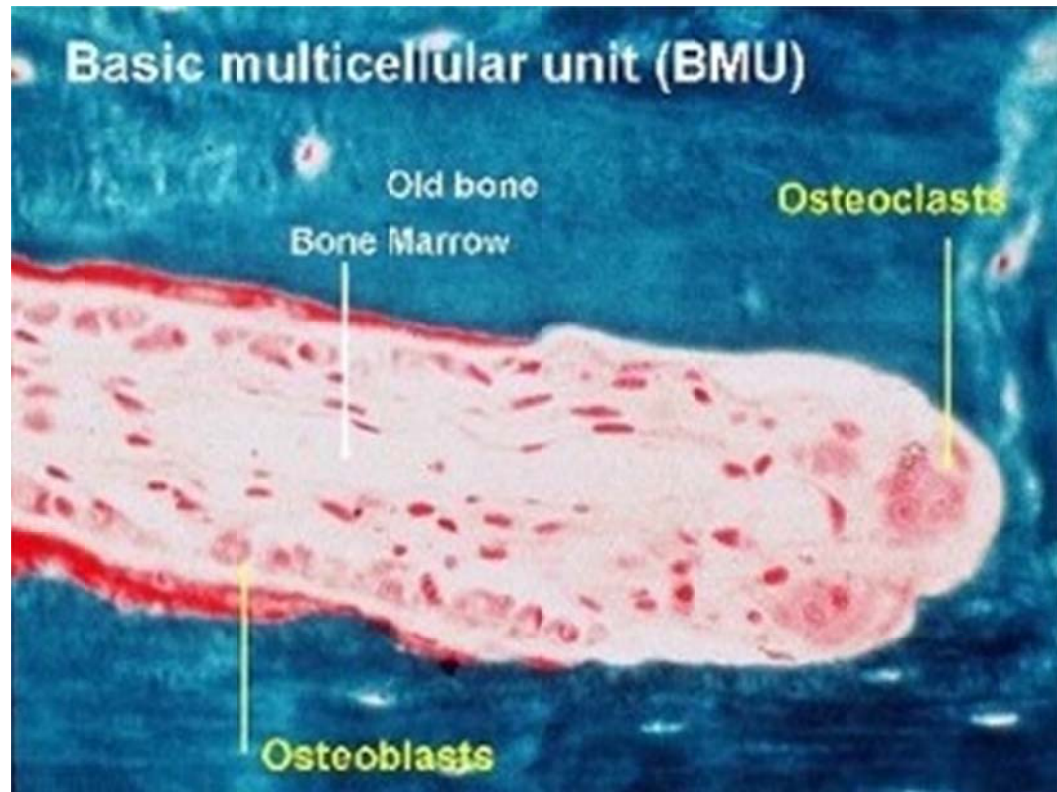


Figure 52. Basic Multicellular Unit [126].

As mentioned earlier, numerical models that applied adaptive bone remodeling theories assumed the material properties to change with the mechanical signals. The first theory to predict both the orientation and apparent density of cancellous bone was proposed by Carter and Hayes, where an empirical relationship was developed between the mechanical signal “stress” and density [131]. They assumed bone to be a self-optimizing material and derived the following Equation 1.

$$\rho = Aeff^2 \quad (1)$$

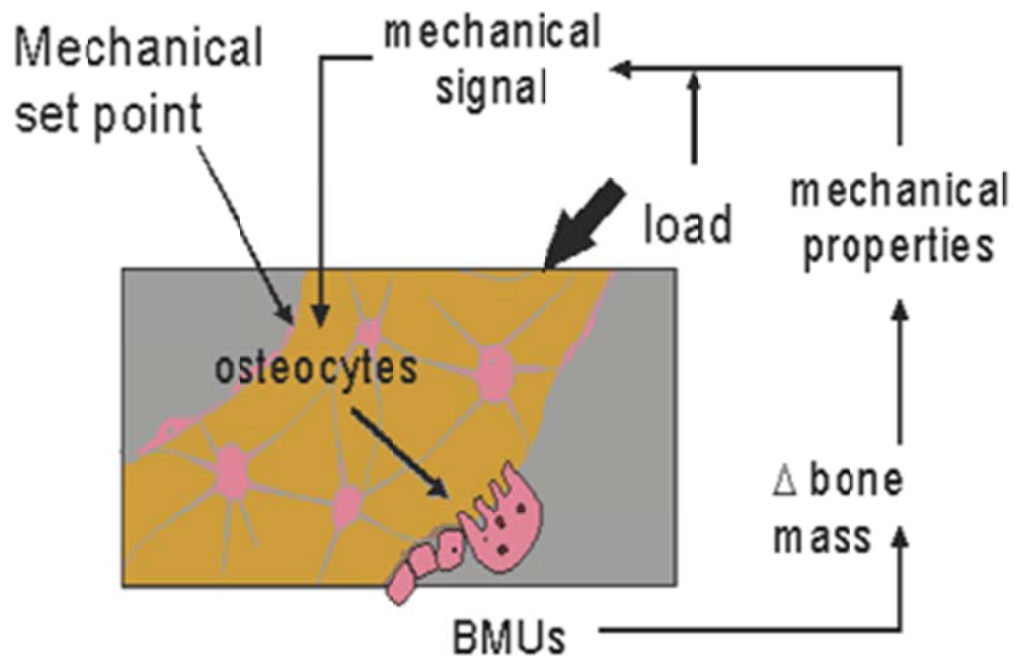


Figure 53. Biological control mechanism of adaptive bone remodeling [130].

The theory of adaptive elasticity was developed to predict the behavior of bone from one loading configuration to another by assuming a site-specific homeostatic equilibrium strain state [132,133,134]. The authors used strain tensor as the mechanical signal driving the bone adaptation until equilibrium strain state is obtained. The relationship between elastic modulus and strain rate was defined by the following

Equation 2.

$$\frac{dE}{dt} = A_{ij}(e_{ij} - e_{ij}^{\circ}) \quad (2)$$

E : Local modulus of elasticity

e_{ij} : Actual Strain tensor

e_{ij}° : Equilibrium strain tensor

A_{ij} : Remodeling coefficient.

Huiskes and coworkers used strain energy density (SED) as a signal that controls remodeling of the bone [128]. SED was defined as the strain energy per unit volume at any region inside a stress field that can be written as shown in Equation 3.

$$U = \frac{1}{2} e_{ij} s_{ij} \quad (3)$$

s_{ij} : Local stress tensor

e_{ij} : Strain Tensor

The difference between the actual SED (i.e. S), and the site-specific homeostatic SED, (i.e. S_0) was the driving force for internal and external remodeling. He later applied this remodeling algorithm to a two-dimensional FE model of a square plate to observe that the orientation of trabeculae was in correlation with the external principal stresses [135]. It was postulated by Carter that under normal conditions, there is a physiologic band of activity where bone is relatively unresponsive to changes in loading history [127]. Applying this principle to the theory of adaptive bone remodeling, a lazy zone was introduced so that, certain threshold level is exceeded before the bone reacts. Weinans et al. [136] postulated the rate of change of apparent density of the bone at a particular location in terms of mechanical stimulus like strain energy density (SED) (Equation 4).

$$\frac{d\rho}{dt} = \begin{cases} B(S - (1+s) S_0) & S > (1+s) S_0 \\ 0 & (1-s)S_0 \leq S \leq (1+s)S_0 \\ B(S - (1+s) S_0) & S < (1-s) S_0 \end{cases} \quad (4)$$

B: Remodeling Rate

S: Remodeling stimulating signal; $S = U/\rho$

s: Half width of lazy zone interval

S_0 : Reference stimulating signal

ρ : Density

5.2 Methods

5.2.1 Finite Element Model

The previously validated subject-specific 3D finite element model of the cervical spine (C2-T1) was considered [137]. Image based material properties were initially assigned to each element defining the vertebrae based on the relationship between the CT Hounsfield units (HU) and apparent density ($\rho = 0.001HU + 1$) and between the density and the elastic modulus ($E = c\rho^3$; $c = 3790$) [131].

The intact C2-T1 finite element model was modified to simulate the open door laminoplasty procedure at levels C3-C6 [138]. The procedure has been described in detail previously in Chapter 3 of the thesis.

5.2.1.1 Loading and Boundary Conditions

The inferior nodes of the T1 vertebra were fixed in all directions. The model was subjected to a compressive load of 50N, and moments of 2Nm in flexion and extension respectively. The loads were applied on the superior surface of C2. Each loading condition was considered separately and the strain energy density (SED) for each element under the three loading conditions was then averaged; thereafter the bone remodeling algorithm was applied. The finite element analysis was performed in ABAQUS 6.9.

5.2.2 Bone Remodeling Algorithm

Bone remodeling was implemented at the C5 vertebra by quantifying the changes in apparent bone density in terms of the mechanical stimulus (i.e. SED/density). Of the various available stimuli like stress, strain, strain energy density; SED, a physical quantity related to both rigidity and strength, was chosen as the signal sensed by osteocytes as it represents both stress and strain induced in bone. Moreover, being a scalar variable, it has the advantage of using a single remodeling coefficient as opposed to many coefficients [128].

The integration between the remodeling code and finite element model is shown in Figure 54. The iterative algorithm starts by determining the SED and stimulus for each element under each loading condition (i.e., compression, flexion, and extension). Thereafter, the bone density for each element was calculated based on the difference between the current stimulus and the reference stimulus (S_{ref}). As seen in Figure 55 the relationship between the mechanical stimulus and rate of change of density is a nonlinear function featuring the dead zone ($1\pm s$) that represents the minimum effective strain. The size of the dead zone depends on species and age combined with genetic, hormonal and metabolic factors. A lazy zone equivalent to $\pm 35\%$ of the reference stimulus was assumed; within these limits bone is unresponsive, yielding no net apposition or resorption. The time step in each incremental step was determined such that the maximum change in density does not exceed $1/2 \rho_{max}$ ($=0.865\text{g/cm}^3$). Subsequently, the material property assignments for each element were updated accordingly and the algorithm repeated until convergence was met. Bone remodeling algorithm was implemented using Intel Fortran Compiler 11.1.

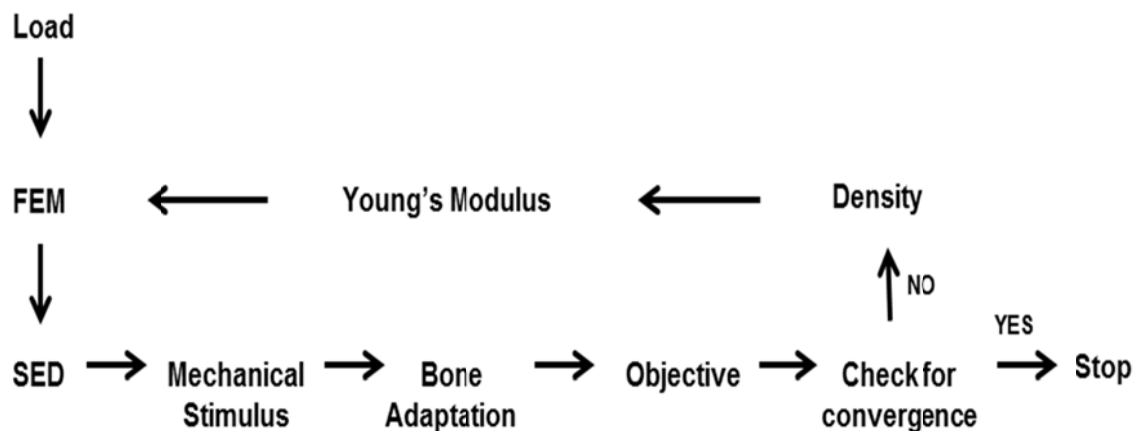


Figure 54. Adaptive bone remodeling algorithm.

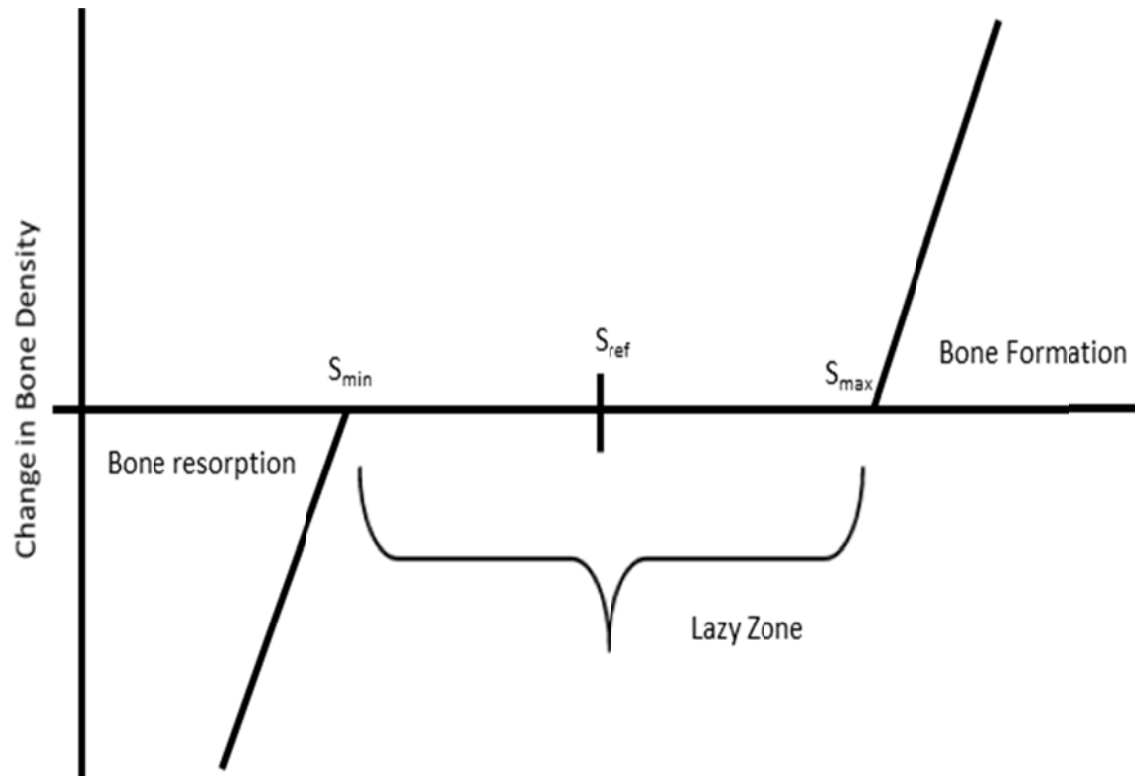


Figure 55. Graphical representation of the rate of change of bone density with the remodeling signal (strain energy density) [139].

Convergence Criteria: After each iteration, the objective function (F/N) was calculated to determine the state of convergence; where F is defined in Equation 5

$$F = \sum |S_i - (1 \pm s)S_{0,i}| \quad (5)$$

N = Number of elements satisfying the objective criteria

The model was considered to have converged when no change in the density values were observed or when the density of all the elements reached a minimum (0.01 gm/cm^3) or maximum value (1.73 gm/cm^3).

The flowchart illustrated in Figure 56 describes the site-specific bone remodeling process applied to the cervical laminoplasty model, initiating from the optimal intact state.

a) *Intact Model:* The image based material properties were applied to the intact finite element at time $t_i=0$. The bone remodeling algorithm was applied to the C5 vertebra to determine the intact optimal bone density distribution. The anterior and posterior regions of the vertebra were considered separately to avoid one being driven by the other [140]. The individual reference values (i.e., S_{ref} , anterior and posterior) were calculated as the average SED value for all elements defining each region, for each of the three loading conditions. Hence, a constant S_{ref} was assigned to each of the anterior and posterior regions. The bone remodeling algorithm was implemented separately for the anterior and posterior elements until convergence was met.

b) *Laminoplasty Model:* In order to predict the bone remodeling changes in response to laminoplasty, a site specific analysis was performed, initiating from the optimal intact configuration. The optimized bone properties were assigned to the laminoplasty model at time $t_i=0$. Moreover, the optimal site-specific SED values from the intact model served as the reference values (S_{ref}) for the laminoplasty model. Hence, S_{ref} was specific for each element. Bone remodeling was performed until convergence was met.

5.2.3 Analysis

Bone remodeling was evaluated by comparing the changes in the bone density before and after convergence in the regions of interest. The regions of interest include primarily the cortical and cancellous shells of the vertebral bodies and the laminar regions of the posterior parts of vertebra.

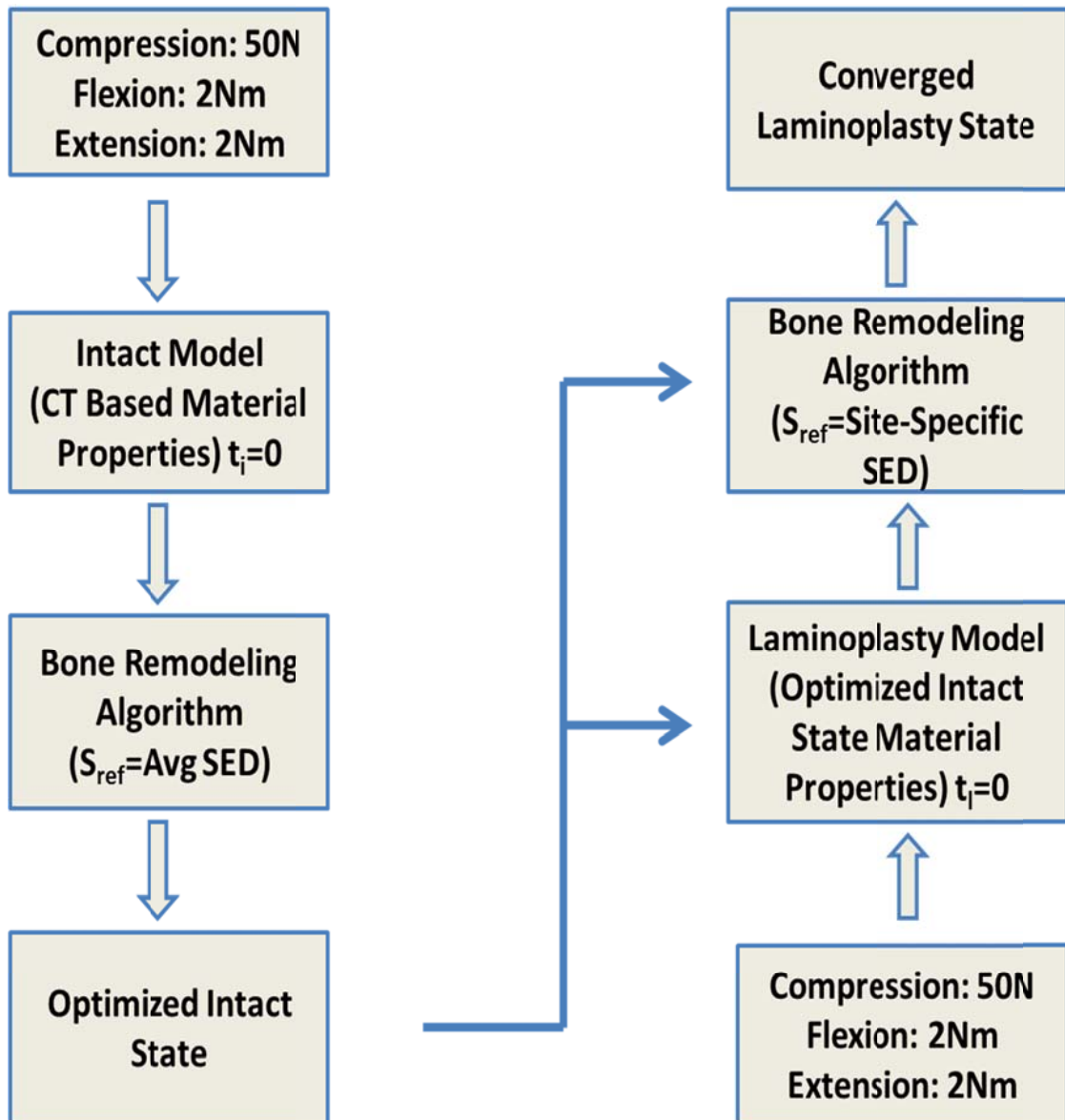


Figure 56. Flowchart showing the application of site-specific bone remodeling algorithm to cervical laminoplasty.

5.3 Results

For better visualization, the changes in the bone density distribution post bone remodeling are represented on a scale of 0.01-1.73gm/cm³. The red color corresponds to

the highest value (1.73gm/cm^3) of bone density and the blue color corresponds to the lowest value (0.01gm/cm^3) of bone density.

Figure 57A shows the initial density distribution of a C5 vertebra based on the CT measurements ($t_i=0$). This model was run through the algorithm until convergence was met (Figure 57B and Figure 57C). This is the optimal state where no further change in the density distribution was observed. The superior and mid-sagittal view of the optimal density distribution of the C5 vertebra showed an increase in the density values in the antero-superior, mid-infero cortical and pedicle regions. No significant changes in the density values were observed in posterior elements. Moments of 2Nm in the sagittal plane resulted in a flexion of 49° and extension of 43° , while a compressive load of 50N resulted in 5° of flexion. Considering the three loading modes, the increased load during flexion resulted in increased bone density in the anterior regions. No differences in the C2-T1 motion were observed with bone remodeling.

Compared to the intact model, the open door laminoplasty model resulted in a 5.4% and 1.3% increase in motion during flexion and extension respectively. Figure 58A shows the initial density distribution ($t_i=0$) in a C5 vertebra after ODL with the material properties from the optimized intact model. Bone remodeling algorithm was applied to this initial configuration of C5 vertebra until convergence was met. The converged C5 vertebra showed an increase in the density values at the hinge region and around the implants suggesting bone formation (Figure 58B). No significant changes in the bone density were observed in the anterior regions of vertebral bodies.

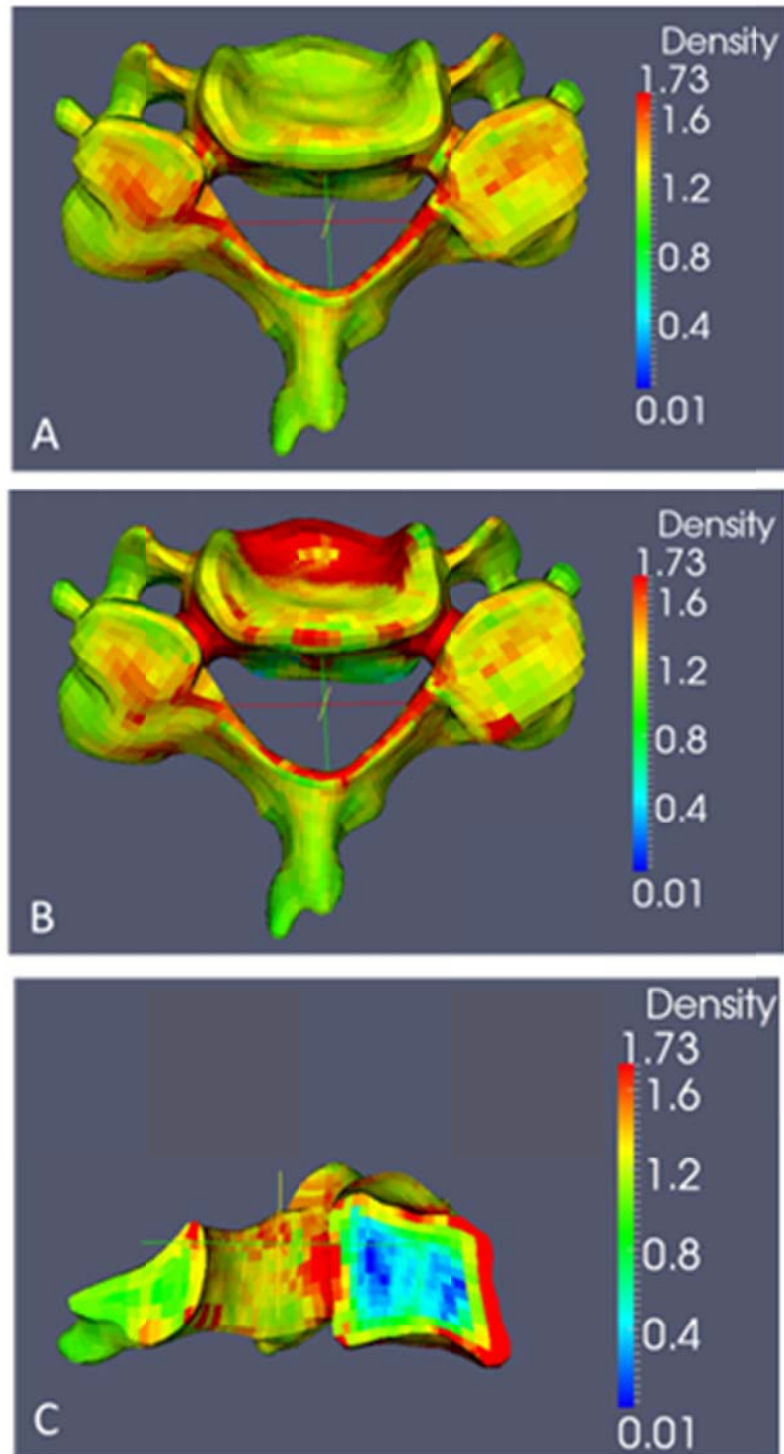


Figure 57. Density distribution in an intact C5 vertebrae (A) CT based material properties (B) Optimized material properties (Superior View) (C) Optimized material properties (Sagittal View).

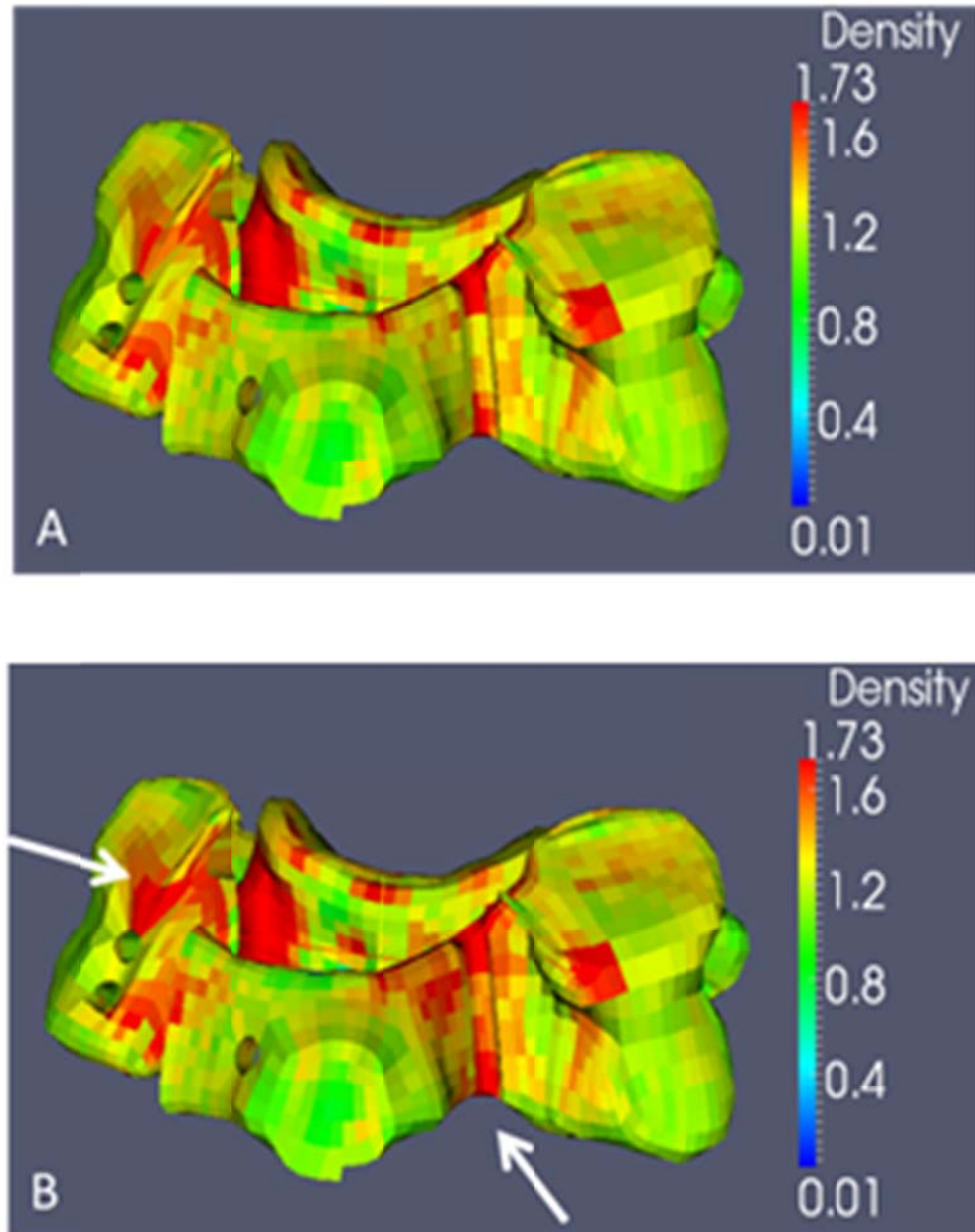


Figure 58. Density distribution in a C5 vertebra after open door laminoplasty (A) site-specific material properties from the optimized intact model (B) Optimized material properties after convergence.

5.4 Discussion

The greatest density changes in the optimized intact vertebra occurred mainly in the superior and inferior endplate regions. Bone density increased along the cortical

shells while the cancellous regions demonstrated a decrease in the density. This is in accordance with the work done by other authors, where the center of the endplate and the region between the endplates were less dense compared to other regions of the vertebrae [141,142]. These changes in the internal structure of bone can be related to the external loads. After laminoplasty, the increased load distribution through the bony hinge region led to the increased bone density during extension. This increased bone density could eventually lead to bone formation in those regions through external remodeling. These results correspond to the radiographic findings obtained from axial CT scans where complete bony union was observed at the hinge region by the end of two years [143].

Wienans et al.[144] compared quantitative adaptive bone remodeling theory to cross-sectional measurements of the canine femur after two years. They observed a good correlation in the morphology of the bone around femoral components of total hip replacements. Several other authors have successfully applied this theory in the area of hip replacement to predict stress shielding post implantation. It has also been effectively used to optimize the material and design of an implant [136,139,145,146]. With the successful application of bone remodeling theories in hip studies, several researchers considered applying it to other areas of human body like the spine [142,147] and dental regions.

The study has the general limitation associated with most of the finite element studies where the effect of muscles on the stability of the spine has been neglected. Because of the various approximations involved in the simulation of bone remodeling post laminoplasty, validation of these models is necessary. This can be performed by looking at the bone remodeling phenomena on a large scale to see if the predictions are similar to that obtained in reality or by comparing it with subject specific experimental/animal models [135]. Moreover, emphasis should be laid on testing these models under physiologic loading and boundary conditions and, by applying the

appropriate adaptive bone remodeling theory with a realistic representation of material properties of bone.

This study concentrates on internal remodeling; however the changes in the internal bone density can be correlated to changes in the external morphology by nodal surface movement. The current study shows that bone adaptation depends on the applied loading conditions and predicts changes in bone density to an altered stress/strain state. It can be concluded that adaptive bone remodeling theory can be applied to understand the process of bone remodeling following surgical simulations like open door laminoplasty. Future studies should consider correlating clinical data with subject-specific bone remodeling response.

CHAPTER 6: CONCLUSION

Cervical spondylotic myelopathy is a medical condition caused by the narrowing of the spinal canal, possibly leading to the compression of the spinal cord or other nerve roots [76,148]. Surgical options can be broadly classified into two categories namely, anterior and posterior approaches. The optimal surgical approach to treat myelopathy has been the subject of considerable debate. While each has its own share of advantages, the posterior approach is preferable in cases of multi-level involvement and posterior pathological conditions [112,113].

Laminoplasty techniques vary with type of laminar opening and hinge placement. Open door [7,8] and double door laminoplasty [86] , for example result in asymmetrical and symmetrical expansion of the spinal canal respectively. To date, numerous clinical studies [6,43,65,149] have been done to observe the effect of multi-level laminoplasty and laminectomy on the kinematics of spine. Very few *in vitro* studies have been performed and to our knowledge, this is the first computational study performed to compare the biomechanical response of the spine to multi-level laminectomy and laminoplasty. The current study employed both computational and experimental methods to understand the effect of laminoplasty and laminectomy on the operated and adjacent levels. Adaptive bone remodeling theory was also applied to determine the effect of open door laminoplasty on the internal bone density.

A validated intact finite element model was modified to simulate the surgical techniques of open door, double door laminoplasty and laminectomy techniques. To closely mimic the *in vitro/ in vivo* situation, the initial stresses developed while opening the lamina for laminoplasty were fed back into the model as initial conditions. All the four models were tested in six loading modes to determine the ranges of motion, stresses in the intervertebral discs and the laminoplasty constructs. Open door laminoplasty preserved the total C2-T1 motion but predicted increased motion at the unaltered levels

(C2-C3 and C6-C7) during flexion. Double door laminoplasty showed an inclination towards increased motion at all the levels during flexion, thereby explaining the role of the lamina-ligamentum flavum complex in the stability of spine. Maximum von Mises stresses in the laminoplasty constructs were within the yield strength of the implants. Laminectomy resulted in a profound increase in range of motion at all levels during flexion. Significant changes observed in the annular stresses after laminoplasty and laminectomy during flexion correlated with the changes in the intersegmental rotations.

In-vitro biomechanical study was conducted to address the effects of laminoplasty (two-level and multi-level) and multi-level laminectomy on the flexibility of the cervical spine. For the two-level laminoplasty during extension, the C4 spinous process impinged the C5 lamina, thereby resulting in decreased motion at C4-C5. This is attributed to the resection of spinous process only at the operated levels. Both two-level and multi-level laminoplasty resulted in minimal changes in ranges of motion while laminectomy resulted in a statistically significant increase in the range of motion compared to the intact condition during the three loading modes. The titanium miniplates used to stabilize the lamina in the open position provided the posterior stability by reconstructing the laminar arch while laminectomy can cause instability of spine.

The experimental and computational studies allowed a direct comparison of flexibility among the intact and surgically simulated models. Both studies showed preservation of motion after open door laminoplasty and a significant increase in the motion after laminectomy. Finite element simulation predicted an increase in the motion at the unaltered levels (C2-C3 and C6-C7) after open door laminoplasty while the *in vitro* study on cadaveric specimens predicted a decreased motion at the superior unaltered level. The finite element simulations showed the significant role of ligaments in the stability of spine. On the other hand, it has to be noted that the decrease in the motion observed in the cadaveric spines was statistically insignificant and was not consistent among all the specimens. The decrease was mostly observed in older specimens and

specimens with adjacent laminae close to each other; thus leading to the encroachment of the spinous process into the opened lamina. Since, the finite element model was developed from a different specimen; these geometrical differences could not be taken into account.

Stabilizing the lamina in the open position and re-creating the posterior arch is one of the primary goals of laminoplasty. The adaptive bone remodeling algorithm applied to open door laminoplasty predicted an increase in the bone density around the hinge region and the implants; thus predicting bone growth in those regions.

6.1 Future Work

The finite element model supplements *in vitro* studies in understanding the effect of the surgical procedure on the biomechanics of spine. Hence, more emphasis should be placed on finite element models mimicking the *in vitro/ in vivo* conditions. Future studies could incorporate muscle data into the finite element models. To further evaluate the effect of the surgical procedure on each level, the finite element predictions could be correlated with clinical segmental data.

Due to the limited availability of the specimens, the experimental study was restricted to only five specimens. To minimize the effect of age-, and geometry-, related differences on the flexibility of spines; more specimens will be needed to further evaluate the effect of surgical procedure on the unaltered levels.

The main aim of the current study was to compare the laminoplasty technique with the traditional method of decompression that is laminectomy. It also aimed at evaluating the motion preservation technique in detail. Future studies could consider evaluating the biomechanical effects of laminectomy and fusion, another commonly employed posterior-based surgical technique.

The current study successfully applied adaptive bone remodeling theory to simulate internal bone remodeling after open door laminoplasty. In the future, external

bone remodeling could be implemented to help determine the thickness of the bone growth. Additional loading scenarios (i.e. different magnitudes and directions) could be considered. More effort should be placed to relate HU values to density, and then with the mechanical properties of bone. Furthermore, emphasis should be placed on validating the bone remodeling theory and this could be best obtained by developing subject-specific finite element models and comparing the results with the clinical data.

REFERENCES

- [1] Bernhardt M, Hynes R,A., Blume H,W., White A,A. Cervical spondylotic myelopathy. *The Journal of Bone and Joint Surgery* 1993;75(1):119-128.
- [2] Hilibrand AS, Carlson GD, Palumbo MA, Jones PK, Bohlman HH. Radiculopathy and myelopathy at segments adjacent to the site of a previous anterior cervical arthrodesis. *The Journal of Bone and Joint Surgery* 1999;81(4):519-528.
- [3] Weinhoffer SL, Guyer RD, Herbert M, Griffith SL. Intradiscal pressure measurements above an instrumented fusion: a cadaveric study. *Spine* 1995;20(5):526-531.
- [4] Bohlman H, Emery S, Goodfellow D, Jones P. Robinson anterior cervical discectomy and arthrodesis for cervical radiculopathy. Long-term follow-up of one hundred and twenty-two patients. *The Journal of Bone and Joint Surgery* 1993;75(9):1298-1307.
- [5] Baisden J, Voo LM, Cusick JF, Pintar FA, Yoganandan N. Evaluation of cervical laminectomy and laminoplasty: a longitudinal study in the goat model. *Spine* 1999;24(13):1283-1289.
- [6] Matsunaga S, Sakou T, Nakanisi K. Analysis of the cervical spine alignment following laminoplasty and laminectomy. *Spinal Cord* 1999;37(1):20-24.
- [7] Hirabayashi K. Expansive open-door laminoplasty for cervical spondylotic myelopathy. *Jpn J Surg* 1978;32:1159-1163.
- [8] Hirabayashi K, Watanabe K, Wakano K, Suzuki N, Satomi K, Ishii Y. Expansive open-door laminoplasty for cervical spinal stenotic myelopathy. *Spine* 1983;8(7):693-699.
- [9] Nowinski GP, Visarius H, Nolte LP, Herkowitz HN. A biomechanical comparison of cervical laminoplasty and cervical laminectomy with progressive facetectomy. *Spine* 1993;18(14):1995-2004.
- [10] Kubo S, Goel VK, Yang SJ, Tajima N. Biomechanical evaluation of cervical double-door laminoplasty using hydroxyapatite spacer. *Spine* 2003;28(3):227-234.
- [11] Tadepalli S, Kallameyn N, Shivanna K, Smucker J, Fredericks D, Grosland N. Cervical Laminoplasty Construct Stability: A Finite Element Study. In the Proceedings of ASME Summer Bioengineering Conference June 2008.
- [12] Tadepalli S, Gandhi A, Fredericks D, Smucker J, Grosland N. Cervical laminoplasty construct stability: experimental and finite element investigation. In the Proceedings of American Society of Biomechanics August 2009.

[13] Subramaniam V, Chamberlain RH, Theodore N, Baek S, Safavi-Abbasi S, Senoglu M, et al. Biomechanical effects of laminoplasty versus laminectomy: stenosis and stability. *Spine* 2009;34(16):E573-E578.

[14] Wang M, Yokoyama T, Numasawa T, Toh S, McGrady L, Toth J. Biomechanical Evaluation of a Modified Cervical Laminoplasty. *The Spine Journal* 2006;6:141S-142S.

[15] U.S. Market for Spinal Laminoplasty 2009. iData Research Inc. 2009.

[16] Spine Universe. <http://www.spineuniverse.com/anatomy/vertebral-column>.

[17] Hughston Clinic. <http://www.hughston.com/hha/a.cspine.htm>.

[18] Hochman M, Tuli S. Cervical Spondylotic Myelopathy: A Review. *The Internet Journal of Neurology* 2005;4(1).

[19] Bao QB, McCullen GM, Higham PA, Dumbleton JH, Yuan HA. The artificial disc: theory, design and materials. *Biomaterials* 1996;17(12):1157-1167.

[20] Nachemson A. Lumbar intradiscal pressure. Experimental studies on post-mortem material. *Acta Orthop Scand Suppl* 1960;43:1-104.

[21] King AI, Prasad P, Ewing CL. Mechanism of spinal injury due to caudocephalad acceleration. *Orthop Clin North Am* 1975 Jan;6(1):19-31.

[22] Spine Universe.
<http://www.spineuniverse.com/treatments/surgery/cervical/posterior-cervical-foraminotomy-surgical-technique>.

[23] Simeone FA, Rothman R. Cervical disc disease. *The Spine*. Philadelphia, WB Saunders 1982:440-496.

[24] Fehlings MG, Skaf G. A review of the pathophysiology of cervical spondylotic myelopathy with insights for potential novel mechanisms drawn from traumatic spinal cord injury. *Spine* 1998;23(24):2730-2736.

[25] Penning L, Wilmsink J, Van Woerden H, Knol E. CT myelographic findings in degenerative disorders of the cervical spine: clinical significance. *Am J Roentgenol* 1986;146(4):793.

[26] Neo Spine. <http://www.neospine.com/cervical-epidural-injection.php>.

[27] Young WF. Cervical spondylotic myelopathy: a common cause of spinal cord dysfunction in older persons. *Am Fam Physician* 2000 Sep 1;62(5):1064-70, 1073.

[28] Brain WR, Knight GC, Bull JW. Discussion of rupture of the intervertebral disc in the cervical region. *Proc R Soc Med* 1948 Aug;41(8):509-516.

[29] Mair W, Druckman R. The pathology of spinal cord lesions and their relation to the clinical features in protrusion of cervical intervertebral discs (a report of four cases). *Brain* 1953;76(1):70-91.

[30] Bushell G, Ghosh P, Taylor T, Sutherland J, Braund K. The effect of spinal fusion on the collagen and proteoglycans of the canine intervertebral disc. *J Surg Res* 1978;25(1):61-69.

[31] Huang RC, Girardi FP, Lim MR, Cammisa FP. Advantages and disadvantages of nonfusion technology in spine surgery. *Orthop Clin North Am* 2005;36(3):263-269.

[32] Synthes. <http://www.synthes.com>.

[33] Rhee JM, Basra S. Posterior Surgery for Cervical Myelopathy: Laminectomy, Laminectomy with Fusion, and Laminoplasty. *Asian Spine Journal* 2008;2(2):114-126.

[34] Rogers L. The treatment of cervical spondylitic myelopathy by mobilisation of the cervical cord into an enlarged spinal canal. *J Neurosurg* 1961;18:490.

[35] Scoville WB. Cervical spondylosis treated by bilateral facetectomy and laminectomy. *J Neurosurg* 1961 Jul;18:423-428.

[36] Stoops WL, King RB. Neural complications of cervical spondylosis: their response to laminectomy and foramenotomy. *J Neurosurg* 1962 Nov;19:986-999.

[37] Brain BWRB. *Cervical Spondylosis and Other Disorders of the Cervical Spine*: Edited by Lord Brain and Marcia Wilkinson. : Saunders; 1967.

[38] Mixter WJ, Ayer JB. Herniation or rupture of the intervertebral disc into the spinal canal. *N Engl J Med* 1935;213(9):385-393.

[39] eOrthopod. <http://www.eorthopod.com/content/cervical-laminectomy>.

[40] Steinmetz MP, Resnick DK. Cervical laminoplasty. *The Spine Journal* 2006;6(6):S274-S281.

[41] Edwards CC, Heller JG, Murakami H. Corpectomy versus laminoplasty for multilevel cervical myelopathy: an independent matched-cohort analysis. *Spine* 2002;27(11):1168.

[42] Koakutsu T, Morozumi N, Ishii Y, Kasama F, Sato T, Tanaka Y, et al. Anterior decompression and fusion versus laminoplasty for cervical myelopathy caused by soft disc herniation: a prospective multicenter study. *Journal of Orthopaedic Science* 2010;15(1):71-78.

[43] Herkowitz HN. A comparison of anterior cervical fusion, cervical laminectomy, and cervical laminoplasty for the surgical management of multiple level spondylotic radiculopathy. *Spine* 1988;13(7):774.

[44] Brekelmans WAM, Poort HW, Slooff T. A new method to analyse the mechanical behaviour of skeletal parts. *Acta Orthopaedica* 1972;43(5):301-317.

[45] Yoganandan N, Kumaresan S, Voo L, Pintar FA. Finite element applications in human cervical spine modeling. *Spine* 1996;21(15):1824.

[46] Clausen JD, Goel VK, Traynelis VC, Scifert J. Uncinate processes and Luschka joints influence the biomechanics of the cervical spine: Quantification using a finite element model of the C5-C6 segment. *Journal of orthopaedic research* 1997;15(3):342-347.

[47] Kallemeyn N, Shivanna K, Gandhi A, Kode S, Grosland N. Subject-Specific Experimental Validation of a C27 cervical spine finite element model. Summer Bioengineering Conference 2009.

[48] Kallemeyn N, Gandhi A, Kode S, Shivanna K, Smucker J, Grosland N. Validation of a C2-C7 cervical spine finite element model using specimen-specific flexibility data. *Med Eng Phys* 2010;32(5):482-489.

[49] Magnotta VA, Harris G, Andreasen NC, O'Leary DS, Yuh WTC, Heckel D. Structural MR image processing using the BRAINS2 toolbox. *Comput Med Imaging Graphics* 2002;26(4):251-264.

[50] DeVries NA, Gassman EE, Kallemeyn NA, Shivanna KH, Magnotta VA, Grosland NM. Validation of phalanx bone three-dimensional surface segmentation from computed tomography images using laser scanning. *Skeletal Radiol* 2008;37(1):35-42.

[51] Kallemeyn NA, Tadepalli SC, Shivanna KH, Grosland NM. An interactive multiblock approach to meshing the spine. *Comput Methods Programs Biomed* 2009;95(3):227-235.

[52] Sharma M, Langrana NA, Rodriguez J. Role of ligaments and facets in lumbar spinal stability. *Spine* 1995;20(8):887.

[53] Percy M,J., Tibrewal S,B. Lumbar intervertebral disc and ligament deformations measured in vivo. *Clin Orthop* 1984;191:281.

[54] Fagan M,J., Julian S, Siddall D,J., Mohsen A,M. Patient-specific spine models. Part 1: finite element analysis of the lumbar intervertebral disc—a material sensitivity study. *Proc Inst Mech Eng Part H J Eng Med* 2002;216(5):299-314.

[55] Schmidt H, Heuer F, Simon U, Kettler A, Rohlmann A, Claes L, et al. Application of a new calibration method for a three-dimensional finite element model of a human lumbar annulus fibrosus. *Clin Biomech* 2006;21(4):337-344.

[56] Panjabi MM. Biomechanical evaluation of spinal fixation devices: I. A conceptual framework. *Spine* 1988;13(10):1129.

[57] Zhang QH, Teo EC, Ng HW, Lee VS. Finite element analysis of moment-rotation relationships for human cervical spine. *J Biomech* 2006;39(1):189-193.

[58] CT Based Three Dimensional Finite Element Model of Cervical Spine. *Biomedical and Pharmaceutical Engineering, 2006. ICBPE 2006. International Conference on: IEEE; 2006.*

[59] del Palomar AP, Calvo B, Doblaré M. An accurate finite element model of the cervical spine under quasi-static loading. *J Biomech* 2008;41(3):523-531.

[60] Wheeldon JA, Pintar FA, Knowles S, Yoganandan N. Experimental flexion/extension data corridors for validation of finite element models of the young, normal cervical spine. *J Biomech* 2006;39(2):375-380.

[61] Epstein JA. The surgical management of cervical spinal stenosis, spondylosis, and myeloradiculopathy by means of the posterior approach. *Spine* 1988;13(7):864.

[62] xzzzoijm-Live Journal. <http://xzzzoijm.livejournal.com/41079.html>.

[63] Kaptain GJ, Simmons NE, Replogle RE, Pobereskin L. Incidence and outcome of kyphotic deformity following laminectomy for cervical spondylotic myelopathy. *Journal of Neurosurgery: Spine* 2000;93(2):199-204.

[64] Sim FH, Svien HJ, Bickel WH, Janes JM. Swan-neck deformity following extensive cervical laminectomy: A review of twenty-one cases. *The Journal of Bone and Joint Surgery* 1974;56(3):564.

[65] Epstein N,E. Laminectomy for cervical myelopathy. *Spinal Cord* 2003;41(6):317-327.

[66] Heller JG, Edwards CC, Murakami H, Rodts GE. Laminoplasty versus laminectomy and fusion for multilevel cervical myelopathy: an independent matched cohort analysis. *Spine* 2001;26(12):1330.

[67] Nakamura K, Toyama Y, Hoshino Y editors. Cervical Laminoplasty. 1st ed.: Springer; 2003.

[68] Park AE, Heller JG. Cervical laminoplasty: use of a novel titanium plate to maintain canal expansion-surgical technique. *Journal of spinal disorders & techniques* 2004;17(4):265.

[69] Pal G, Routal R. The role of the vertebral laminae in the stability of the cervical spine. *J Anat* 1996;188(Pt 2):485-489.

[70] Hosono N, Sakaura H, Mukai Y, Fujii R, Yoshikawa H. C3-6 laminoplasty takes over C3-7 laminoplasty with significantly lower incidence of axial neck pain. *European Spine Journal* 2006;15(9):1375-1379.

[71] Wang JM, Roh KJ, Kim DJ, Kim DW. A new method of stabilising the elevated laminae in open-door laminoplasty using an anchor system. *Journal of Bone and Joint Surgery-British Volume* 1998;80(6):1005.

[72] Lee JY, Hanks SE, Oxner W, Tannoury C, Donaldson III WF, Kang JD. Use of small suture anchors in cervical laminoplasty to maintain canal expansion: a technical note. *Journal of Spinal Disorders & Techniques* 2007;20(1):33.

[73] Matsumoto M, Watanabe K, Tsuji T, Ishii K, Takaishi H, Nakamura M, et al. Risk factors for closure of lamina after open-door laminoplasty. *Journal of Neurosurgery: Pediatrics* 2008;9(6).

[74] Buffalo Neurosurgery Group.
http://buffaloneuro.com/cervical/cervical_post_laminectomy.htm.

[75] O'Brien MF, Peterson D, Casey ATH, Crockard HA. A novel technique for laminoplasty augmentation of spinal canal area using titanium miniplate stabilization: a computerized morphometric analysis. *Spine* 1996;21(4):474-483.

[76] Ratliff JK, Cooper PR. Cervical laminoplasty: a critical review. *Journal of Neurosurgery: Spine* 2003;98(3):230-238.

[77] Hyun SJ, Rhim SC, Roh SW, Kang SH, Riew KD. The time course of range of motion loss after cervical laminoplasty: a prospective study with minimum two-year follow-up. *Spine* 2009;34(11):1134.

[78] Kang SH, Rhim SC, Roh SW, Jeon SR, Baek HC. Postlaminoplasty cervical range of motion: early results. *Journal of Neurosurgery: Spine* 2007;6(5):386-390.

[79] Vitarbo E, Sheth RN, Levi AD. Open-door expansile cervical laminoplasty. *Neurosurgery* 2007;60(1):S1.

[80] Frank E, Keenen TL. A technique for cervical laminoplasty using mini plates. *Br J Neurosurg* 1994;8(2):197-199.

[81] Deutsch H, Mummaneni PV, Rodts GE, Haid RW. Posterior cervical laminoplasty using a new plating system: technical note. *Journal of spinal disorders & techniques* 2004;17(4):317-320.

[82] Dimar 2nd J, Bratcher KR, Brock D, Glassman SD, Campbell MJ, Carreon LY. Instrumented open-door laminoplasty as treatment for cervical myelopathy in 104 patients. *Am J Orthop (Belle Mead NJ)* 2009;38:E123-E128.

[83] Shaffrey CI, Wiggins GC, Piccirilli CB, Young JN, Lovell LVR. Modified open-door laminoplasty for treatment of neurological deficits in younger patients with congenital spinal stenosis: analysis of clinical and radiographic data. *Journal of Neurosurgery: Pediatrics* 1999;90(2).

[84] Grosland NM, Shivanna KH, Magnotta VA, Kallemeyn NA, DeVries NA, Tadepalli SC, et al. IA-FEMesh: An open-source, interactive, multiblock approach to anatomic finite element model development. *Comput Methods Programs Biomed* 2009;94(1):96-107.

[85] Puttlitz CM, Goel VK, Traynelis VC, Clark CR. A finite element investigation of upper cervical instrumentation. *Spine* 2001;26(22):2449.

[86] Kurokawa T, Tsuyama N, Tanaka H, Kobayashi M, Machida H, Nakamura K. Double-door laminoplasty. *Bessatsu Seikeigeka* 1982;2:234-240.

[87] Miyata M, Neo M, Fujibayashi S, Takemoto M, Nakamura T. Double-door cervical laminoplasty with the use of suture anchors: technical note. *Journal of Spinal Disorders & Techniques* 2008;21(8):575.

[88] Nakano K, Harata S, Suetsuna F, Araki T, Itoh J. Spinous process-splitting laminoplasty using hydroxyapatite spinous process spacer. *Spine* 1992;17:41.

[89] Ueyama K, Harata S, Okada A, Echigoya N, Yokoyama T. Midline Spinous Process Splitting Laminoplasty Using Hydroxyapatite Spacers. *Cervical Laminoplasty* 2003:111.

[90] Hirabayashi S, Kumano K. Finite Element Analysis of the Space Created by Split Spinous Processes in Double-Door Laminoplasty to Optimize Shape of an Artificial Spacer. *J Musculoskeletal Res* 2000;4(1):47-54.

[91] Aita I, Yabuki T, Wadano Y. Bilateral Open Laminoplasty Using the Spinous Process as Bone Blocks. *Cervical Laminoplasty* 2003:119.

[92] Kaito T, Hosono N, Makino T, Kaneko N, Namekata M, Fuji T. Postoperative displacement of hydroxyapatite spacers implanted during double-door laminoplasty. *Journal of Neurosurgery: Spine* 2009;10(6):551-556.

[93] Patel CK, Cunningham BJ, Herkowitz HN. Techniques in cervical laminoplasty. *The Spine Journal* 2002;2(6):450-455.

[94] Takayasu M, Takagi T, Nishizawa T, Osuka K, Nakajima T, Yoshida J. Bilateral open-door cervical expansive laminoplasty with hydroxyapatite spacers and titanium screws. *Journal of Neurosurgery: Spine* 2002;96(1):22-28.

[95] Saruhashi Y, Hukuda S, Katsuura A, Miyahara K, Asajima S, Omura K. A long-term follow-up study of cervical spondylotic myelopathy treated by "French window" laminoplasty. *Journal of Spinal Disorders & Techniques* 1999;12(2):99.

[96] Morimoto T, Matsuyama T, Hirabayashi H, Sakaki T, Yabuno T. Expansive laminoplasty for multilevel cervical OPLL. *Journal of Spinal Disorders & Techniques* 1997;10(4):296.

[97] Tomita K, Kawahara N, Toribatake Y, Heller JG. Expansive midline T-saw laminoplasty (modified spinous process-splitting) for the management of cervical myelopathy. *Spine* 1998;23(1):32.

[98] Seichi A, Takeshita K, Ohishi I, Kawaguchi H, Akune T, Anamizu Y, et al. Long-term results of double-door laminoplasty for cervical stenotic myelopathy. *Spine* 2001;26(5):479.

[99] Goto T, Ohata K, Takami T, Nishikawa M, Tsuyuguchi N, Morino M, et al. Hydroxyapatite laminar spacers and titanium miniplates in cervical laminoplasty. *Journal of Neurosurgery: Spine* 2002;97(3):323-329.

[100] Puttlitz CM, Deviren V, Smith JA, Kleinstueck FS, Tran QNH, Thurlow RW, et al. Biomechanics of cervical laminoplasty: kinetic studies comparing different surgical techniques, temporal effects and the degree of level involvement. *European Spine Journal* 2004;13(3):213-221.

[101] Liu DM. Preparation and characterisation of porous hydroxyapatite bioceramic via a slip-casting route. *Ceram Int* 1998;24(6):441-446.

[102] Iguchi T, Kanemura A, Kurihara A, Kasahara K, Yoshiya S, Doita M, et al. Cervical laminoplasty: evaluation of bone bonding of a high porosity hydroxyapatite spacer. *Journal of Neurosurgery: Pediatrics* 2003;98(2).

[103] Rasband WS, ImageJ U. National Institutes of Health, Bethesda, Maryland, USA 1997.

[104] Wang XY, Dai LY, Xu HZ, Chi YL. Prediction of spinal canal expansion following cervical laminoplasty: a computer-simulated comparison between single and double-door techniques. *Spine* 2006;31(24):2863.

[105] Benglis Jr DM, Guest JD, Wang MY. Clinical feasibility of minimally invasive cervical laminoplasty. *Journal of Neurosurgery: Pediatrics* 2008;25(2).

[106] Kumaresan S, Yoganandan N, Pintar FA, Voo LM, Cusick JF, Larson SJ. Finite element modeling of cervical laminectomy with graded facetectomy. *Journal of Spinal Disorders & Techniques* 1997;10(1):40.

[107] Hong-Wan N, Ee-Chon T, Qing-Hang Z. Biomechanical effects of C2-C7 intersegmental stability due to laminectomy with unilateral and bilateral facetectomy. *Spine* 2004;29(16):1737.

[108] Goel VK, Clark CR, Harris KG, Schulte KR. Kinematics of the cervical spine: effects of multiple total laminectomy and facet wiring. *Journal of orthopaedic research* 1988;6(4):611-619.

[109] Ding S, Zhang Z, Jiang Z, Gu X, Li H, Wang Y. Biomechanical evaluation of cervical spine instability after multiple level laminectomy. *Chin Med J* 1991;104(8):626.

[110] Detwiler PW, Spetzler CB, Taylor SB, Crawford NR, Porter RW, Sonntag VKH. Biomechanical comparison of facet-sparing laminectomy and Christmas tree laminectomy. *Journal of Neurosurgery: Spine* 2003;99(2):214-220.

[111] Kode S, Gandhi AA, Fredericks DC, Grosland NM, Smucker JD. Effect of Multi-Level Open Door Laminoplasty and Laminectomy on Flexibility of the Cervical Spine: An Experimental Investigation. Manuscript submitted to *Spine* (Under Review) 2011.

[112] White A,III, Panjabi MM. Biomechanical considerations in the surgical management of cervical spondylotic myelopathy. *Spine* 1988;13(7):856-860.

[113] Orr RD, Zdeblick TA. Cervical spondylotic myelopathy: approaches to surgical treatment. *Clin Orthop* 1999;359:58-66.

[114] Fields MJ, Hoshijima K, Feng AHP, Richardson WJ, Myers BS. A biomechanical, radiologic, and clinical comparison of outcome after multilevel cervical laminectomy or laminoplasty in the rabbit. *Spine* 2000;25(22):2925-2931.

[115] Panjabi MM. Hybrid multidirectional test method to evaluate spinal adjacent-level effects. *Clin Biomech* 2007;22(3):257-265.

[116] Goel VK, Nye TA, Clark CR, Nishiyama K, Weinstein JN. A technique to evaluate an internal spinal device by use of the Selspot system: an application to Luque closed loop. *Spine* 1987;12(2):150.

[117] Crawford NR, Brantley AGU, Dickman CA, Koeneman EJ. An apparatus for applying pure nonconstraining moments to spine segments in vitro. *Spine* 1995;20(19):2097.

[118] Cunningham BW, Gordon JD, Dmitriev AE, Hu N, McAfee PC. Biomechanical evaluation of total disc replacement arthroplasty: an in vitro human cadaveric model. *Spine* 2003;28(20S):S110.

[119] DiAngelo DJ, Foley KT. An improved biomechanical testing protocol for evaluating multilevel cervical instrumentation in a human cadaveric corpectomy model. *Spinal Implants: Are We Evaluating Them Appropriately* 2003.

[120] Panjabi M, Malcolmson G, Teng E, Tominaga Y, Henderson G, Serhan H. Hybrid testing of lumbar CHARITE discs versus fusions. *Spine* 2007;32(9):959.

[121] Grassmann S, Oxland TR, Gerich U, Nolte LP. Constrained testing conditions affect the axial rotation response of lumbar functional spinal units. *Spine* 1998;23(10):1155.

[122] Eguizabal J, Tufaga M, Scheer JK, Ames C, Lotz JC, Buckley JM. Pure moment testing for spinal biomechanics applications: Fixed versus sliding ring cable-driven test designs. *J Biomech* 2010;43(7):1422-1425.

[123] Rhee JM, Register B, Hamasaki T, Franklin B. Plate-Only Open Door Laminoplasty Maintains Stable Spinal Canal Expansion with High Rates of Hinge Union and No Plate Failures. *Spine* 2011;36(1):9-14.

[124] Guigui P, Benoist M, Deburge A. Spinal deformity and instability after multilevel cervical laminectomy for spondylotic myelopathy. *Spine* 1998;23(4):440-447.

[125] Frost HM. Dynamics of bone remodeling. *Bone biodynamics* 1964:315.

[126] Talos Project. <http://www.talosproject.nl/index.cfm?p=7B5FF46F-E2D3-5E8F-A05DBE04A7DCA3F1>.

[127] Carter DR. Mechanical loading histories and cortical bone remodeling. *Calcif Tissue Int* 1984;36:19-24.

[128] Huiskes R, Weinans H, Grootenboer H, Dalstra M, Fudala B, Slooff T. Adaptive bone-remodeling theory applied to prosthetic-design analysis. *J Biomech* 1987;20(11-12):1135-1150.

[129] The effect of adaptive bone remodelling threshold levels on resorption around noncemented hip stems. The winter annual meeting of the American society of mechanical engineers. United States: Atlanta, Georgia; 1991.

[130] Mullender M, Huiskes R. Proposal for the regulatory mechanism of Wolff's law. *Journal of orthopaedic research* 1995;13(4):503-512.

[131] Carter DR, Hayes WC. The compressive behavior of bone as a two-phase porous structure. *The journal of bone and joint surgery* 1977;59(7):954.

[132] Cowin SC, Firoozbakhsh K. Bone remodeling of diaphysial surfaces under constant load: theoretical predictions. *J Biomech* 1981;14(7):471-484.

[133] Cowin S, Hegedus D. Bone remodeling I: theory of adaptive elasticity. *Journal of Elasticity* 1976;6(3):313-326.

[134] Hegedus D, Cowin S. Bone remodeling II: small strain adaptive elasticity. *Journal of Elasticity* 1976;6(4):337-352.

[135] Huiskes R. Validation of adaptive bone-remodeling simulation models. *Bone research in biomechanics* 1997:33-48.

[136] Weinans H, Huiskes R, Grootenboer H. The behavior of adaptive bone-remodeling simulation models. *J Biomech* 1992;25(12):1425-1441.

[137] Kode S, Gandhi AA, Smucker JD, Fredericks DC, Grosland NM. *Biomechanical Testing of Multi-Level Laminoplasty and Laminectomy Procedures*. American Society of Biomechanics 2011.

[138] Kode S, Kallemeyn NA, Fredericks DC, Grosland NM, Smucker JD. A Finite Element study on the effect of multi-level laminoplasty and laminectomy on the biomechanics of cervical spine. Submitted to *Spine* 2011.

[139] Pawlikowski M. *Computer Simulation of Bone Adaptation Process Under Various Load Cases*.

[140] Grosland NM. *Spinal adaptations in response to interbody fusion systems: a theoretical investigation*. Thesis (Ph D), University of Iowa 1998.

[141] Grant JP, Oxland TR, Dvorak MF. Mapping the structural properties of the lumbosacral vertebral endplates. *Spine* 2001;26(8):889.

[142] Grosland NM, Goel VK. Vertebral endplate morphology follows bone remodeling principles. *Spine* 2007;32(23):E667.

[143] Rhee JM, Register B, Hamasaki T, Yoon ST, Franklin B. Rate of Hinge Healing after Open Door Laminoplasty. Spine Journal Meeting Abstracts; 2007.

[144] Weinans H, Huiskes R, Van Rietbergen B, Sumner D, Turner T, Galante J. Adaptive bone remodeling around bonded noncemented total hip arthroplasty: a comparison between animal experiments and computer simulation. Journal of orthopaedic research 1993;11(4):500-513.

[145] Bougherara H, Bureau MN, Yahia LH. Bone remodeling in a new biomimetic polymer-composite hip stem. Journal of Biomedical Materials Research Part A 2010;92(1):164-174.

[146] Pawlikowski M, Skalski K, Haraburda M. Process of hip joint prosthesis design including bone remodeling phenomenon. Comput Struct 2003;81(8-11):887-893.

[147] Goel VK, Seenivasan G. Applying bone-adaptive remodelling theory to ligamentous spine. Preliminary results of partial nucleotomy and stabilization. Engineering in Medicine and Biology Magazine, IEEE 2002;13(4):508-516.

[148] Emery SE. Cervical spondylotic myelopathy: diagnosis and treatment. J Am Acad Orthop Surg 2001;9(6):376-388.

[149] Hale JJ, Gruson KI, Spivak JM. Laminoplasty: a review of its role in compressive cervical myelopathy. The Spine Journal 2006;6(6):S289-S298.